

Anna Lifen Tennfjord

Synthesis of enantiopure β -blocker (S)-esmolol

Master's thesis in Chemistry

Supervisor: Elisabeth Egholm Jacobsen

June 2021

Anna Lifen Tennfjord

Synthesis of enantiopure β -blocker (S)- esmolol

Master's thesis in Chemistry
Supervisor: Elisabeth Egholm Jacobsen
June 2021

Norwegian University of Science and Technology
Faculty of Natural Sciences
Department of Chemistry



I hereby declare that this thesis is an independent work in accordance with examination regulations at the Norwegian University of Science and Technology (NTNU).

Trondheim, June 13, 2021

Anna L. Tennfjord

Anna Lifen Tennfjord

Preface

This thesis has been performed as a part of the Master of Technology in Industrial Chemistry and Biotechnology (MTKJ) at the Department of Chemistry at the Norwegian University of Science and Technology. All work was carried out under the supervision of Associate Professor Elisabeth Egholm Jacobsen, and performed in the period between January 2021 and June 2021.

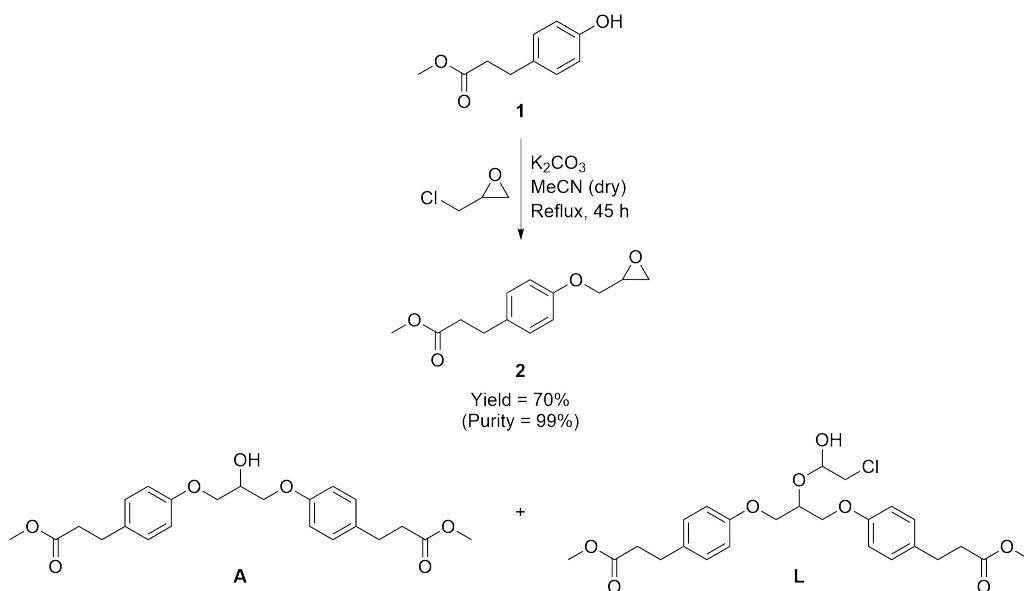
I would like to thank Elisabeth for great professional guidance, her engagement, and motivation. I would also like to thank Mari Rødseth for being good company in the lab, and answering many of my countless questions. Thanks to Raymond Trohjell and Kristoffer Klungseth for also being good company in the lab, and Susanne Hansen Troøyen and Lucas Hugo Yvan for teaching me about natural product chemistry. In general, a big thank you to all the people in the Biocatalysis research group for great group meetings and discussions. Further, I would like to thank Roger Aarvik for providing chemicals, Julie Asmussen for the assistance with HPLC, Susana Villa Gonzalez for LC-MS assistance, and Torun Melø for the NMR assistance.

I would also like to thank my friends and family for their support, and especially my boyfriend, Bendik Bogfjellmo, for calming me down in stressful times and making me dinner when I had late hours at the university.

Abstract

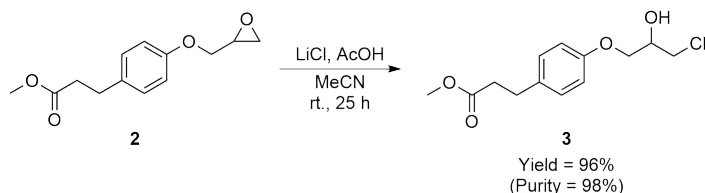
β -blockers are β -adrenergic antagonists blocking the natural cellular response of adrenaline at β -receptors. β -Blockers are drugs which can be used in treatment of common diseases such as hypertension and angina pectoris, and most β -blockers are sold with a racemic active pharmaceutical ingredient (API) which often have side-effects. Esmolol is a β -blocker which is sold with racemic API, but it is the (*S*)-enantiomer of esmolol that has the desired effects. The aim of this thesis was to synthesize (*S*)-esmolol ((*S*)-**5**) in an environmentally friendly and efficient fashion.

The building block for esmolol (**5**), methyl 3-(4-(3-chloro-2-hydroxypropoxy)phenyl)propanoate (**3**) was synthesized in a two-step synthesis. The first synthesis step formed methyl 3-(4-(oxiran-2-ylmethoxy)phenyl)propanoate (**2**) in 70% yield with 99% purity (determined by ¹H-NMR) from methyl 3-(4-hydroxyphenyl)propanoate (**1**), epichlorohydrin, and base (Scheme 0.1). The reaction forming epoxide **2** formed two by-products; 3,3'-(((2-hydroxypropane-1,3-diyl)bis(oxy))bis(4,1-phenylene))dipropanoate (**A**) and dimethyl 3,3'-(((2-(2-chloro-1-hydroxy-ethoxy)propane-1,3-diyl)bis(oxy))bis(4,1-phenylene))dipropionate (**L**). Both by-product **A** and **L** was discovered by LC-MS, and by-product **A** were isolated and characterized by NMR.



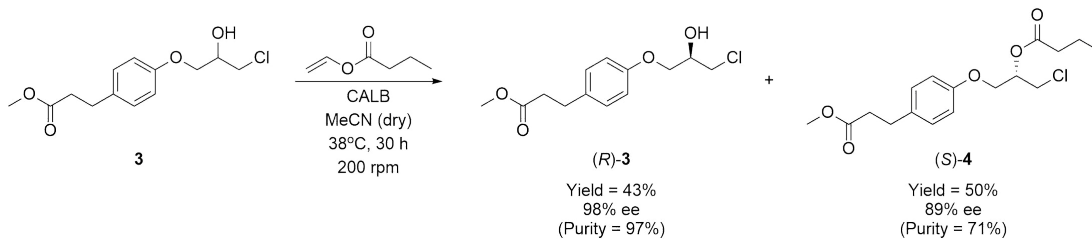
Scheme 0.1: Synthesis of methyl 3-(4-(oxiran-2-ylmethoxy)phenyl)propanoate (**2**) from methyl 3-(4-hydroxyphenyl)propanoate (**1**), epichlorohydrin, and base. By-product 3,3'-(((2-hydroxypropane-1,3-diyl)bis(oxy))bis(4,1-phenylene))-dipropanoate (**A**) and dimethyl 3,3'-(((2-(2-chloro-1-hydroxy-ethoxy)propane-1,3-diyl)bis(oxy))bis(4,1-phenylene))dipropionate (**L**) were discovered by LC-MS.

The second synthesis step was ring-opening of epoxide **2** with lithium chloride and protonation by acetic acid. The reaction formed chlorohydrin **3** in 96% yield with 98% purity, see Scheme 0.2.



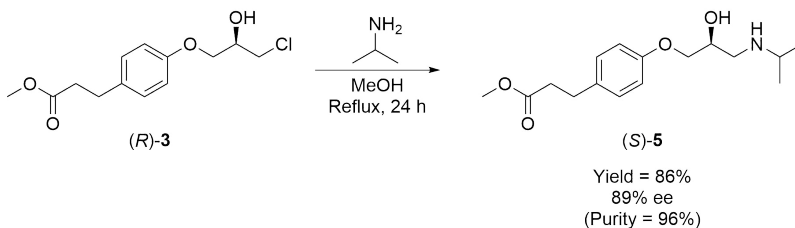
Scheme 0.2: Synthesis of chlorohydrin **3** by ring-opening of epoxide **2** with lithium chloride and acetic acid.

Kinetic resolution of racemic chlorohydrin **3** was performed with *Candida antarctica* Lipase B (CALB) as catalyst and vinyl butanoate as acyl donor, see Scheme 0.3. Enantiopure (*R*)-**3** was obtained in 43% yield with 97% purity and 98% ee (determined by HPLC). (*S*)-1-chloro-3-(4-(3-methoxy-3-oxopropyl)phenoxy)propan-2-yl butanoate ((*S*)-**4**) was formed in 50% yield with 71% purity and 89% ee. The enantiomeric ratio (*E*) was determined to be 157.



Scheme 0.3: Kinetic resolution of racemic chlorohydrin **3** performed with CALB as catalyst and vinyl butanoate as acyl donor forming enantiopure (*R*)-**3** and (*S*)-1-chloro-3-(4-(3-methoxy-3-oxopropyl)phenoxy)propan-2-yl butanoate ((*S*)-**4**).

(*S*)-esmolol ((*S*)-**5**) was synthesized from (*R*)-**3** and isopropylamine upon heating, see Scheme 0.4. This gave enantiopure (*S*)-**5** in 86% yield with 96% purity and 89% ee.

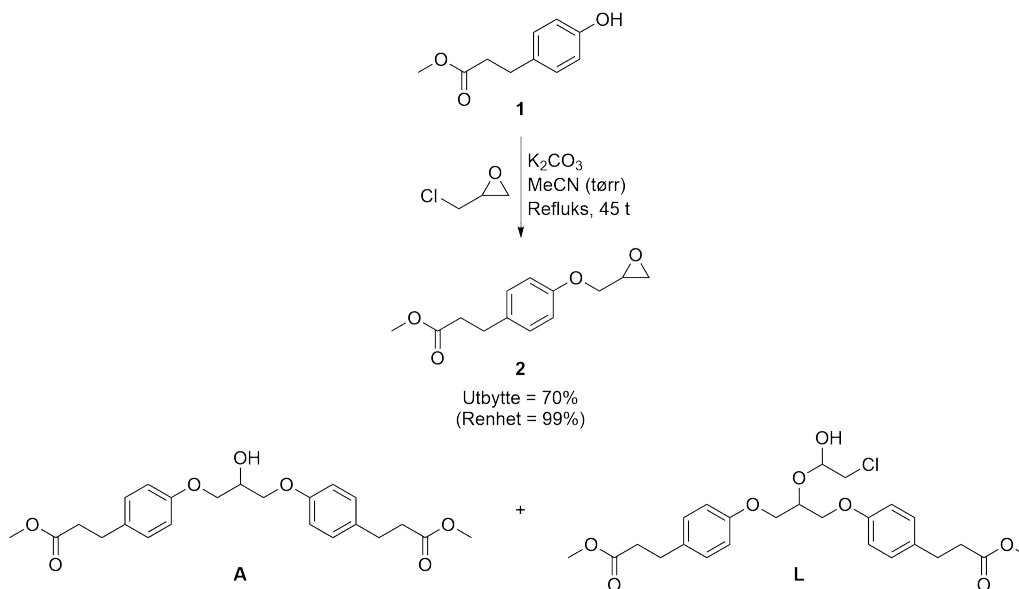


Scheme 0.4: Synthesis of enantiopure (*S*)-esmolol ((*S*)-**5**) from (*R*)-**3** and isopropylamine.

Sammendrag

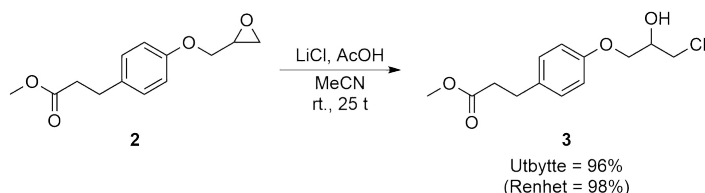
β -Blokkere er β -adrenerge antagonister som blokkerer den naturlige cellulære responsen til adrenalin i β -reseptorer. β -Blokkere er medisiner som kan bli brukt i behandling av vanlige sykdommer som hypertensjon og angina pectoris, og de fleste β -blokkere selges med en rasemisk *active pharmaceutical ingredient* (API) som ofte har bivirkninger. Esmolol er en β -blokker som selges med rasemisk API, men det er (*S*)-enantiomeren av esmolol som har de ønskede effektene. Formålet med denne oppgaven var å syntetisere (*S*)-esmolol ((*S*)-**5**) på en miljøvennlig og effektiv måte.

Byggesteinen til esmolol, metyl 3-(4-(3-klor-2-hydroksypropoksy)fenyl)propanoat (**3**), ble syntetisert i en tostegssyntese. Det første syntese­steget dannet 3-(4-(oksiran-2-ylmetoksy)fenyl)-propanoat (**2**) i 70% utbytte med 99% renhet (bestemt ved $^1\text{H-NMR}$) fra metyl 3-(4-hydroksyfenyl)propanoat (**1**), epiklorhydrin og base (Skjema 0.5). Reaksjonen som dannet epoksid **2** dannet to biprodukter; 3,3'-(((2-hydroksypropan-1,3-diyl)bis(oksy))bis(4,1-fenylen))dipropanoat (**A**) og dimetyl 3,3'-(((2-(2-klor-1-hydroksy-etoksy)propan-1,3-diyl)bis(oksy))bis(4,1-fenylen))dipropanoat (**L**). Både biprodukt **A** og **L** ble oppdaget ved LC-MS, og biprodukt **A** ble isolert og karakterisert ved NMR.



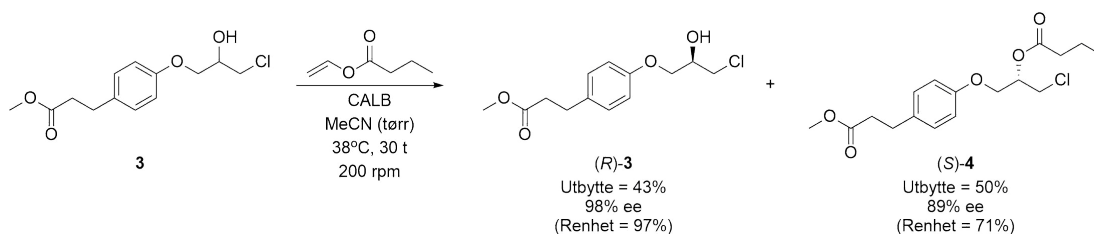
Skjema 0.5: Syntese av metyl 3-(4-(oksiran-2-ylmetoksy)fenyl)propanoat (**2**) fra metyl 3-(4-hydroksyfenyl)propanoat (**1**), epiklorhydrin og base. Biprodukt 3,3'-(((2-hydroksypropan-1,3-diyl)bis(oksy))bis(4,1-fenylen))dipropanoat (**A**) og dimetyl 3,3'-(((2-(2-klor-1-hydroksy-etoksy)propan-1,3-diyl)bis(oksy))bis(4,1-fenylen))dipropanoat (**L**) ble oppdaget ved LC-MS.

Det andre syntesesteget var ringåpning av epoksid **2** med litiumklorid og protonering med eddiksyre. Reaksjonen dannet klorhydrin **3** i 96% utbytte med 98% renhet, se Skjema 0.6.



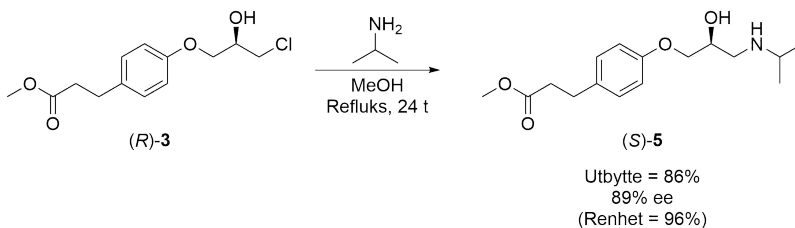
Skjema 0.6: Syntese av klorhydrin **3** ved ringåpning av epoksid **2** med litiumklorid og eddiksyre.

Kinetisk oppløsning av rasemisk klorhydrin **3** ble utført med *Candida antarctica* Lipase B (CALB) som katalysator og vinylbutanoat som acyldonor, se Skjema 0.7. Enantiomert ren (*R*)-**3** ble oppnådd i 43% utbytte med 97% renhet og 98% ee (bestemt ved HPLC). (*S*)-1-klor-3-(4-(3-metoksy-3-oksypopyl)fenoksy)propan-2-yl butanoat ((*S*)-**4**) ble dannet i 50% utbytte med 71% renhet og 89% ee. Det enantiomeriske forholdet (*E*) ble bestemt til å være 157.



Skjema 0.7: Kinetisk oppløsning av rasemisk klorhydrin **3** utført med CALB som katalysator og vinylbutanoat som acyldonor, som dannet enantiomert ren (*R*)-**3** og (*S*)-1-klor-3-(4-(3-metoksy-3-oksypopyl)fenoksy)propan-2-yl butanoat ((*S*)-**4**).

(*S*)-esmolol ((*S*)-**5**) ble syntetisert fra (*R*)-**3** og isopropylamin ved oppvarming, se Skjema 0.8. Dette ga enantiomert ren (*S*)-**5** i 86% utbytte med 96% renhet og 89% ee.



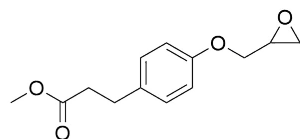
Skjema 0.8: Syntese av enantiomert ren (*S*)-esmolol ((*S*)-**5**) fra (*R*)-**3** and isopropylamin.

Symbols and Abbreviations

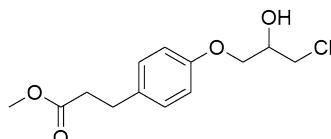
δ	Chemical shift
λ	Wavelength
API	Active pharmaceutical ingredient
c	Conversion
CALB	<i>Candida antarctica</i> Lipase B
COSY	Correlation spectroscopy
d	Doublet
dd	Doublet of doublet
DAD	Diode array detector
DBE	Double bond equivalent
ee	Enantiomeric excess
ee _S	Enantiomeric excess of substrate
ee _P	Enantiomeric excess of product
E	Enantiomeric ratio
Equiv.	Equivalents
h	Hours
HMBC	Heteronuclear Multiple Bond Correlation
HPLC	High-Performance Liquid Chromatography
HSQC	Heteronuclear Single Quantum Coherence
Hz	Hertz
ID	Inner diameter
Int.	Integral
J	Coupling constant
LC	Liquid chromatography
m	Multiplet
m/z	Mass to charge ratio
MS	Mass spectroscopy
NME	New Molecular Entity
NMR	Nuclear Magnetic Resonance
PCL	<i>Pseudomonas cepacia</i> Lipase
ppm	Parts per million
quint.	Quintet
R _f	Retention factor
R _S	Resolution
rpm	Rotations per minute
rt.	Room temperature

s	Singlet
t	Triplet
TLC	Thin Layer Chromatography
t_R	Retention time
UV	Ultraviolet Light
VWD	Variable wavelength detector

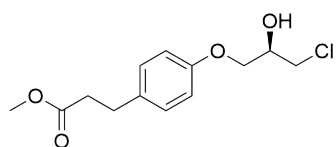
List of Synthesized Compounds



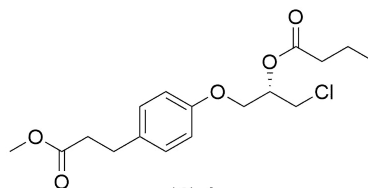
2



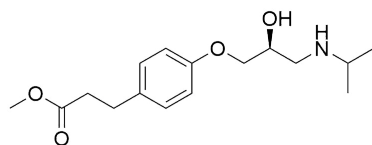
3



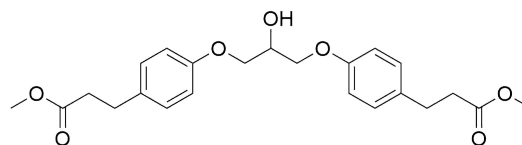
(R)-3



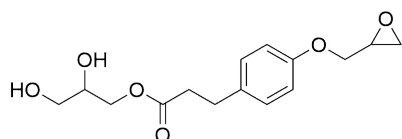
(S)-4



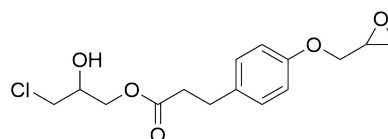
(S)-5



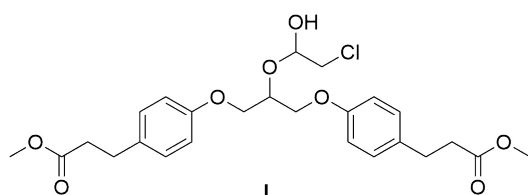
A



H



J



L

Contents

1	Introduction	1
1.1	Aim of the thesis	1
1.2	Importance of enantiopure compounds in medicinal chemistry	2
1.2.1	β -Blockers	4
1.2.2	Esmolol	5
1.3	Green chemistry	6
1.4	Biocatalysis in organic chemistry	6
1.4.1	Kinetic resolution	7
1.4.2	Classification of enzymes	9
1.4.3	Lipases	10
1.4.4	<i>Candida antarctica</i> Lipase B (CALB)	11
1.4.5	Factors that effect the enzyme activity and selectivity	12
1.5	Synthetic pathways to enantiopure (<i>S</i>)-esmolol	14
1.5.1	Previous studies in the synthesis of β -blocker precursors similar to the esmolol precursor	15
1.5.2	Formation of by-products in previous studies in the synthesis of (<i>S</i>)-esmolol precursors, and other similar β -blocker precursors	16
1.6	Analytical methods for chiral chemical compounds	18
1.6.1	Chiral chromatography	18
1.6.2	Polarimetry	20
1.7	Organic synthesis theory	21
1.7.1	Nucleophilic substitution reactions, S_N2 and S_N1	21
1.7.2	Ring-opening of epoxides	21
1.7.3	Amine alkylation (amino-de-halogenation)	22
1.7.4	Transesterification	23
1.7.5	Reaction kinetics	24
2	Results and Discussion	25
2.1	Synthesis of a mixture of methyl 3-(4-(oxiran-2-ylmethoxy)phenyl)propanoate (2) and methyl 3-(4-(3-chloro-2-hydroxypropoxy)phenyl)propanoate (3) with sodium hydroxide	25
2.1.1	Mechanistic studies of reaction between deprotonated phenol 1 and epichlorohydrin	28
2.1.2	Formation of by-products	29
2.2	Synthesis of methyl 3-(4-(oxiran-2-ylmethoxy)phenyl)propanoate (2)	33
2.2.1	Characterization of epoxide 2	36
2.2.2	The effect of using NaOH and K_2CO_3 as base	37

2.3	Synthesis of methyl 3-(4-(3-chloro-2-hydroxypropoxy)phenyl)propanoate (3) by ring- opening of methyl 3-(4-(oxiran-2-ylmethoxy)phenyl)propanoate (2)	38
2.3.1	Mechanistic studies of ring-opening of epoxide 2	40
2.3.2	Characterization of chlorohydrin 3	40
2.3.3	Impact of acetic acid equivalents, and the concentration	41
2.4	Formation of dimers as by-products	42
2.4.1	Mechanistic studies of dimer A formation	43
2.4.2	Characterization of dimer A	44
2.4.3	Formation of a dimer derivative	46
2.5	Derivatization reaction of methyl 3-(4-(3-chloro-2-hydroxypropoxy)phenyl)propanoate (3)	46
2.6	Small-scale kinetic resolution of methyl 3-(4-(3-chloro-2-hydroxypropoxy)phenyl)propanoate (3) with CALB	49
2.7	Large-scale kinetic resolution of methyl 3-(4-(3-chloro-2-hydroxypropoxy)phenyl)propanoate (3) with CALB	54
2.7.1	Characterization of ester 4	56
2.8	Synthesis of enantiopure (<i>S</i>)-esmolol ((<i>S</i>)- 5)	58
2.8.1	Characterization of esmolol (5)	61
2.9	Optical rotation of enantiopure compounds	63
3	Conclusion	65
4	Future Work	67
5	Experimental	69
5.1	General methods	69
5.1.1	Chemicals, solvents and enzymes	69
5.1.2	Chromatographic analyzes	69
5.1.3	Spectroscopic analyzes	71
5.1.4	Other methods	71
5.2	Synthesis of racemic building blocks and achiral compounds	71
5.2.1	Synthesis of a mixture of methyl 3-(4-(oxiran-2-ylmethoxy)phenyl)propanoate (2) and methyl 3-(4-(3-chloro-2-hydroxypropoxy)phenyl)propanoate (3) with NaOH	71
5.2.2	Synthesis of methyl 3-(4-(oxiran-2-ylmethoxy)phenyl)propanoate (2) with K ₂ CO ₃	72

5.2.3	Synthesis of methyl 3-(4-(3-chloro-2-hydroxypropoxy)phenyl)propanoate (3) by ring-opening of methyl 3-(4-(oxiran-2-ylmethoxy)phenyl)propanoate (2)	72
5.3	Enzyme catalyzed kinetic resolutions of racemates	73
5.3.1	Derivatization reaction of methyl 3-(4-(3-chloro-2-hydroxypropoxy)phenyl)propanoate (3)	73
5.3.2	Small-scale kinetic resolution of methyl 3-(4-(3-chloro-2-hydroxypropoxy)phenyl)propanoate (3) with CALB	73
5.3.3	Large-scale kinetic resolution of methyl 3-(4-(3-chloro-2-hydroxypropoxy)phenyl)propanoate (3) with CALB	74
5.4	Synthesis of (<i>S</i>)-esmolol ((<i>S</i>)- 5)	74
References		75
A Characterization of		
	methyl 3-(4-(oxiran-2-ylmethoxy)phenyl)propanoate (2)	i
A.1	¹ H-NMR spectrum of epoxide 2	i
A.2	¹³ C-NMR spectrum of epoxide 2	ii
A.3	H,H-COSY-NMR spectrum of epoxide 2	iii
A.4	HSQC-NMR spectrum of epoxide 2	iv
A.5	HMBC-NMR spectrum of epoxide 2	v
B Characterization of methyl		
	3-(4-(3-chloro-2-hydroxypropoxy)phenyl)propanoate (3)	vi
B.1	¹ H-NMR spectrum of chlorohydrin 3	vi
B.2	¹³ C-NMR spectrum of chlorohydrin 3	vii
B.3	H,H-COSY-NMR spectrum of chlorohydrin 3	viii
B.4	HSQC-NMR spectrum of chlorohydrin 3	ix
B.5	HMBC-NMR spectrum of chlorohydrin 3	x
C Characterization of		
	1-chloro-3-(4-(3-methoxy-3-oxopropyl)phenoxy)propan-2-yl butyrate (4)	xi
C.1	¹ H-NMR spectrum of ester 4	xi
C.2	¹³ C-NMR spectrum of ester 4	xii
C.3	H,H-COSY-NMR spectrum of ester 4	xiii
C.4	HSQC-NMR spectrum of ester 4	xiv
C.5	HMBC-NMR spectrum of ester 4	xv

D	Characterization of esmolol (5)	xvi
D.1	¹ H-NMR spectrum of esmolol (5)	xvi
D.2	¹³ C-NMR spectrum of esmolol (5)	xvii
D.3	H,H-COSY-NMR spectrum of esmolol (5)	xviii
D.4	HSQC-NMR spectrum of esmolol (5)	xix
D.5	HMBC-NMR spectrum of esmolol (5)	xx
E	Characterization of	
	3,3'-(((2-hydroxypropane-1,3-diy)bis(oxy))bis(4,1-phenylene))dipropanoate	
	(A)	xxi
E.1	¹ H-NMR spectrum of dimer A	xxi
E.2	¹³ C-NMR spectrum of dimer A	xxii
E.3	H,H-COSY-NMR spectrum of dimer A	xxiii
E.4	HSQC-NMR spectrum of dimer A	xxiv
E.5	HMBC-NMR spectrum of dimer A	xxv
F	Characterization of 3-chloro-2-hydroxypropyl	
	3-(4-(oxiran-2-ylmethoxy)phenyl)propanoate (J)	xxvi
F.1	¹ H-NMR spectrum of by-product J	xxvi
F.2	¹³ C-NMR spectrum of by-product J	xxvii
F.3	H,H-COSY-NMR spectrum of by-product J	xxviii
F.4	HSQC-NMR spectrum of by-product J	xxix
F.5	HMBC-NMR spectrum of by-product J	xxx
G	LC-MS-analysis of by-products	xxxix
G.1	LC-MS-chromatogram for reaction with NaOH	xxxix
G.2	MS-spectrum of by-product H or I	xxxix
G.3	MS-spectrum of by-product J or K	xxxix
G.4	LC-MS-chromatogram for reaction with K ₂ CO ₃	xxxix
G.5	MS-spectrum of dimer A	xxxix
G.6	MS-spectrum of dimer L	xxxix

1 Introduction

In this section the aim of the thesis will be presented first. This will lay the foundation for the rest of the topics addressed in this section.

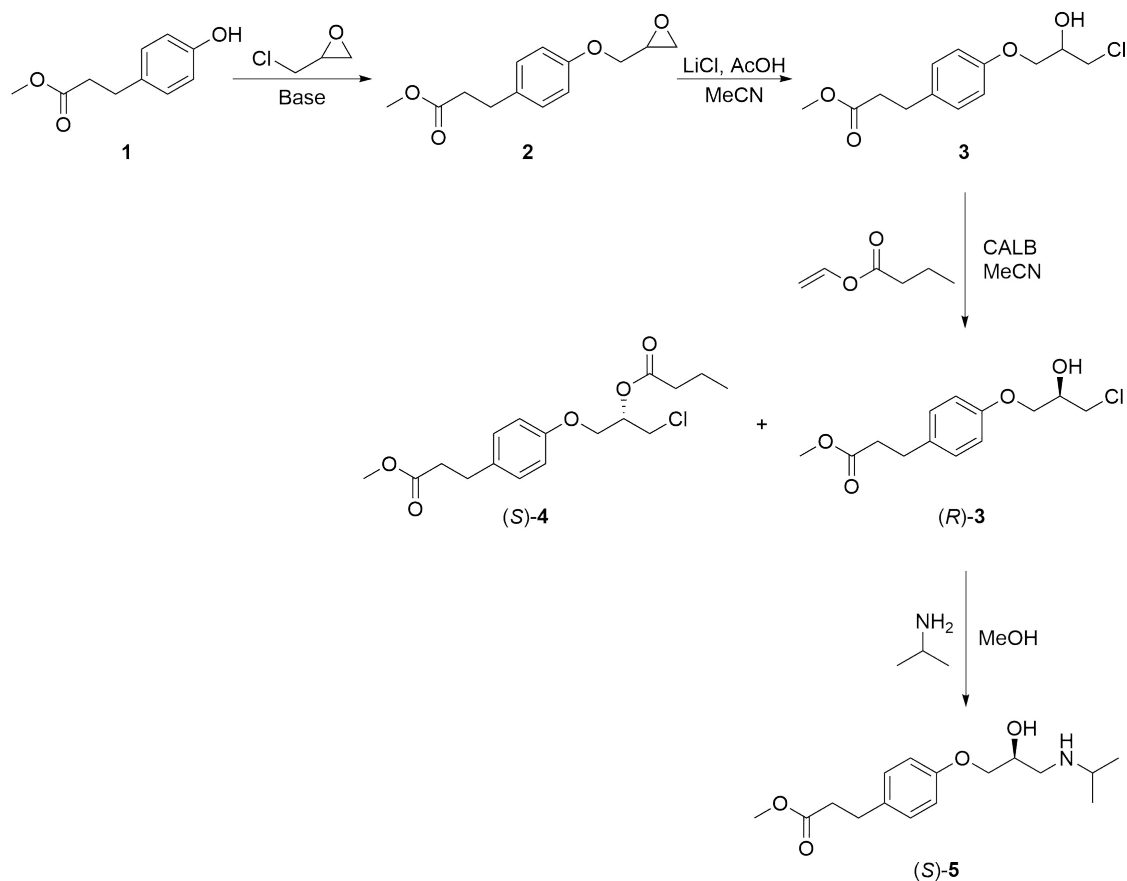
1.1 Aim of the thesis

Several studies of enzymatic kinetic resolutions have been performed in the synthesis of various enantiopure β -blocker precursors in the Biocatalysis research group. The main aim of this thesis was to synthesize (*S*)-esmolol ((*S*)-**5**) in an environmentally friendly and efficient fashion by the use of biocatalysis, specifically kinetic resolution. The total synthesis of (*S*)-**5** is shown in Scheme 1.1. In order to achieve the main goal, there were three sub-goals.

The first sub-goal was to synthesize the racemic building block for esmolol, methyl 3-(4-(3-chloro-2-hydroxypropoxy)phenyl)propanoate (**3**), through a two-step synthesis. Different reaction conditions for the first and the second step were investigated in order to synthesize pure chlorohydrin **3**.

The second sub-goal was to synthesize enantiopure (*R*)-**3** by performing enzymatic kinetic resolution with *Candida antarctica* Lipase B (CALB) as catalyst. It was tried to achieve an enantiomeric excess of (*R*)-**3** of at least 96% as this is the requirement for classifying a pharmaceutical as enantiopure. CALB has shown to be stereoselective in kinetic resolution of structurally similar chlorohydrins as chlorohydrin **3**.¹

Finally, the third sub-goal was to synthesize enantiopure (*S*)-esmolol ((*S*)-**5**) by alkylating isopropylamine with (*S*)-**3** as alkylating agent.



Scheme 1.1: Synthesis of enantiopure (*S*)-esmolol ((*S*)-5), the main aim of the thesis.

1.2 Importance of enantiopure compounds in medicinal chemistry

For several years a drug called thalidomide was used to relieve the symptoms of morning sickness in pregnant women, and in 1963 it was discovered that thalidomide caused horrible birth defects in many babies exposed to this drug.² Later, it was discovered that whereas one of the enantiomers of thalidomide (the right-handed molecules) had the desired effect of curing morning sickness, the other enantiomer, which was also present in the drug, caused the terrible birth defects.² Side effects from pharmaceuticals like this are not unusual, but they are often not this severe. This has led to that the amount of approved new racemic drugs, so-called New Molecular Entities (NME's), has decreased especially in the past 20 years. To further understand what happened in the case with thalidomide, we are going to examine the properties of enantiomers.

Enantiomers are two three-dimensional molecules with a center of asymmetry, thus two nonsuperimposable mirror images of one another (Figure 1.1). Their configuration is denoted as *S* or *R* depending on the ordering of substituents; counterclockwise or clockwise respectively. An important property of enantiomers with a single chiral center, is that an interchange of groups at the chiral center converts one enantiomer into the other. A chiral center with such a property is also called a stereogenic center.

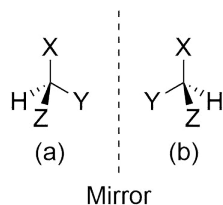


Figure 1.1: An example of a tetrahedral carbon atom that bears four different groups, giving two enantiomers, where (a) is a nonsuperimposable mirror image of (b).²

Two enantiomers have identical chemical and physical properties, but different optical rotation. Furthermore, the chirality determines the biological properties of enantiomers, which can vary. This is often likened to the specificity of our hands for their respective gloves; the binding specificity for a chiral molecule (like a hand) at a chiral binding site (a glove) is favorable in one way only.² This applies, among other things, to enzymes which have chiral building blocks such as L- and D-amino acids, giving stereospecific binding sites favoring binding of one enantiomer over the other. Figure 1.2 illustrates how the enzyme chooses an exact structure.

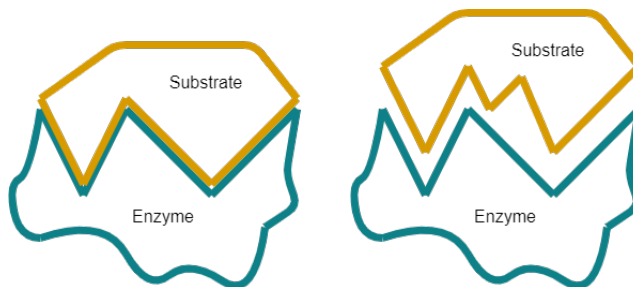


Figure 1.2: An illustration of enzyme specificity. The substrate to the left fits perfectly in the enzyme, while the substrate to the right does not.

In racemic drugs, one of the enantiomers is the active enantiomer (eutomer) giving the desired effects, while the other enantiomer can have adverse effects or no effect at all (distomer). In pharmaceutical drugs the active substance is called the active

pharmaceutical ingredient (API). The API can be sold in both racemic and enantiomerically pure form. When it is referred to pharmaceuticals in this project it is always the API that is in question.

The replacement of an already approved racemic pharmaceutical by an enantiomeric pure pharmaceutical is called "chiral switching". This is usually performed by the company that already has the license for the racemate. In this way they can extend their patent and protect themselves against generic competition with the racemate.³ Since the copyright of a patent of a pharmaceutical is usually on the racemate, and not the individual enantiomers, it has allowed other companies to specialize in chiral synthesis, showing an increase in patents for "chiral switching".³ In the period from 1994 to 2011, two studies combined showed that the US Food and Drug Administration (FDA) approved 15 enantiomerically pure versions of racemic drugs, i.e. 15 chiral switches had been launched in less than 20 years.⁴⁻⁶

β -Blockers are good examples of pharmaceuticals sold as racemates, where mostly the (*S*)-enantiomers are the active enantiomers, while some of the (*R*)-enantiomers have adverse effect rather than any effects at all.⁷

1.2.1 β -Blockers

β -Blockers are one of the classes of drugs which plays a relevant role in the treatment of various human diseases such as hypertension, angina pectoris, migraines, and tremors.⁸

β -Blockers are β -adrenergic antagonists, which affects the β -adrenergic receptors found in a variety of places in the human body, with most efficiency in the heart and vascular system.^{8,9} The β -receptors are divided into β_1 -, β_2 -, and β_3 -receptors, where β_1 -receptors are mainly found in the the heart and β_2 in the lungs. All the receptors are regulated by epinephrine and norepinephrine, also known as adrenaline and noradrenaline, which regulates the "fight and flight" response through interactions with the receptors. The structures of epinephrine and norepinephrine are shown in Figure 1.3.¹⁰

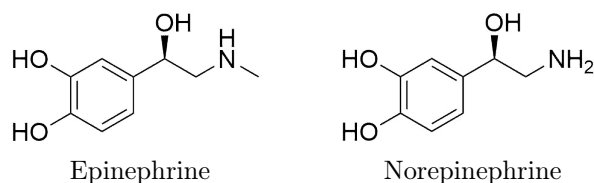


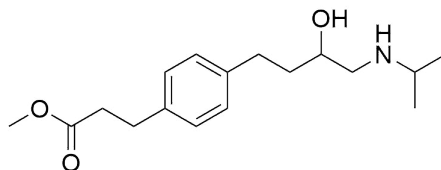
Figure 1.3: The structures of epinephrine and norepinephrine, the natural regulators of β -receptors.¹⁰

Among β -blockers there are agonists and antagonists. Agonists are structural analogues binding to the receptor sites and mimicking the response of epinephrine, while antagonists are structural analogues binding to the same receptor sites as the agonists, thus blocking the cellular response.⁹ β -Antagonists can be both selective and non-selective towards the β -receptors, meaning that they are selective towards either the β_1 - or the β_2 -receptors or both receptors. Selective β -blockers are safer to use as they give less side effects.¹⁰ An example is if you are treating heart failure in a patient that is also suffering from asthma. Using a non-selective β -blocker can therefore treat both the heart failure, and the asthma with possibly negative side-effects.

In 2010, only a few β -blockers were sold as the single enantiomer even though most β -blockers are dependent on the (*S*)-enantiomers, which usually are more potent than the distomers.⁷

1.2.2 Esmolol

Esmolol is a unique cardioselective β_1 -antagonist with a rapid onset and a short duration of action. It is an intravenous administrated hydrophilic β -blocker quickly metabolized in red blood cells.^{11,12} It is sold under the trade name Brevibloc, and is widely used in the treatment of hypertension, cardiac arrhythmia, and angina pectoris. The structure of esmolol is shown in Figure 1.4.¹³



Esmolol

Figure 1.4: The structure of the β -blocker esmolol.¹³

Esmolol is currently marketed as the racemic form, but it is the (*S*)-enantiomer of esmolol that is the eutomer and the (*R*)-enantiomer is the distomer.¹³ (*S*)-esmolol as a β -blocker has two times higher potency than that of (*RS*)-esmolol.¹³

At higher dosages, esmolol has shown to inhibit β_2 -receptors in the bronchial and vascular smooth muscle. After infusion of esmolol, the onset of action occurs within two minutes, and within 5 minutes 90% of the β -blocker activity is reached.⁷ The elimination half-life of esmolol is approximately 9 minutes, with full recovery from its beta blocking properties occurring 18-30 minutes after stopping the infusion.¹¹ Because of esmolol's uniquely short half-life and β_1 -selectivity, it can be used effectively in patients with congestive heart failure and chronic obstructive lung diseases.¹⁴

1.3 Green chemistry

P. T. Anastas describes green chemistry as "*the utilization of a set of principles that reduces or eliminates the use or generation of hazardous substances in the design, manufacture, and applications of chemical products*".¹⁵ This means that green chemistry is an approach to prevent pollution, which involves the reduction or elimination of hazardous chemicals as feeding stocks, reagents, solvents, products, and by-products from chemical processes. In addition, it means to execute energy-effective syntheses if possible, reduce reaction temperature, pressure, and reaction time. This is generally called optimization. The use of degradable substances also has a positive effect on the environment.¹⁵ In other words, green chemistry is a chemical process or a chemical product that is greener or more environmentally friendly. An example of this type of a process is biocatalysis.

1.4 Biocatalysis in organic chemistry

The area of research for achieving enantiomerically pure compounds has grown enormously over the past 20 years because of the recognition that enantiomerically pure pharmaceuticals can be more potent and safer than their racemic ones, as described earlier. A widely used method in the 1900s for achieving enantiopure compounds was using a chiral pool, which is a collection of naturally occurring enantiopure building blocks such as sugars and amino acids.¹⁶ Most pharmaceuticals were synthesized from chiral building blocks, but in recent times it has become less popular, as other synthesis methods have been used more frequently.¹⁷ However, it has become important to find environmentally friendly methods for synthesis of enantiomerically pure compounds, and this is what green chemistry takes into account.

Enzymes are catalysts that meet most of the requirements of green chemistry, as they are biodegradable and can be used under mild conditions. All chemical processes that uses enzymes as catalysts are called biocatalysis. Like other catalysts, enzymes accelerate chemical reactions by lowering the activation energy. Biocatalysis by the use of enzymes in organic chemistry have several advantages; enzymes are biodegradable, react under mild conditions, and tolerate large variations in the substrate. Enzymes can catalyze almost all types of organic reactions; hydrolysis, oxidation-reduction, addition-elimination, and halogenation- and dehalogenation of a variety of compounds.

Biocatalysis also has several advantages when looking from an economical perspective. Enzymes can easily be washed and reused after a reaction. Additionally, biocatalysis replaces several reaction steps compared to traditional processes, as well as no powerful heating is necessary. Reducing reaction steps also leads to less waste, which is environmentally friendly.

Enzymes' selectivity is the basis for their utilization in organic chemistry. Enzymes can be chemoselective, regioselective, diastereoselective, and enantioselective. Chemoselective enzymes are able to selectively transform a specific functional group within the substrate, while regio- and diastereoselective enzymes perform transformations in a specific location within the substrate. An enantioselective enzyme prefers transformation of one substrate enantiomer over the other in a racemic mixture. This is called kinetic resolution.

1.4.1 Kinetic resolution

Kinetic resolution is defined as a process in a racemic mixture where one of the enantiomers is more readily transformed into a product than the other.¹⁸ Figure 1.5 shows the formation of products P and Q from the (R)- and (S)-enantiomers with rate constants k_R and k_S respectively.¹⁸

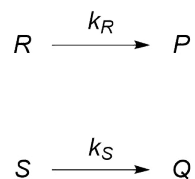


Figure 1.5: Transformation of the (R)- and (S)-enantiomers with rate constants k_R and k_S forming product P and Q respectively.¹⁸

If $k_R \neq k_S$ and the reaction is stopped at a point between 0 and 100% conversion, a kinetic resolution occurs.¹⁸ In an ideal situation, only one of the enantiomers reacts, for example the (R)-enantiomer. Therefore, at 50% conversion a mixture of 50% of the (S)-enantiomer and 50% product P is obtained. The difference in the specific rate constants comes from the fact that the transformation is mediated by a chiral catalyst or a chiral reagent.

In special cases the slower reacting enantiomer can be converted into the mirror image isomer using kinetic resolution. In this way the starting racemate is formed into the desired enantiomer. This is called dynamic kinetic resolution. Dynamic kinetic resolution allows the undesired enantiomer to be converted into the desired enantiomer with 100% conversion instead of 50%, which is the theoretically upper limit of conversion by "regular" kinetic resolution.

Enzymes are often used as chiral catalysts in kinetic resolution as they are stereospecific and thereby binds and favor formation of one enantiomer over the other. To determine the degree of enantioselectivity in a kinetic resolution some concepts need to be defined.

Enantiomeric excess, ee

Enantiomeric excess, ee, is a measurement of purity used for chiral substances, and it reflects the degree to which a sample contains the desired enantiomer relative to the other. The enantiomeric excess in percent is given by Equation (1.1) and can be calculated using the area of the chromatogram peaks from chromatographic analyses.¹⁹

$$ee [\%] = \frac{R - S}{R + S} \times 100, \quad (1.1)$$

R is the area of the chromatogram peak of the enantiomer in excess and S is the area of the chromatogram peak of the enantiomer in deficit.

Conversion, c

To follow a reaction pathway conversion, c , in percent is an important parameter. It describes the conversion to desired product in a reaction, and can be calculated using the enantiomeric excess of the substrate and product, ee_S and ee_P respectively. Conversion is defined in Equation (1.2).¹⁹

$$c[\%] = \frac{ee_S}{ee_S + ee_P} \times 100 \quad (1.2)$$

Enantiomeric ratio, E

To describe the selectivity of a resolution, a parameter called the enantiomeric ratio, E , needs to be defined. The enantiomeric ratio corresponds to the ratio of the relative second-order rate constants, ν_A and ν_B , of the individual substrate enantiomers, A and B. ν_A and ν_B are related to ratio of the specificity constants k_{cat}/K_M of the enantiomers according to the Michaelis-Menten kinetics as given in Equation (1.3).¹⁹

$$E = \frac{\nu_B}{\nu_A} = \frac{\left[\frac{k_{cat}}{K_M} \right]_A}{\left[\frac{k_{cat}}{K_M} \right]_B} \quad (1.3)$$

The ratio of the initial reaction rates of the substrate enantiomers ($E = \nu_A/\nu_B$) can be mathematically linked to the conversion of the reaction and the enantiomeric excess of the substrate and product.¹⁹ Equation (1.4) and (1.5) show two other ways to calculate the enantiomeric ratio.¹⁹

$$E = \frac{\ln[1 - c(1 + ee_P)]}{\ln[1 - c(1 - ee_P)]} \quad (1.4)$$

$$E = \frac{\ln[(1-c)(1-ee_S)]}{\ln[(1-c)(1+ee_S)]} \quad (1.5)$$

Equation (1.4) and (1.5) however, does not give reliable results for very low and high levels of conversion, where accurate measurement is hindered by errors derived from sample manipulation.¹⁹ Furthermore, Equation (1.4) and (1.5) is based on one substrate forming one product. However, in a kinetic resolution with an acyl donor, there are two substrates which forms two products. This type of kinetic resolution is called a bi-bi-reaction. Bi-bi-reactions can further be derived into the ping-pong mechanism, where the first product is released before the next substrate is bound to the enzyme. Figure 1.6 describes the generalized ping-pong bi-bi reaction.^{20,21}

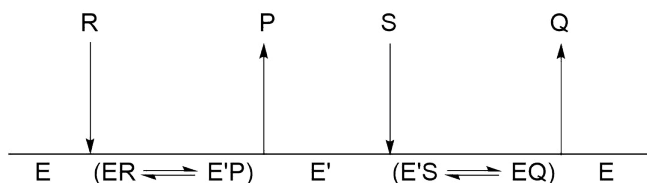


Figure 1.6: Ping-pong bi-bi reaction system (Cleland's nomenclature); E = enzyme; ER = enzyme-substrate complex; E'P = enzyme-product complex; E' = acyl enzyme; E'S = acyl enzyme-substrate complex; EQ = enzyme-product complex; R and S = substrates; P and Q = products.^{20,21}

To calculate the enantiomeric ratio for the ping-pong bi-bi reaction, Equation (1.6) is recommended as it only depends on relative quantities in contrast to the conversion.¹⁹ Another possibility is using the computer program called *E & K calculator*, which also is based on ping-pong bi-bi resolutions.²²

$$E = \frac{\ln \frac{[ee_P(1-ee_S)]}{(ee_P+ee_S)}}{\ln \frac{[ee_P(1+ee_S)]}{(ee_P+ee_S)}} \quad (1.6)$$

As a rule of thumb, enantiomeric ratios below 15 are invalid. In organic syntheses, $30 < E < 200$, is the desired interval for *E*-values. An *E*-value of 30 reflects $ee > 95\%$, while an $E > 200$ is inaccurate due to formation of small amounts of the slow reacting enantiomer, which in turn leads to inaccurate analyses by chiral chromatography.²³

1.4.2 Classification of enzymes

Enzymes are classified by the type of reaction they catalyze, and they are divided into six main classes. Table 1.1 show the six classes of enzymes and the reaction type they catalyze.¹⁹

Table 1.1: Classification of enzymes by the type of reaction they catalyze.¹⁹

Enzyme class	Reaction type
Oxidoreductases	Oxidation-reduction
Transferases	Transfer of functional groups (e.g. aldehydes, ketones, acyl)
Hydrolases	Hydrolysis of various bonds (e.g. esters, amides, epoxides)
Lyases	Addition-elimination of small molecules on double bonds (e.g. alkenes, imines, carbonyls)
Isomerases	Isomerization (e.g. racemization, epimerization, rearrangement)
Ligases	Formation-cleavage of C-O, C-S, C-N, C-C bonds

The most used enzyme class for organic chemists the past two decades is the hydrolases.¹⁹ The key features that have made hydrolases the most used enzymes are the hydrolases' lack of sensitive cofactors, and the large number of readily available enzymes possessing relaxed substrate specificities to choose from. Hydrolases can be divided in the sub-classes proteases, esterases, and lipases, and can catalyze reactions involving hydrolysis or formation of ester- and amide-bonds.

1.4.3 Lipases

Lipases are a group of enzymes that catalyzes the decomposition of triglycerides to di- and monoglycerides, glycerol, and fatty acids by hydrolysis. They are therefore important in the digestion of fats. Lipases are a subcategory of hydrolases, which follows the ping-pong bi-bi reaction mechanism. What makes lipases special, is that they work very well at organic-aqueous interfaces, and most of them express higher catalytic activity under such conditions than in aqueous solution with the dissolved substrate. This phenomenon is called interfacial activation.²⁴ In general, lipases have very broad substrate specificity, and therefore they are used in a wide range of applications, both in research and industry.²⁴ Other benefits with lipases are that they do not require cofactors, and their catalytic reactions results in almost no side products. In addition, the majority of practically used lipases are obtained by microbiological synthesis, which makes them very affordable.²⁵

The active site of lipases comprises serine, aspartic or glutamic acid residues, and histidine. Research has shown that lipases are more active against alcohol-containing substrates than acid-containing substrates.²⁵ In lipase-catalyzed kinetic resolution of alcohols, the enzyme is selective towards one of the enantiomers. This is illustrated in Scheme 1.2, where the transesterification takes place by addition of an acyl donor (Ac) in excess.²⁶



R₁, R₂, R₃ = alkyl, halogen, etc.

Scheme 1.2: Lipase-catalyzed kinetic resolution of a secondary alcohol.²⁶

To determine the stereochemical preference of lipase-catalyzed transesterifications of a secondary alcohols, Jing and Kazlauskas²⁷ developed predictive rules based on the relative size of the substituents. Analysis of lipases showed that the binding site for alcohols consists of one large hydrophobic pocket and one smaller, and that lipases differentiates between enantiomers based on the placing and size of two substituents (Figure 1.7). In this way, the stereochemical preference of lipases can be used to determine the absolute configuration of secondary alcohols. For reliable determination the substituents should have large difference in size, the lipase used in kinetic resolution should have high enantioselectivity, and the enantiomeric preference of the desired lipase is known for similar secondary alcohols with established configuration.²⁷

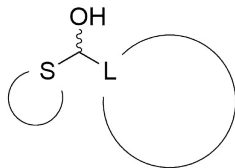
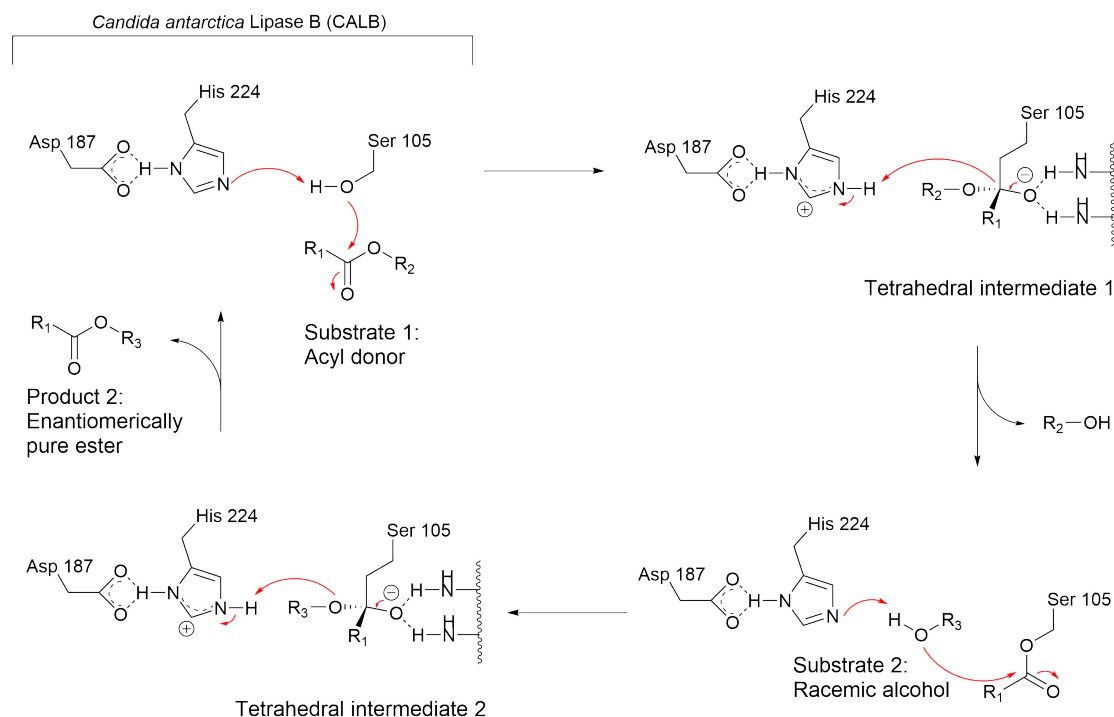


Figure 1.7: Model for lipase stereospecificity. S is the small group relative to L, which is the large group.²⁷

1.4.4 *Candida antarctica* Lipase B (CALB)

Lipase B from *Candida antarctica*, CALB, is an enzyme from the lipase group, isolated from the antarctic yeast *Candida antarctica*. CALB is widely used as a biocatalyst in biochemical and pharmaceutical reactions.²⁸ CALB has a catalytic triad consisting of Ser, His, and Asp/Glu, and the binding site for the substrate consists of an acyl binding pocket, and a binding pocket for the moiety of secondary alcohols.²⁹ The structure of CALB is open conformation, meaning there is no lid covering the entrance to the active site, however the lipase does not show any signs of interfacial activation. Because of the narrow entrance to the active site, and the lack of a lid covering the active site, it is believed that this may be the reason the substrate selectivity and stereospecificity is high in CALB.³⁰ By transesterification of alcohols, CALB follows the serine-hydrolase mechanism as shown in Scheme 1.3.^{31,32}



Scheme 1.3: General transesterification of alcohols with CALB following the serine-hydrolase mechanism.^{31,32}

CALB has shown to be selective towards secondary alcohols with one large and one small group connected to the stereocenter. Given that the large group has higher priority than the small according to IUPAC's nomenclature, the (*R*)-enantiomer will react faster, and the other way around.³³

1.4.5 Factors that effect the enzyme activity and selectivity

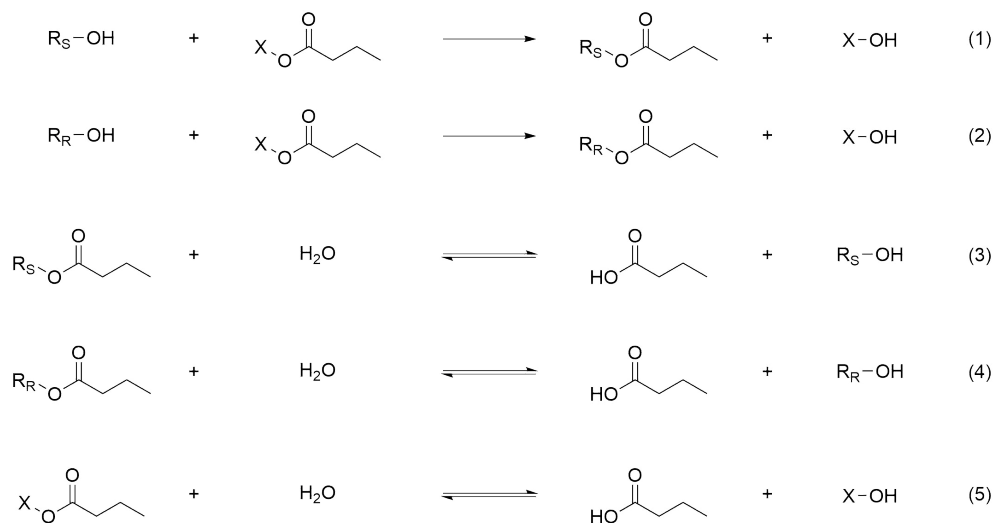
There are several factors that can effect the activity and selectivity of an enzyme like the solvent, pH, temperature, immobilization of the enzyme, and the acyl donor used for the enzyme reaction. In worst case, the enzyme can denaturate and therefore loose its catalytic activity.

Effect of solvent

Since enzymes have become more commonly used for catalysis, there have been several studies of how the enzymes work in both aqueous medium and organic medium. Generally, the activity of the enzyme is increased in aqueous medium and decreased in non-aqueous medium. It has also been shown that enzymes have less activity in polar medium and higher activity in non-polar medium.³⁴ On the other hand,

the enantiomeric ratio, E , becomes higher in solvents where the enzyme has lower activity.³⁵

The water content of the organic solvent in which an enzyme-catalyzed reaction takes place has shown through several studies to be of great importance. This is important for both enzyme stability and reactivity as well as enzyme specificity. A higher water content in the solvent decreases the reaction rate, but the enantioselectivity does not necessarily get worse. In polar solvents like acetonitrile, a high water content can stop the reaction at low conversions. The reason why is because the irreversible reactions shown in Scheme 1.4 can become reversible. In addition, unwanted side-reactions are more likely to occur.³⁶ These side-reactions hydrolyses both esters and acyl donors to form acids as shown by reaction (3)-(5) in Scheme 1.4.^{34,36}



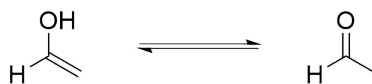
Scheme 1.4: Transesterification by lipase yielding reaction (1)-(5), where reaction (1) and (2) are irreversible and (3)-(5) are reversible.³⁶

Effect of acyl donor

The choice of acyl donor can also effect the enzyme activity. In transesterification reactions with enzymes it is necessary to add an acyl donor in order to react the undesired enantiomer of the alcohol to an ester. Transesterifications are often reversible reactions because the concentration of the substrate is low. However, transesterifications with vinyl esters as acyl donors are irreversible in anhydrous environment as shown in Scheme 1.4. The equilibria in Scheme 1.4 also show that hydrolysis reactions can be irreversible if there are large quantities of water that shifts the equilibria towards hydrolyzed product.

Another advantage using vinyl esters is tautomerization of the vinyl alcohol yielding acetaldehyde which evaporates at room temperature. The tautomerization reaction

is shown in Scheme 1.5.

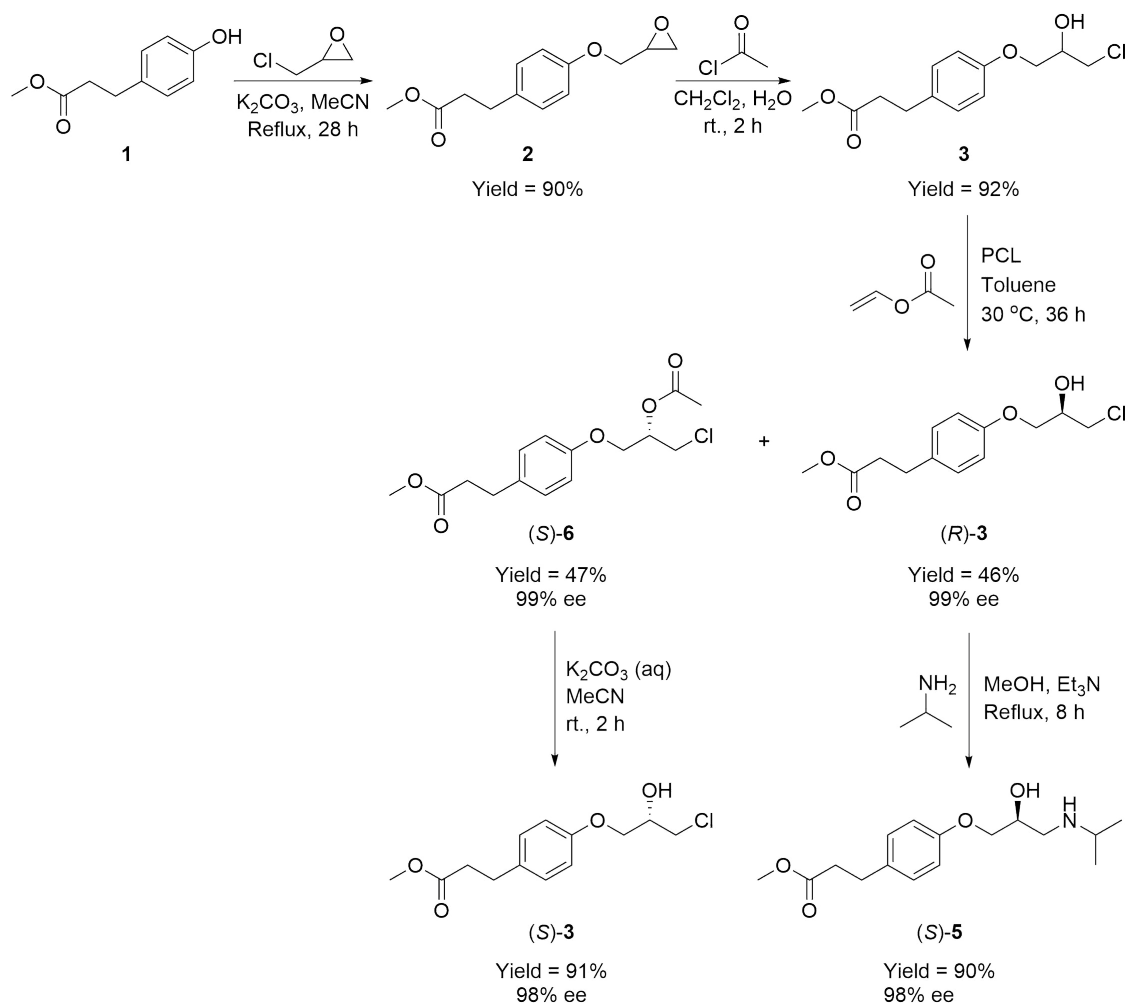


Scheme 1.5: Tautomerization of the vinylalcohol in a transesterification.

1.5 Synthetic pathways to enantiopure (*S*)-esmolol

There are several methods to achieve enantiopure compounds. As discussed, kinetic resolution is, among other possible methods, used in the synthesis of enantiopure (*S*)-esmolol. Banoth and Banerjee¹³ reported in 2017 a chemo-enzymatic synthesis of (*S*)-esmolol ((*S*)-**5**) which consisted of four synthesis steps. The total synthesis of (*S*)-esmolol ((*S*)-**5**) performed by Banoth and Banerjee¹³ is shown in Scheme 1.6.

The first synthesis step is a base-catalyzed S_N2-reaction between methyl 3-(4-hydroxyphenyl)propanoate (**1**) and epichlorohydrin, which gave methyl 3-(4-(oxiran-2-ylmethoxy)phenyl)propanoate (**2**) in 90% yield. In the second step, epoxide **2** was ring-opened with acetyl chloride giving methyl 3-(4-(3-chloro-2-hydroxypropoxy)phenyl)propanoate (**3**), the precursor for esmolol (**5**), in 92% yield. Further, chlorohydrin **3** was subjected to kinetic resolution with vinyl acetate as acyl donor and lipase from *Pseudomonas cepacia* (PCL) giving enantiopure (*R*)-**3** in 46% yield with 99% ee, and methyl (*S*)-3-(4-(2-acetoxy-3-chloropropoxy)phenyl)propanoate (**6**) in 47% yield with 99% ee. Lastly, (*S*)-esmolol ((*S*)-**5**) was synthesized by subjecting (*R*)-**3** to isopropylamine giving (*S*)-**5** in 90% yield with 98% ee.¹³

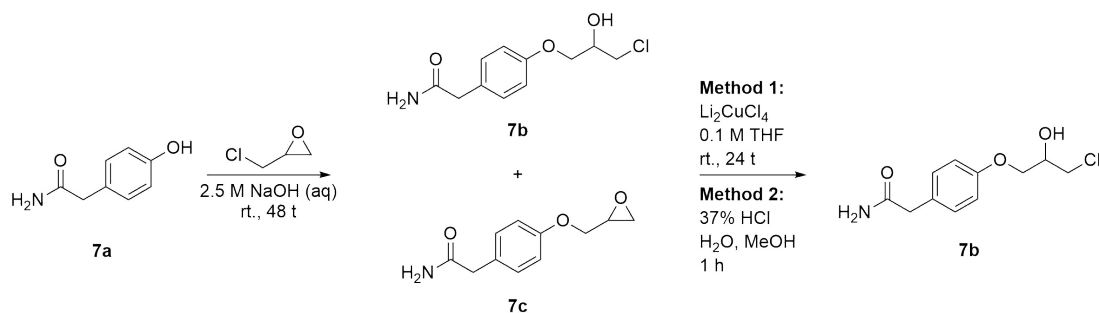


Scheme 1.6: A chemo-enzymatic pathway to enantiopure (*S*)-esmolol ((*S*)-**5**) as a four step synthesis, which gave the esmolol precursor methyl 3-(4-(3-chloro-2-hydroxypropoxy)phenyl)propanoate (**3**) in 92% yield and (*S*)-**5** in 90% yield with 98% ee.¹³

1.5.1 Previous studies in the synthesis of β -blocker precursors similar to the esmolol precursor

Extensive studies of the reactions forming the atenolol precursor 2-(4-(3-chloro-2-hydroxypropoxy)phenyl)acetamide (**7b**) have previously been performed in the Biocatalysis research group. Scheme 1.7 shows a synthetic pathway to the atenolol precursor **7b** by the use of sodium hydroxide to form chlorohydrin **7b** and 2-(4-(oxiran-2-ylmethoxy)-phenyl)acetamide (**7c**), and ring-opening of epoxide **7c** by the use of dilithium tetrachlorocuprate (Method 1) or hydrochloric acid (Method 2) as chloro donors.^{37,38}

The studies showed that the use of sodium hydroxide as base at room temperature in the first synthesis step formed a mixture of chlorohydrin **7b** and epoxide **7c**. Further, the studies of the synthesis of the atenolol precursor **7b** showed favored formation of chlorohydrin **7b** using catalytic amounts of base indicating that chlorohydrin **7b** is kinetically favored and epoxide **7c** thermodynamically favored.³⁹ Master candidate Mari Bergan Hansen³⁹ concluded that using 0.3 equivalents of sodium hydroxide and running the reaction for 7 hours was optimal to achieve full conversion of 2-(4-hydroxyphenyl)acetamide (**7a**) and avoid formation of by-products in the first synthetic step. Furthermore, studies showed that lithium chloride and acetic acid can be used in the ring-opening of similar epoxides like epoxide **2** to form chlorohydrin precursors.³⁹



Scheme 1.7: Formation of atenolol precursor 2-(4-(3-chloro-2-hydroxypropoxy)-phenyl)acetamide (**7b**) with sodium hydroxide forming chlorohydrin **7b** and 2-(4-(oxiran-2-ylmetoxy)-phenyl)acetamide (**7c**), and ring-opening of epoxide **7c** by dilithium tetrachlorocuprate or hydrochloric acid as chloro donors.^{37,38}

1.5.2 Formation of by-products in previous studies in the synthesis of (*S*)-esmolol precursors, and other similar β -blocker precursors

Previous studies in the Biocatalysis research group have shown formation of two by-products in the synthesis of (*S*)-esmolol ((*S*)-**5**). The first by-product is shown in Figure 1.8, and it's 3,3'-(((2-hydroxypropane-1,3-diyl)bis(oxy)))bis(4,1-phenylene))-dipropoanoate (**A**) with molecular mass 416.45 g/mol. This by-product has not been observed on LC-MS, but has been isolated and characterized by NMR spectroscopy.⁴⁰

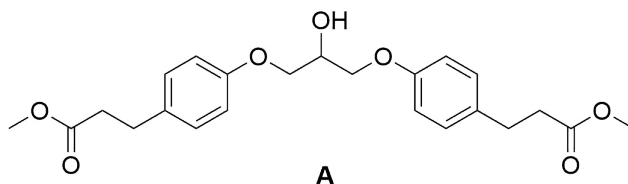


Figure 1.8: Structure of 3,3'-(((2-hydroxypropane-1,3-diyl)bis(oxy))bis(4,1-phenylene))dipropionate (**A**) with molecular mass 416.45 g/mol.⁴⁰

The second by-product that has been isolated and characterized by NMR spectroscopy in the Biocatalysis research group is 1,2-dichloro-2-propanol (**B**) with molecular mass 128.99 g/mol.⁴⁰ By-product **B** is shown in Figure 1.9.

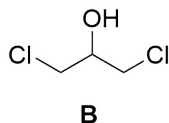


Figure 1.9: Structure of 1,2-dichloro-2-propanol (**B**) with molecular mass 128.99 g/mol.⁴⁰

The formation of a dimer has been observed in the synthesis of other similar β -blocker precursors as atenolol (**7**) and practolol (**8**), which formed dimer 2,2'-(((2-hydroxypropane-1,3-diyl)bis(oxy))bis(4,1-phenylene))diacetamide (**C**) and *N,N'*-(((2-hydroxypropane-1,3-diyl)bis(oxy))bis(4,1-phenylene))diacetamide (**D**) (Figure 1.10).^{39,41} In the synthesis of atenolol (**7**) studies showed that formation of dimer **C** is avoided by using catalytic amounts of base and reduced reaction times, thereby being thermodynamically favored.³⁹ Favored formation of dimer **D** in the synthesis of practolol (**8**) was observed in base-catalyzed reactions performed at 80°C.⁴¹

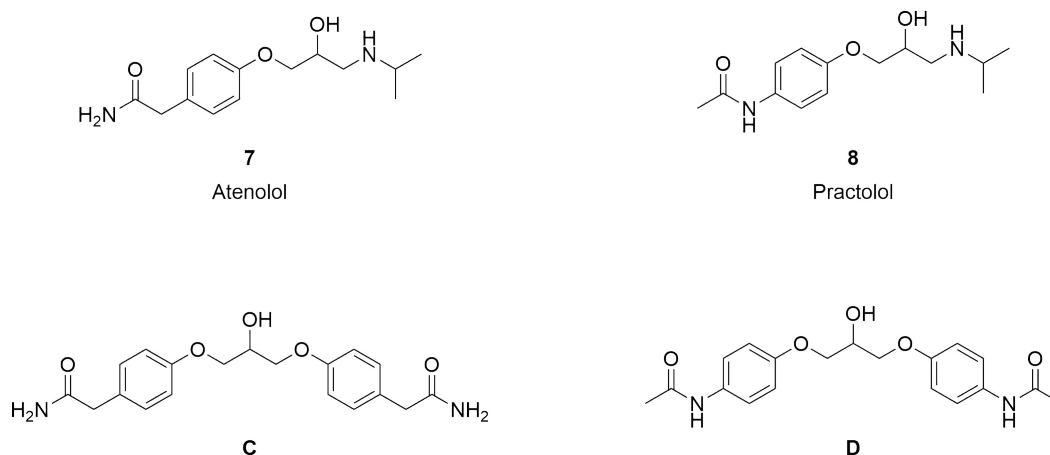
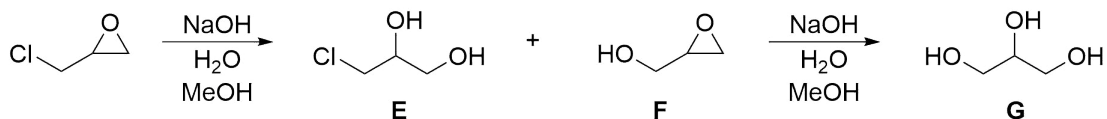


Figure 1.10: Structure of atenolol (**7**) and practolol (**8**), and their respective dimers 2,2'-(((2-hydroxypropane-1,3-diyl)bis(oxy))bis(4,1-phenylene))diacetamide (**C**) and *N,N'*-(((2-hydroxypropane-1,3-diyl)bis(oxy))bis(4,1-phenylene))diacetamide (**D**). The dimers **C** and **D** were discovered under different conditions in base-catalyzed reactions.^{39,41}

Other by-products that have been observed by LC-MS are 3-chloropropane-1,2-diol (**E**), oxiran-2-ylmethanol (**F**) and propane-1,2,3-triol (**G**). These by-products may be formed in side-reactions between epichlorohydrin and sodium hydroxide, and have been found in previous studies in the Biocatalysis research group in the synthesis of similar β -blocker precursors.¹



Scheme 1.8: Formation of 3-chloropropane-1,2-diol (**E**), oxiran-2-ylmethanol (**F**) and propane-1,2,3-triol (**G**) as side-reactions between epichlorohydrin and sodium hydroxide found by LC-MS in previous studies in the synthesis of similar β -blocker precursors in the Biocatalysis research group.¹

1.6 Analytical methods for chiral chemical compounds

1.6.1 Chiral chromatography

Chiral chromatography is used to determine the enantiomeric excess, ee, either by chiral high pressure liquid chromatography (HPLC) or chiral gas-liquid chromatography (GLC). The peaks in the chromatogram is compared in order to determine the enantiomeric excess. In this master's thesis, only chiral HPLC has been performed,

therefore chiral GLC will not be discussed further.

In chiral HPLC, the most common method is to use a chiral stationary phase such as amino acid derivatives, cyclodextrin derivatives, or polysaccharide derivatives. For enantiomers with low volatility, chiral HPLC is the most used method. An advantage of using chiral HPLC is that there are a large number of chiral stationary phases commercially available.⁴² Another advantage, is that there are both normal phase, and reverse phase columns, meaning enantiomers with both poor and good solubility in water can be separated by chiral HPLC.⁴³

To calculate the enantiomeric excess from chromatograms, baseline separation needs to be achieved for reliable results. The resolution factor, R_S , is a parameter that denotes how good the baseline separation is, and for chiral columns it's calculated from Equation (1.7).⁴⁴

$$R_S = 1.177 \times \frac{t_R(2) - t_R(1)}{t_{w0.5}(1) + t_{w0.5}(2)} \quad (1.7)$$

$t_R(1)$ and $t_R(2)$ are the retention times of the enantiomers, and $t_{w0.5}(1)$ and $t_{w0.5}(2)$ are the peak widths at half heights.⁴⁴ R_S -values equal to 1.5 denotes baseline separation, and higher R_S -values denotes even better separation.⁴⁵

In a Chiralcel OD-H column, the stationary phase is composed of cellulose coated on silica gel, which forms a hydrogen-bonding- π -complex phase. This type of stationary phase bases its enantioselectivity on the formation of diastereomeric complexes from the enantiomers through interactions between the chiral stationary phase, where at least one of the interactions are stereochemical dependent.⁴² Figure 1.11 is a geometrical representation where it appears that a minimum of three simultaneous interactions is required for recognition of the chirality of molecules by a second chiral compound.⁴² Enantiomer I interacts with the chiral stationary phase through three interactions while enantiomer II only interacts through two interactions. Therefore, enantiomer I forms a more stable complex than enantiomer II, which results in enantiomer I being more retained. Thereby, the enantiomers are separated. The strength between the interactions defines the difference in retention, and therefore determines the degree of separation between the enantiomers.

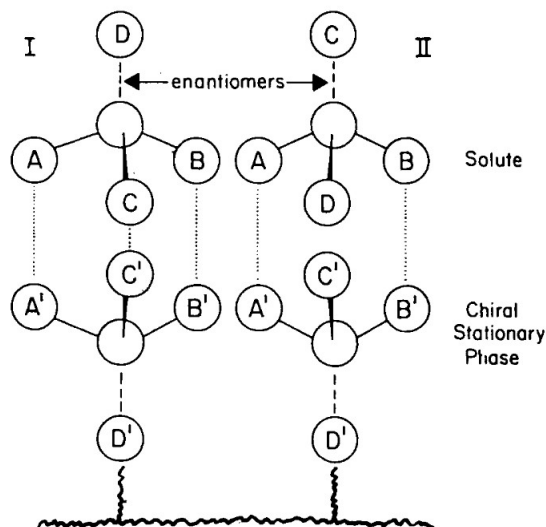


Figure 1.11: Three-point chiral interaction model for separation of enantiomers by a chiral stationary phase.⁴²

1.6.2 Polarimetry

In Section 1.2 it was briefly mentioned that enantiomers have different optical rotation. This means that they possess the property of rotating the plane of polarized light as it passes through them, thereby being optically active. One way to determine the enantiomeric excess of a chemical compound is to measure the optical rotation, α , of resolved enantiomers using a polarimeter.

The measurement of optical rotation requires specific parameters to be known. These are the concentration, solvent, wavelength of the light, and the temperature at which the measurement was taken. The optical rotation measured can then be used to calculate the specific rotation by Equation (1.8).⁴⁶

$$[\alpha]_{\lambda}^t = \frac{100 \cdot \alpha'}{l \cdot c} \quad (1.8)$$

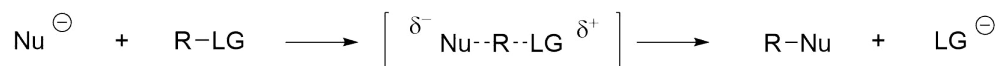
Here α' is the observed rotation, l is the cell's length in decimeters, c is the concentration in grams per 100 mL solvent, t is the temperature in celcius, and λ is the wavelength of the incident beam of the light in nanometer.⁴⁶

1.7 Organic synthesis theory

1.7.1 Nucleophilic substitution reactions, S_N2 and S_N1

Nucleophilic substitution reactions are among the most fundamental types of organic reactions where a nucleophile replaces a leaving group in the molecule that undergoes substitution.²

Substitution reactions are divided into bimolecular S_N2 and unimolecular S_N1. Bimolecular substitution reactions are concerted reactions, which means they proceed simultaneously in a single step through a single transition state, where both the leaving group and the nucleophile are partly bonded to the substrate carbon atom. This is illustrated in Scheme 1.9. Furthermore, the nucleophile attacks from behind, inverting the stereochemistry.²



Scheme 1.9: General S_N2-reaction where Nu corresponds to the nucleophile and LG to the leaving group.²

In S_N2-reactions, the reaction rate depends on the concentration of both the nucleophile and the electrophile, hence the name bimolecular substitution. Further, the reaction rate may depend on the solvent. A polar protic solvent can stabilize the charges formed during a reaction, thus hindering the nucleophile's approach to the carbon atom. This might slow down the reaction rate. On the contrary, a polar aprotic solvent is unable to stabilize negative charges, and the nucleophile would therefore favor attack on the electrophile. The trend in the reaction rate for halogens as leaving groups is the same in S_N2- and S_N1-reactions; R-I > R-Br > R-Cl > R-F.²

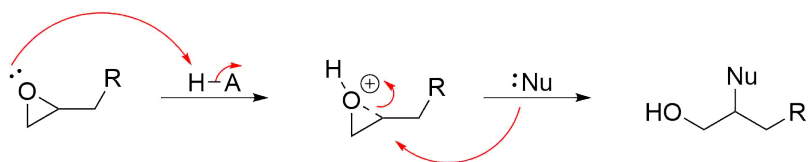
Unimolecular substitution reactions proceed in two steps; firstly an initial slow step where a carbocation is formed by heterolytical cleavage of the leaving group, and secondly a fast step where the nucleophile attacks the carbocation.

One typical reaction that proceeds through an S_N2-reaction is called a Williamson ether synthesis. This is a reaction which forms an ether from an organohalide and a deprotonated alcohol (alkoxide). The organohalide is typically an alkyl halide, and the best results of the reaction are obtained if the alkyl halide is primary.²

1.7.2 Ring-opening of epoxides

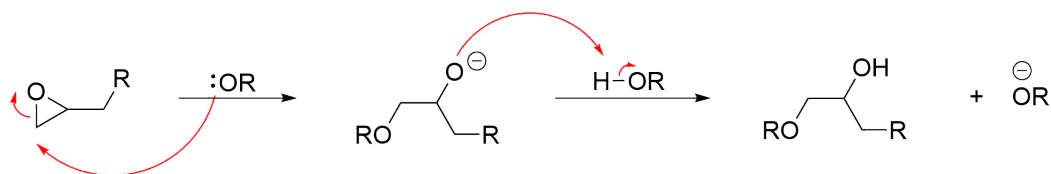
Epoxides are highly strained three-membered rings which makes them much more reactive toward nucleophilic substitution than other ethers. Ring-opening of epoxides can be both acid- and base-catalyzed.²

Acid-catalyzed ring-opening of epoxides follows an S_N1 -like mechanism where the nucleophilic attack is likely to happen at the most sterically hindered carbon atom, as shown in Scheme 1.10. The reason why the nucleophile attacks the highly substituted carbon atom is because bonding in the protonated epoxide is unsymmetrical, with the most substituted carbon atom bearing a considerable positive charge. This carbon atom resembles a tertiary carbocation which is more stable than the other carbon atom in the ring.²



Scheme 1.10: Acid-catalyzed ring-opening of unsymmetrical epoxide. Nucleophilic attack at the most sterically hindered carbon atom.²

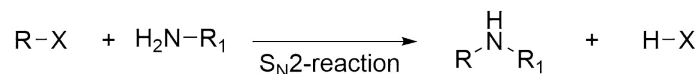
Base-catalyzed ring-opening of unsymmetrical epoxides occurs primarily by attack of the nucleophile at the less substituted carbon atom, and with strong nucleophiles, the opening is a direct S_N2 -reaction. This is illustrated in Scheme 1.11.²



Scheme 1.11: Base-catalyzed ring-opening of unsymmetrical epoxide. Nucleophilic attack at the least sterically hindered carbon atom.²

1.7.3 Amine alkylation (amino-de-halogenation)

A reaction between an alkyl halide and ammonia or an amine is called an amine alkylation reaction or an amino-de-halogenation reaction. Amine alkylation is a type of nucleophilic aliphatic substitution which gives a higher substituted amine. The reaction between alkyl halides and primary amines is not usually a feasible method for preparation of secondary amines, since they are stronger bases than ammonia and preferentially attack the substrate. In order to use this method for preparation of secondary amines, a large excess of primary amine is necessary. Amine alkylation is a type of a S_N2 -reaction, and a general illustration of the reaction is shown in Scheme 1.12.⁴⁷

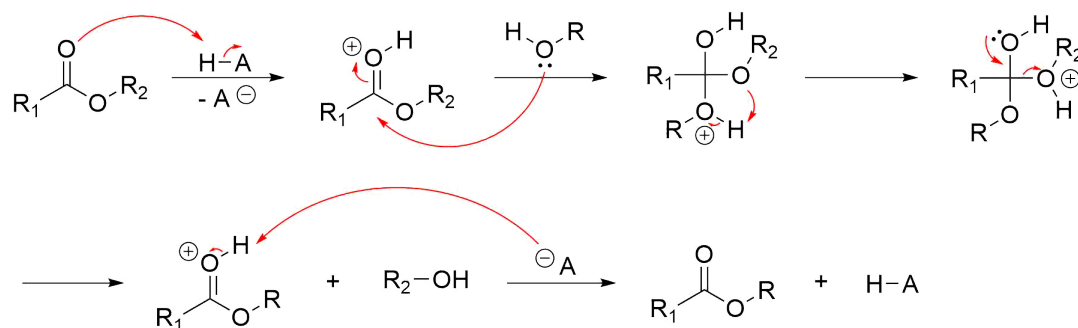


Scheme 1.12: General amine alkylation reaction, a type of $\text{S}_{\text{N}}2$ -reaction, between an alkyl halide and a primary amine forming a secondary amine.⁴⁷

1.7.4 Transesterification

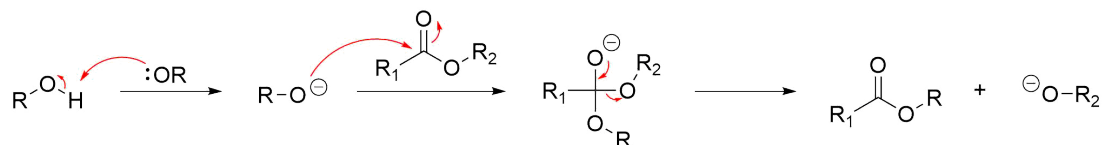
Transesterification is a conversion of an ester into a different ester. A transesterification reaction occurs when an ester is placed in a large excess of an alcohol with presence of either an acid or a base. This leads to the possibility of exchange of alkoxy groups. The large excess of alcohol is used to drive the reaction, and the most common method of transesterification is the reaction between an ester and a alcohol in the presence of an acid catalyst.⁴⁸

Acid-catalyzed transesterification starts with a protonation of the carbonyl by the acid. The carbonyl is activated towards a nucleophilic attack by the alcohol, as illustrated in Scheme 1.13. Further, there is a proton shift, and removal of the leaving group forming a new alcohol. The new ester is then deprotonated.⁴⁸



Scheme 1.13: Acid-catalyzed transesterification by reaction between an ester and an alcohol. Nucleophilic attack at the carbonyl carbon.⁴⁸

Base-catalyzed transesterification starts with a nucleophilic attack by the deprotonated alcohol at the carbonyl carbon. Then the leaving group is removed forming the new ester. The reaction mechanism is illustrated in Scheme 1.14.⁴⁸



Scheme 1.14: Base-catalyzed transesterification by reaction between an ester and an alcohol. Nucleophilic attack at the carbonyl carbon.⁴⁸

1.7.5 Reaction kinetics

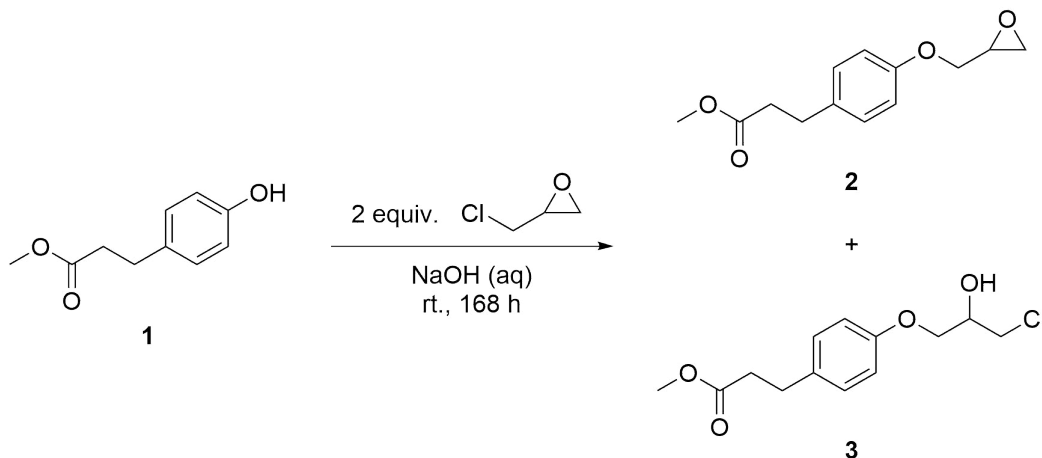
The effect of kinetic and thermodynamic control can be seen in a chemical reaction when a reaction has two competing pathways to form a product mixture. The different pathways are influenced by the reaction conditions which affects the selectivity of the reaction.⁴⁹ Under kinetic control the ratio of the products formed is determined by the relative energies of the transition states leading to the products, while under thermodynamic control the ratio of the products formed is determined only by the relative energies of the products.⁴⁹ In other words, the kinetically favored product is the product formed fastest, while the thermodynamically favored product is the most stable product.⁵⁰

2 Results and Discussion

The main aim of this thesis was to synthesize (*S*)-esmolol in an environmentally friendly and efficient fashion by the use of biocatalysis, specifically kinetic resolution. This section describes the syntheses of the racemic compounds methyl 3-(4-(oxiran-2-ylmethoxy)phenyl)propanoate (**2**) and methyl 3-(4-(3-chloro-2-hydroxypropoxy)phenyl)propanoate (**3**), and the enantiomerically pure compounds (*S*)-**3**, (*S*)-1-chloro-3-(4-(3-methoxy-3-oxopropyl)phenoxy)propan-2-yl butanoate ((*S*)-**4**), and (*S*)-esmolol ((*S*)-**5**).

2.1 Synthesis of a mixture of methyl 3-(4-(oxiran-2-ylmethoxy)phenyl)propanoate (**2**) and methyl 3-(4-(3-chloro-2-hydroxypropoxy)phenyl)propanoate (**3**) with sodium hydroxide

The synthesis of a mixture of epoxide (**2**) and chlorohydrin (**3**) was carried out with basis in master candidate Mari Bergan Hansen's³⁹ description and Lund *et al.*'s³⁷ publication. Epoxide **2** and chlorohydrin **3** was synthesized from deprotonated methyl 3-(4-hydroxyphenyl)propanoate (**1**) and epichlorohydrin. Sodium hydroxide was chosen as base, as this base has been successfully used in similar reactions in the synthesis of other β -blocker precursors.¹ The synthesis performed is a base-catalyzed S_N2 -reaction, and it's shown in Scheme 2.1.



Scheme 2.1: Base-catalyzed synthesis of methyl 3-(4-(oxiran-2-ylmethoxy)phenyl)propanoate (**2**) and methyl 3-(4-(3-chloro-2-hydroxypropoxy)phenyl)propanoate (**3**) from methyl 3-(4-hydroxyphenyl)propanoate (**1**) and epichlorohydrin with sodium hydroxide as base.

To monitor the reaction several different eluent systems for TLC-analysis were tested. These are shown in Table 2.1. The eluent system of dichloromethane and methanol (20:1) gave best separation of phenol **1**, epoxide **2** and chlorohydrin **3**. The R_f -values were determined to be R_f (**1**) = 0.52, R_f (**2**) = 0.77, R_f (**3**) = 0.61.

Table 2.1: Test of different eluent systems for separation of **1**, **2**, and **3** by TLC.

Eluent	Mixing ratio
Dichloromethane:acetonitrile	11:1
Dichloromethane:methanol	20:1
<i>n</i> -Hexane:ethyl acetate	9:1
<i>n</i> -Pentane:acetone	3:1
<i>n</i> -Pentane:ethyl acetate	7:3

As discussed in Section 1.5, this synthesis has been successfully performed with 0.3 equivalents of sodium hydroxide and 2 equivalents epichlorohydrin to form the atenolol precursor. Since the amide group in the starting material for atenolol and the ester group in starting material **1** for esmolol are electronically quite similar, it was believed that the synthesis shown in Scheme 2.1 would proceed in approximately the same fashion as for the atenolol precursor (Scheme 1.7). After running the reaction shown in Scheme 2.1 for 24 hours using 0.3 equivalents sodium hydroxide, the TLC indicated that the reaction did not proceed at the same reaction rate as for the atenolol starting material. Therefore, it was added 1 more equivalent of base. After another 24 hours, in total 48 h, the TLC indicated that both epoxide **2** and chlorohydrin **3** was formed. In addition, one by-product was observed on TLC. The TLC-analysis also showed that it was not achieved full conversion of starting material **1**. The reaction was therefore run for another 120 hours, in total 168 hours. At this point the TLC still indicated a small amount of starting material, but the reaction was stopped and worked up.

The total conversion of the starting material was analyzed by achiral HPLC performed on a ACE Excel 5 C18 column. Different eluent systems were tested in order to achieve baseline separation of phenol **1**, epoxide **2**, chlorohydrin **3**, and possible by-products. Eluent systems tested, both gradient and isocratic are given in Table 2.2. An isocratic mobile phase composition of water and acetonitrile (50:50) gave best separation of phenol **1**, epoxide **2**, chlorohydrin **3**, and by-products. The HPLC chromatogram shown in Figure 2.1 gave t_R (**1**) = 2.8 min, t_R (**2**) = 4.8 min, t_R (**3**) = 4.4 min. The HPLC chromatogram also show what is believed to be by-product 2,3-dihydroxypropyl 3-(4-(oxiran-2-ylmethoxy)phenyl)propanoate (**H**) with t_R = 3.5 min and 3-chloro-2-hydroxypropyl 3-(4-(oxiran-2-ylmethoxy)phenyl)propanoate (**J**) with t_R = 3.8 min. By-product **H** and **J** will be discussed later in Section 2.1.2.

Table 2.2: HPLC methods attempted to achieve baseline separation between phenol **1**, epoxide **2**, chlorohydrin **3**, and by-products. Mobile phase composed of water and acetonitrile with different compositions, both isocratic and gradient. All methods were run with a mobile phase flow of 1 mL/min, and 4 μ L sample injection.

Entry	H ₂ O	MeCN	H ₂ O	MeCN	Analysis time [min]
	[%] _{start}	[%] _{start}	[%] _{stop}	[%] _{stop}	
1	75	25	-	-	30
2	80	20	-	-	30
3	90	10	0	100	25
4	65	35	0	100	25
5	60	40	40	60	20
6	50	50	-	-	12

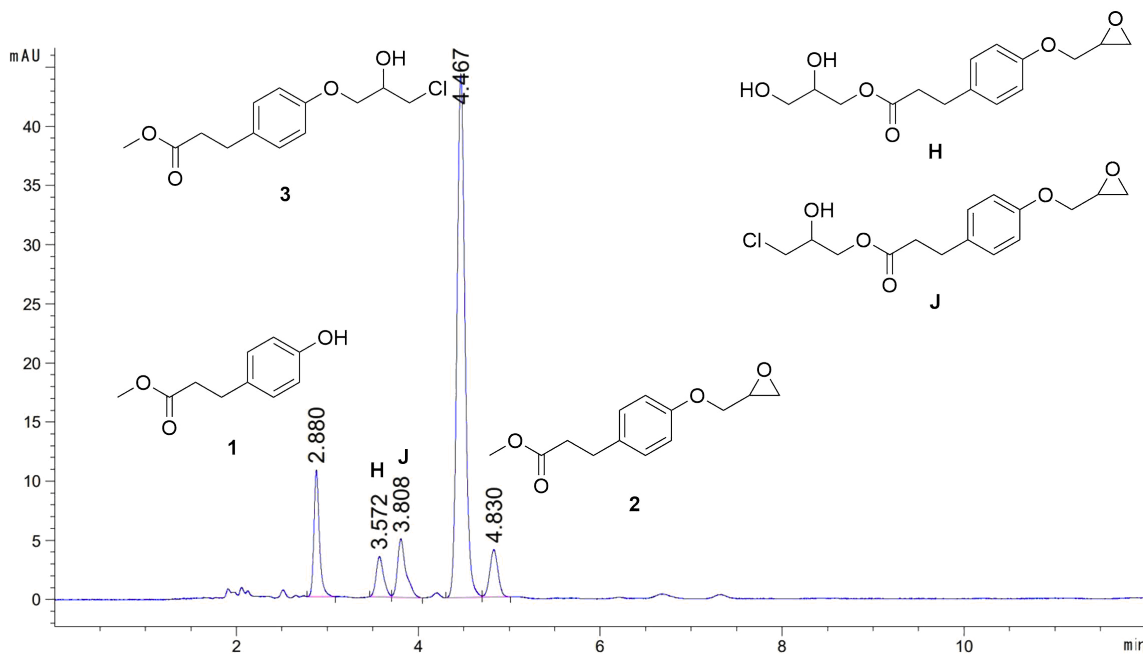
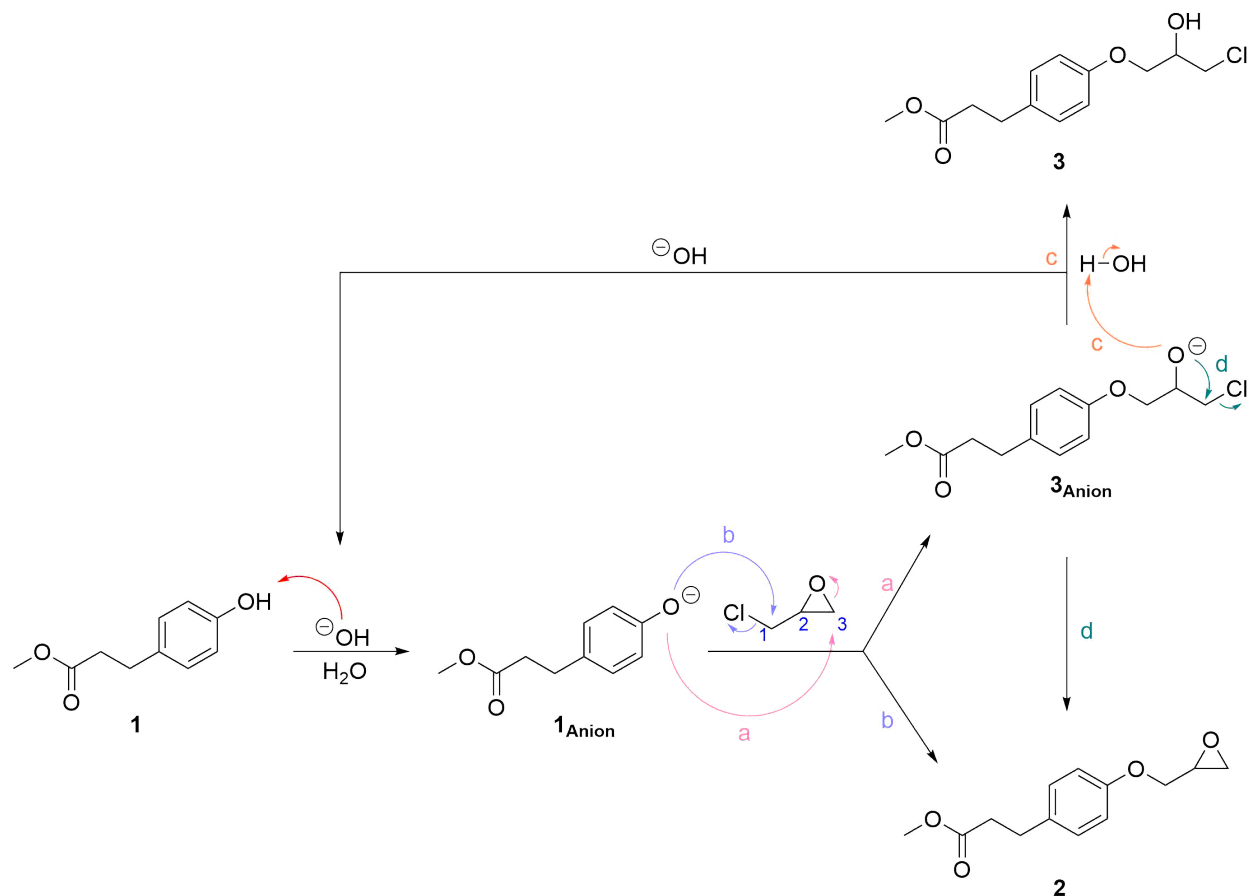


Figure 2.1: Achiral HPLC analysis of the reaction mixture of phenol **1** ($t_R = 2.8$ min), epoxide **2** ($t_R = 4.8$ min), chlorohydrin **3** ($t_R = 4.4$ min), and by-products (t_R (**H**) = 3.5 min and t_R (**J**) = 3.8 min) performed on a ACE Excel 5 C18 column with an isocratic mobile phase composition of water and acetonitrile (50:50) over 12 min, flow 1 mL/min.

To purify the product by flash chromatography it was chosen a different eluent as the R_f -values of epoxide **2** and chlorohydrin **3** with dichloromethane and methanol (20:1) were above 0.6, which is the upper limit of what the R_f -values should be.⁴⁵ Epoxide **2** and chlorohydrin **3** would therefore elute too fast. In addition, the separation of epoxide **2** and chlorohydrin **3** was poor ($\Delta R_f = 0.16$). An eluent of dichloromethane and acetonitrile (11:1) was chosen as the R_f -values were lowered, which would give better separation on the column. Chlorohydrin **3** was obtained in 49% yield with 86% purity, while epoxide **2** was obtained in 2% yield with 96% purity. The purities were determined by ¹H-NMR analysis.

2.1.1 Mechanistic studies of reaction between deprotonated phenol **1** and epichlorohydrin

The first step of the mechanism of the S_N2 -reaction is a deprotonation of phenol **1** under basic conditions forming alkoxide **1_{Anion}**, as shown in Scheme 2.2. Following is a nucleophilic attack in two positions of epichlorohydrin shown as reaction mechanism a and b. An attack at carbon 3 in epichlorohydrin, following reaction mechanism a, is a ring-opening of epichlorohydrin forming alkoxide **3_{Anion}**. An attack at carbon 1, following reaction mechanism b, is a Williamson ether synthesis with chloride as leaving group forming epoxide **2**. In theory, an attack at carbon 2 in epichlorohydrin is possible, but a nucleophilic attack at the most sterically hindered carbon is not likely to happen. If the reaction follows reaction mechanism a, and there are available protons, alkoxide **3_{Anion}** can be protonated and form chlorohydrin **3** following reaction mechanism c. In the absence of available protons the nucleophile can attack at the carbon α to the chlorine, which acts as a leaving group in an intramolecular cyclization forming epoxide **2** through reaction mechanism d.¹

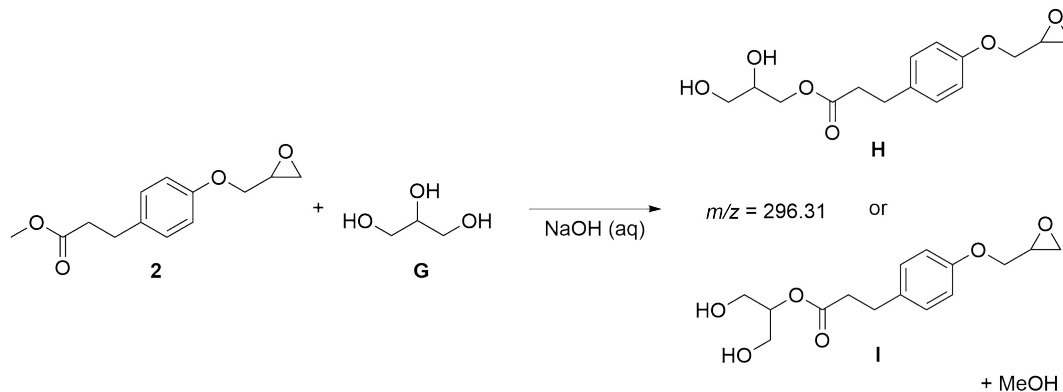


Scheme 2.2: Reaction mechanism for base-catalyzed S_N2 -reaction between deprotonated phenol **1_{Anion}** forming deprotonated chlorohydrin **3_{Anion}** and epoxide **2** by different points of attack at epichlorohydrin (reaction mechanism a and b respectively). Reaction mechanism c shows protonation of alkoxide **3_{Anion}** forming chlorohydrin **3** and regenerating the base, while reaction mechanism d shows an intramolecular S_N2 -reaction of alkoxide **3_{Anion}** forming epoxide **2**.¹

2.1.2 Formation of by-products

As mentioned, the reaction performed in Scheme 2.1 formed two by-products; 2,3-dihydroxypropyl 3-(4-(oxiran-2-ylmethoxy)phenyl)propanoate (**H**) and 3-chloro-2-hydroxypropyl 3-(4-(oxiran-2-ylmethoxy)phenyl)propanoate (**J**). They were observed on HPLC (Figure 2.1) with t_R (**H**) = 3.5 min and t_R (**J**) = 3.8 min. By-product **H** and **J** were believed to be formed due to long reaction time of the reaction shown in Scheme 2.1. The sample analyzed in Figure 2.1 was also analyzed by LC-MS on a ACQUITY UPLC BEH C18 column. Because the LC-MS method was different from the HPLC method, different retention times were obtained. The LC-MS results are given in Appendix G.1.

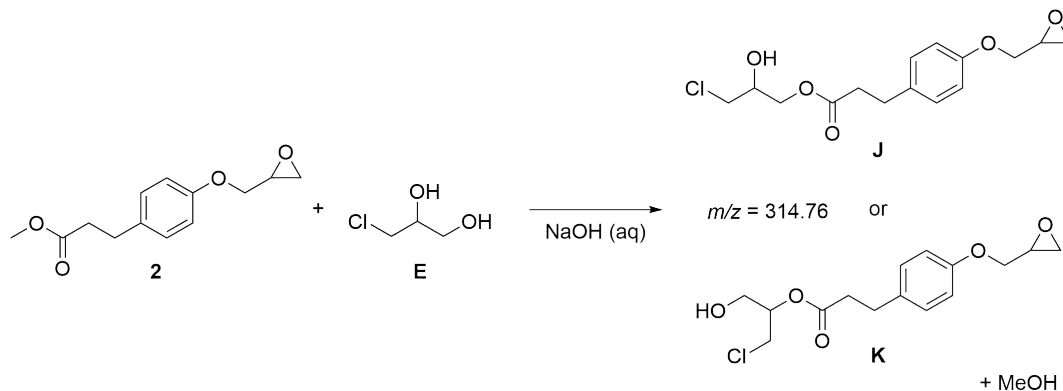
One of the peaks in the LC-MS chromatogram show $m/z = 319.1$ with molecular formula $C_{15}H_{20}O_6Na$ and IHD = 6 (Appendix G.2). It was believed that this was by-product **H** or 1,3-dihydroxypropan-2-yl 3-(4-(oxiran-2-ylmethoxy)phenyl)propanoate (**I**). Both by-product **H** and **I** can be formed in a reaction between epoxide **2** and by-product propane-1,2,3-triol (**G**)¹ (discussed in Section 1.5) as shown in Scheme 2.3.



Scheme 2.3: Side-reaction between epoxide **2** and propane-1,2,3-triol (**G**) forming by-product 2,3-dihydroxypropyl 3-(4-(oxiran-2-ylmethoxy)phenyl)propanoate (**H**) or 1,3-dihydroxypropan-2-yl 3-(4-(oxiran-2-ylmethoxy)phenyl)propanoate (**I**), both with $m/z = 296.31$.

This is a base-catalyzed transesterification where it is believed that MeOH is formed. None of these suggested by-products have been isolated by flash chromatography, and therefore it was not confirmed by NMR analysis if by-product **H** or **I** was formed.

One of the other peaks in the LC-MS chromatogram show $m/z = 337.1$ with molecular formula $C_{15}H_{19}O_5NaCl$ and IHD = 6 (Appendix G.3). This by-product was believed to be formed in a similar reaction as by-product **H** or **I**, but from 3-chloropropane-1,2-diol (**E**)¹ (discussed in Section 1.5). The reaction forming the proposed by-products **J** or 1-chloro-3-hydroxypropan-2-yl 3-(4-(oxiran-2-ylmethoxy)phenyl)propanoate (**K**) is given in Scheme 2.4.



Scheme 2.4: Side-reaction between epoxide **2** and 3-chloropropane-1,2-diol (**E**) forming by-product 3-chloro-2-hydroxypropyl 3-(4-(oxiran-2-ylmethoxy)phenyl)propanoate (**J**) or 1-chloro-3-hydroxypropan-2-yl 3-(4-(oxiran-2-ylmethoxy)phenyl)propanoate (**K**), both with $m/z = 314.76$ g/mol.

Upon purification of epoxide **2** by flash chromatography with dichloromethane and acetonitrile (11:1), the by-product with $t_R = 3.8$ min (Figure 2.1) was isolated with a small amount of chlorohydrin **3**. This was confirmed by achiral HPLC using the same method as before giving t_R (**J**) = 3.8 min and t_R (**3**) = 4.5 min, see Figure 2.2.

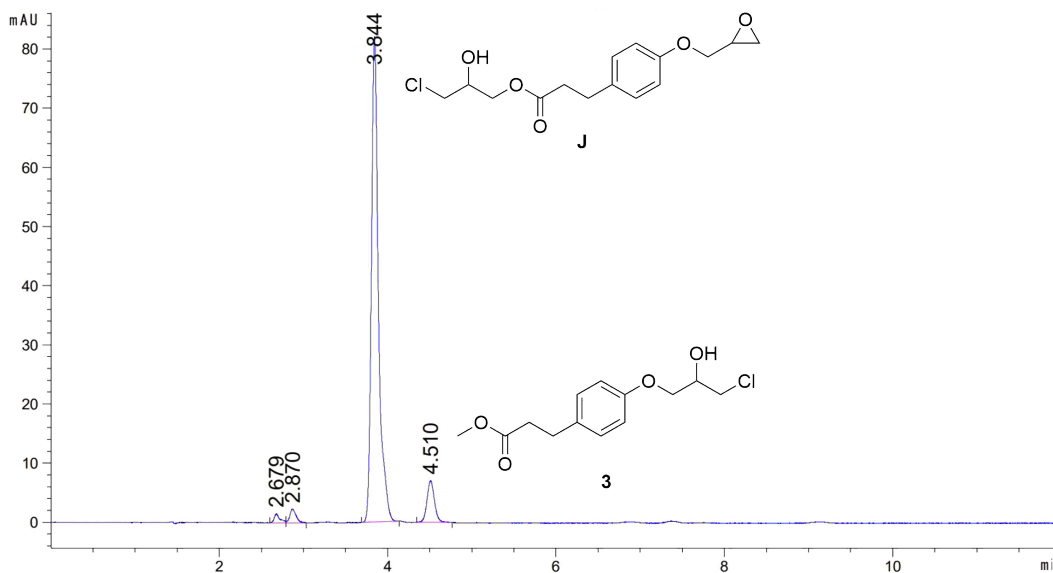


Figure 2.2: Achiral HPLC of isolated by-product **J** ($t_R = 3.8$ min) with a small amount of chlorohydrin **3** ($t_R = 4.5$ min) performed on a ACE Excel 5 C18 column with an isocratic mobile phase composition of water and acetonitrile (50:50) over 12 min, flow 1 mL/min.

By-product **J** was analyzed by NMR spectroscopy, but as it was some chlorohydrin **3** in the isolated by-product **J**, H,H-COSY and HMBC were inconclusive (Appendix F.3 and F.5). From ^1H -, ^{13}C -, and HSQC-NMR analysis (Appendix F.1, F.2, and F.4) by-product **J** was confirmed by comparison with by-product **J** and **K**'s predicted spectra in ChemDraw Professional. The predicted spectra of by-product **J** and **K** showed that the chiral carbon in by-product **J** has chemical shift at 68.7 ppm and that the chiral carbon in by-product **K** has chemical shift at 81.3 ppm. Since there were no chemical shift around 81 ppm in the ^{13}C -NMR spectrum of by-product **J**, but one with chemical shift 69.6 ppm it was concluded that this reaction (Scheme 2.4) formed by-product **J** and not by-product **K**. By-product **J** with numbered carbons is given in Figure 2.3, and the corresponding shifts determined by ^1H -, ^{13}C -, and HSQC-NMR spectroscopy are given in Table 2.3.

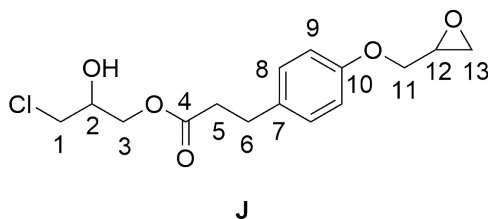


Figure 2.3: By-product **J** with labeled carbon atoms. Assignment of chemical shifts are given in Table 2.3, and all spectra are given in Appendix F.

Table 2.3: Partly characterization of by-product **J** given ^1H -, ^{13}C -, and HSQC-NMR (600 MHz, CDCl_3), see Appendix F.

Position	^1H -NMR [ppm] (mult., int., ^3J)	^{13}C -NMR [ppm]
1	3.55-3.47 (m, 2H)	45.9
2	4.01-3.98 (m, 1H)	69.6
3	4.19-4.18 (m, 2H)	65.2
4	-	172.9
5	2.67-2.64 (t, 2H, 7.76 Hz)	35.9
6	2.92-2.89 (m, 2H)	30.1
7	-	132.8
8	7.14-7.10 (m, 2H)	129.3
9	6.86-6.83 (m, 2H)	114.8
10	-	157.2
11	3.95-3.92 (m, 1H)	68.8
	4.21-4.20 (m, 1H)	
12	3.35-3.33 (m, 1H)	50.2
	2.75-2.74 (m, 1H)	
13	2.92-2.89 (m, 1H)	44.7
OH	2.44-2.43 (m, 1H)	-

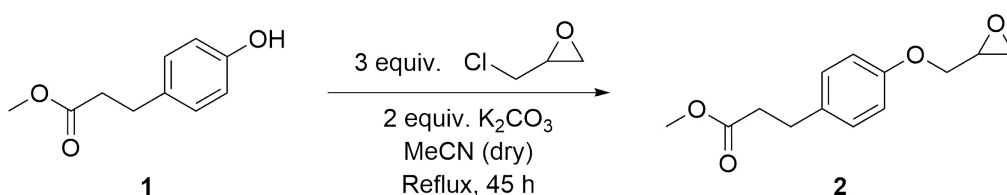
Because of conformation of formation of by-product **J** from the reaction shown in Scheme 2.1 it was also believed that by-product **H** was formed instead of by-product **I**. The reason for this is that the reaction shown in Scheme 2.3 and 2.4 are quite similar. Since oxygen has higher electronegativity than chlorine it is believed that by-product **H** ($t_{\text{R}} = 3.5$ min) eluted before by-product **J** ($t_{\text{R}} = 3.8$ min).

One important point to make is that neither by-product **G**, **E**, or methanol has been observed by NMR analysis. Therefore, there should be performed more studies of the reaction shown in Scheme 2.1. Since this reaction has a low reaction rate, forms several by-products, and the yields and purities obtained for epoxide **2** (yield = 2%, purity = 96%) and chlorohydrin **3** (49%, purity = 86%) were low, no further studies were performed in this project.

2.2 Synthesis of methyl 3-(4-(oxiran-2-ylmethoxy)phenyl)propanoate (**2**)

Since the reaction between deprotonated phenol **1** and epichlorohydrin with sodium hydroxide as base wasn't successful, the reaction was run with potassium carbonate as base instead. The synthesis of epoxide **2** was performed with basis in the publication of Banoth and Banerjee.¹³ The reaction was performed in approximately 14

times smaller scale, but the solvent was only scaled down 4 times as a larger volume of solvent hopefully would give better distribution of potassium carbonate in the reaction mixture. Two equivalents of epichlorohydrin was used instead of one and a half equivalents reported by Banoth and Banerjee¹³ because two equivalents of epichlorohydrin had been successfully performed for similar reactions. Additionally, the equivalents of potassium carbonate was increased by one as the reaction rate turned out to be slower than the one reported by Banoth and Banerjee.¹³ From deprotonated phenol **1**, epichlorohydrin, and potassium carbonate, epoxide **2** was synthesized as in Scheme 2.5.



Scheme 2.5: Base-catalyzed synthesis of epoxide **2** from deprotonated phenol **1** and epichlorohydrin with potassium carbonate as base.

The reaction was monitored by TLC (dichloromethane:acetonitrile) (11:1), which gave best separation of phenol **1** ($R_f = 0.28$) and epoxide **2** ($R_f = 0.50$). TLC-analysis also indicated formation of a by-product ($R_f = 0.13$), which was not reported by Banoth and Banerjee.¹³

The total conversion of the starting material was analyzed by achiral HPLC performed using the same method as discussed in Section 2.1. This gave t_R (**1**) = 2.8 min, t_R (**2**) = 4.8 min, and t_R (**A**) = 9.1 min, see Figure 2.4. The chromatogram also show by-product 3,3'-(((2-hydroxypropane-1,3-diyl)bis(oxy))bis(4,1-phenylene))dipropanoate (**A**), which will be discussed later in Section 2.4.

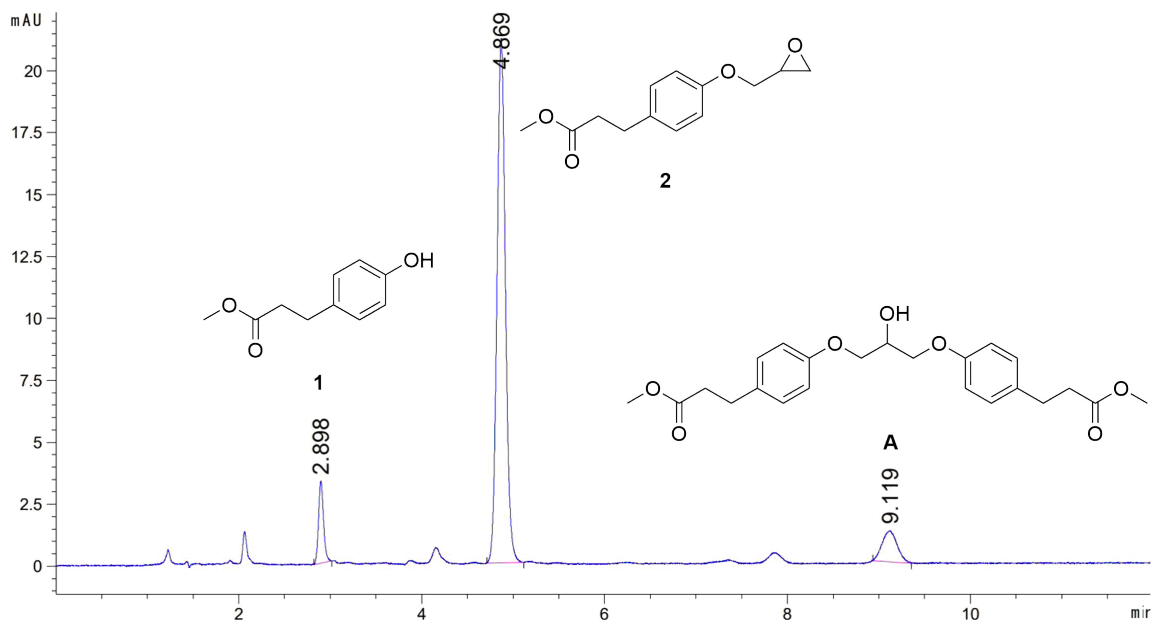


Figure 2.4: Achiral HPLC of phenol **1** ($t_R = 2.8$ min), epoxide **2** ($t_R = 4.8$ min), and by-product **A** ($t_R = 9.1$ min) performed on a ACE Excel 5 C18 column with an isocratic mobile phase composition of water and acetonitrile (50:50) over 12 min, flow 1 mL/min.

To purify the product by flash chromatography the eluent of dichloromethane and acetonitrile (11:1) was used as it in this reaction gave good separation of phenol **1** and epoxide **2** ($\Delta R_f = 0.22$), and R_f -values were also below 0.6. The purified product was analyzed by achiral HPLC giving t_R (**2**) = 4.8 min, see Figure 2.5. The chromatogram show a new by-product, dimethyl 3,3'-(((2-(2-chloro-1-hydroxyethoxy)propane-1,3-diyl)bis(oxy))bis(4,1-phenylene))dipropionate (**L**), with $t_R = 7.8$ min, which also will be discussed later in Section 2.4.

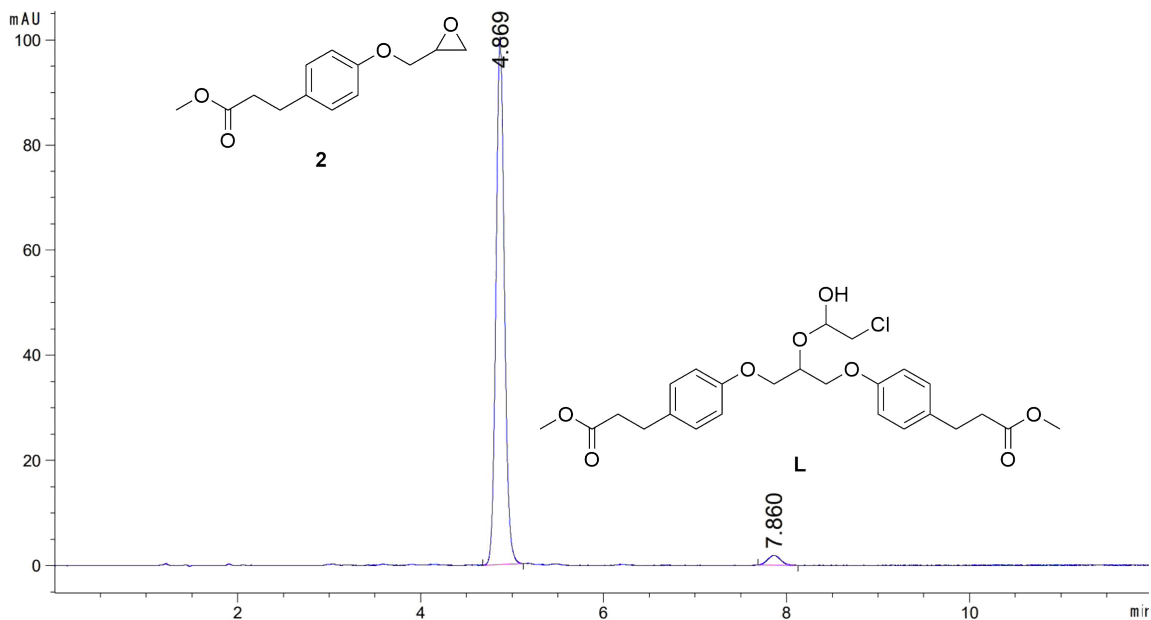


Figure 2.5: Achiral HPLC of epoxide **2** ($t_R = 4.8$ min), and by-product **L** ($t_R = 7.8$ min) after purification by flash chromatography performed on a ACE Excel 5 C18 column with an isocratic mobile phase composition of water and acetonitrile (50:50) over 12 min, flow 1 ml/min.

Epoxide **2** was obtained in 70% yield with 99% purity (determined by $^1\text{H-NMR}$) as a light yellow liquid.

As seen from the chromatogram (Figure 2.4) the reaction did not proceed to full conversion of starting material **1**. Full conversion was only achieved when the reaction shown in Scheme 2.5 was run for 48 hours with vigorously reflux. This also formed more by-product. It would be of interest to do a time analysis in order to find the optimal reaction time and improve the yield of epoxide **2**, but due to limited time, it was not performed in this project.

2.2.1 Characterization of epoxide **2**

Characterization of epoxide **2** was performed by NMR spectroscopy with deuterated chloroform as solvent. Epoxide **2** with numbered carbons is given in Figure 2.6, and the corresponding shifts determined by $^1\text{H-}$, $^{13}\text{C-}$, H,H-COSY, HSQC-, and HMBC-NMR spectroscopy are given in Table 2.4. All spectra for epoxide **2** are given in Appendix A. The $^1\text{H-NMR}$ spectrum (Appendix A.1) showed a water peak at $\delta = 1.74$ ppm, which is shifted from the regular water peak at 1.56 ppm.⁵¹ This is due to potential hydrogen bond acceptors in the sample.⁵² The chemical shifts corresponds to the data reported by Banoth and Banerjee.¹³

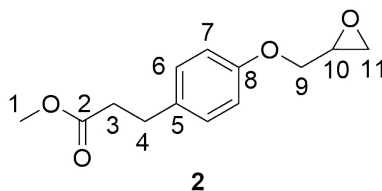


Figure 2.6: Synthesized epoxide **2** with labeled carbon atoms. Assignment of chemical shifts are given in Table 2.4, and all spectra are given in Appendix A.

Table 2.4: Characterization of epoxide **2** given ^1H -, ^{13}C -, H,H-COSY, HSQC- and HMBC-NMR (600 MHz, CDCl_3), see Appendix A.

Position	^1H -NMR [ppm] (mult., int., ^3J)	^{13}C -NMR [ppm]	COSY	HMBC
1	3.65 (s, 3H)	51.6	-	2
2	-	173.4	-	1, 3, 4
3	2.60-2.57 (m, 2H)	35.9	4	2, 4, 5
4	2.89-2.87 (m, 2H)	30.1	3	2, 3, 5, 6
5	-	133.2	-	3, 4, 7
6	7.10-7.09 (m, 2H)	129.3	7	4, 6, 7, 8
7	6.85-6.82 (m, 2H)	114.7	6	5, 6, 7, 8
8	-	157.0	-	6, 7, 9
9	3.94-3.91 (m, 1H)	68.8	9, 10	8, 10, 11
10	4.19-4.17 (dd, 1H, 14.27 Hz)	50.2	9, 10	9, 11
11	3.34-3.31 (m, 1H)	44.7	9, 10, 11	9, 11
	2.74-2.73 (m, 1H)		10, 11	
	2.89-2.87 (m, 1H)		10, 11	9, 10

2.2.2 The effect of using NaOH and K_2CO_3 as base

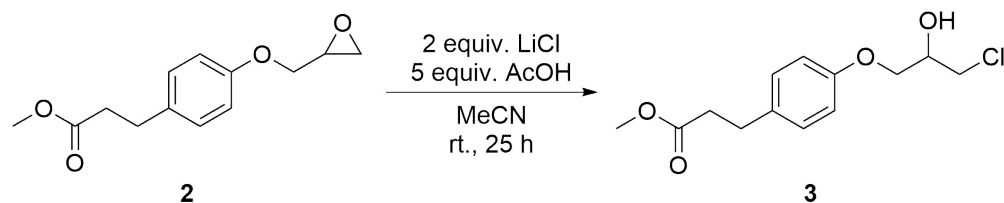
Previous studies have shown favored formation of chlorohydrin **7b** over epoxide **7c** in the synthesis of enantiopure (*S*)-atenolol when using 0.3 equivalents of sodium

hydroxide, as discussed in Section 1.5.³⁹ Sodium hydroxide was chosen as base for the first synthetic step in the total synthesis of (*S*)-esmolol ((*S*)-**5**) due several successful reactions of similar β -blocker precursors.^{1,37} In the synthesis of epoxide **2** and chlorohydrin **3** with sodium hydroxide as base, as shown in Scheme 2.1, chlorohydrin **3** is the favored product (Figure 2.1). After 24 hours, when 0.3 equivalent of base was used, it was only observed formation of chlorohydrin **3** indicating that this is the kinetically favored product when using a catalytic amount of base. Epoxide **2** was only observed when the amount of base wasn't catalytic and the reaction time was long, which indicates that epoxide **2** is thermodynamically favored. This is in line with previous indications for similar β -blocker precursors.

When using potassium carbonate as base, only epoxide **3** was formed (Figure 2.4). A theory is that chlorohydrin **3** was formed, but because the reaction was performed in dry acetonitrile due to clumping of potassium carbonate in hydrous acetonitrile, there were no available protons to protonate alkoxide **3**_{Anion} to form chlorohydrin **3** (Scheme 2.2, reaction mechanism c). Instead, epoxide **2** was formed following reaction mechanism d. When ring-opening epoxide **2**, as indicated in Section 2.3, it seems that alkoxide **3**_{Anion} is quite resistant to protonation, which may also be the reason why only epoxide **2** is formed. Another theory is that alkoxide **1**_{Anion} only attacks epichlorohydrin at carbon 1 (reaction mechanism b) forming epoxide **2** directly. It would be interesting to do a time-analysis of the synthesis of epoxide **2** with potassium carbonate as base in order to get a better understanding of the reaction pathway.

2.3 Synthesis of methyl 3-(4-(3-chloro-2-hydroxypropoxy)phenyl)propanoate (**3**) by ring-opening of methyl 3-(4-(oxiran-2-ylmethoxy)phenyl)propanoate (**2**)

The synthesis of chlorohydrin **3** was performed with basis in master candidate Mari Bergan Hansen's³⁹ description, an optimized method of the one reported by Lund *et al.*³⁷, where the epoxide was ring-opened with dilithium tetrachlorocuprate in tetrahydrofuran. Epoxide **2** was ring-opened with lithium chloride and acetic acid to form chlorohydrin **3**, and the reaction performed is shown in Scheme 2.6.



Scheme 2.6: Ring-opening of epoxide **2** with lithium chloride and acetic acid forming chlorohydrin **3**.

The total conversion of epoxide **2** was analyzed by achiral HPLC which gave t_R (**2**) = 4.8 min and t_R (**3**) = 4.4 min, see Figure 2.7. The chromatogram also showed formation of a small amount of some unknown by-products (t_R = 2.0 min, and t_R = 4.3 min), but due to limited time, chlorohydrin **3** was not purified further.

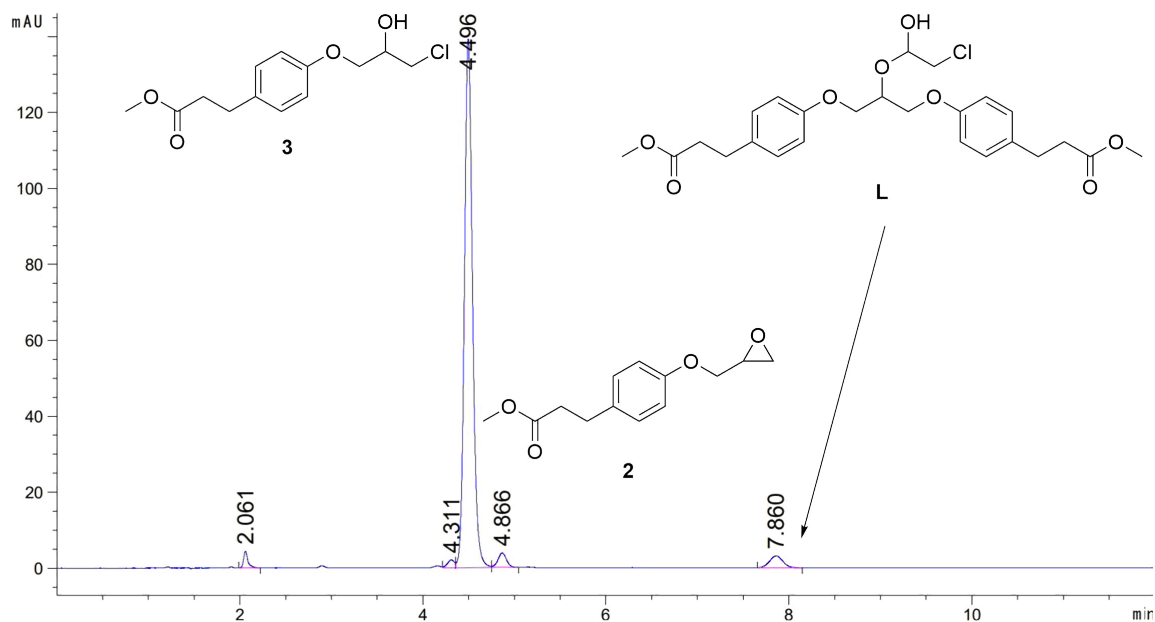
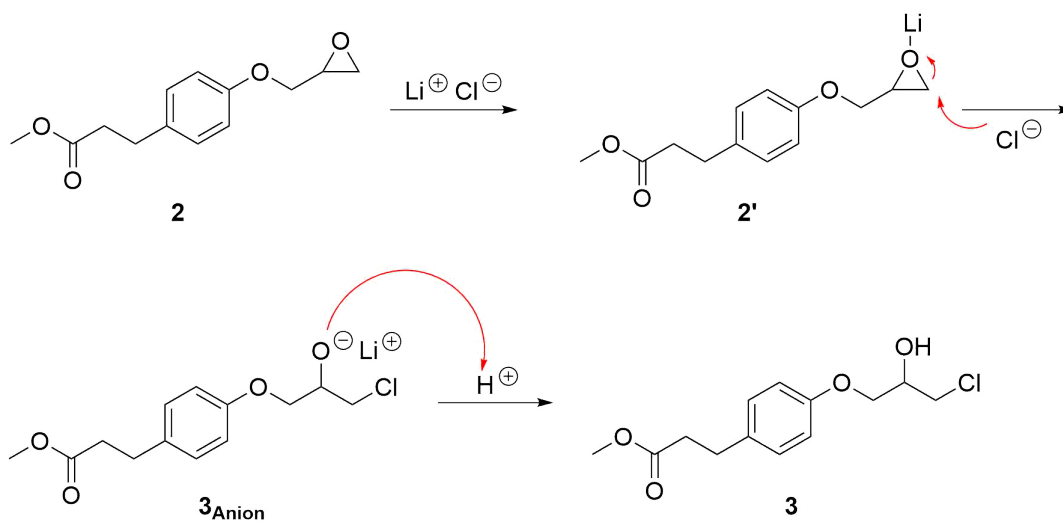


Figure 2.7: Achiral HPLC of chlorohydrin **3** (t_R = 4.4 min), epoxide **2** (t_R = 4.8 min), and by-product **L** (t_R = 7.8 min) after ring-opening of epoxide **2** performed on a ACE Excel 5 C18 column with an isocratic mobile phase composition of water and acetonitrile (50:50) over 12 min, flow 1 ml/min t_R = 2.0 min and t_R = 4.3 min are unknown by-products.

Chlorohydrin **3** was obtained in 96% yield (0.23 g, 1.12 mmol) with 98% purity as a light yellow liquid.

2.3.1 Mechanistic studies of ring-opening of epoxide **2**

The mechanism for ring-opening of epoxide **2** is shown in Scheme 2.7.¹ The lithium ion coordinates to the oxygen in the epoxide, and chlorine is added to the least sterically hindered carbon atom in epoxide **2'**. Followed by protonation of alkoxide **3_{Anion}**, chlorohydrin **3** is formed. An attack at the most sterically hindered carbon atom in epoxide **2'** by the chlorine is theoretically possible, but is not likely to happen.



Scheme 2.7: Reaction mechanism of ring-opening of epoxide **2** in acetic acid forming chlorohydrin **3**. The lithium ion coordinates to the oxygen in the epoxide giving compound **2'**.¹

2.3.2 Characterization of chlorohydrin **3**

Characterization of chlorohydrin **3** was performed by NMR spectroscopy with deuterated chloroform as solvent. Chlorohydrin **3** with numbered carbons is given in Figure 2.8, and the corresponding shifts determined by ¹H-, ¹³C-, H,H-COSY-, HSQC-, and HMBC-NMR spectroscopy are given in Table 2.5. All spectra for chlorohydrin **3** are given in Appendix B. The ¹H-NMR spectrum (Appendix B.1) showed a water peak at 1.61 ppm, which is from the solvent.⁵¹ The chemical shifts corresponds to the data reported by Banoth and Banerjee.¹³ The ¹H-NMR spectrum also showed a doublet with $\delta = 2.56$ - 2.55 ppm which resonates for one proton. This was believed to be the proton in the OH-group, and by performing a deuterated water test the doublet disappeared, confirming this was in fact the OH-proton.

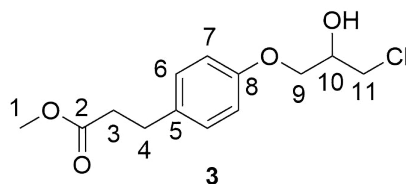


Figure 2.8: Synthesized chlorohydrin **3** with labeled carbon atoms. Assignment of chemical shifts are given in Table 2.5, and all spectra are given in Appendix B.

Table 2.5: Characterization of chlorohydrin **3** given ^1H -, ^{13}C -, H,H-COSY, HSQC- and HMBC-NMR (600 MHz, CDCl_3), see Appendix B.

Position	^1H -NMR [ppm] (mult., int., ^3J)	^{13}C -NMR [ppm]	COSY	HMBC
1	3.66 (s, 3H)	51.6	-	2
2	-	173.4	-	1, 3, 4
3	2.61-2.58 (m, 2H)	36.0	4	2, 4, 5
4	2.91-2.88 (m, 2H)	30.1	3	2, 3, 5, 6
5	-	133.5	-	3, 4, 7
6	7.13-7.10 (m, 2H)	129.4	7	5, 6, 7, 8
7	6.85-6.83 (m, 2H)	114.7	6	5, 6, 7, 9
8	-	156.8	-	6, 7, 9
9	4.09-4.04 (m, 2H)	68.6	9	8, 11, OH
10	4.22-4.18 (m, 1H)	68.9	9, 11	9, 11, OH
11	3.79-3.71 (m, 2H)	46.0	10	10, OH
OH	2.56-2.55 (d, 1H, 5.93 Hz)	-	-	9, 10, 11

2.3.3 Impact of acetic acid equivalents, and the concentration

Four reaction parallels of the reaction shown in Scheme 2.6 were performed using different equivalents of acetic acid. The amounts (%) of starting material **1**, epoxide **2**, and chlorohydrin **3** were determined by ^1H -NMR analysis with deuterated chloroform as solvent. The results are summarized in Table 2.6. All reaction parallels

were performed at room temperature with 2 equivalents of lithium chloride and 5 mL acetonitrile as solvent. c_2 refers to the concentration of epoxide **2**.

Table 2.6: Reaction parallels of ring-opening of epoxide **2** to form chlorohydrin **3**. All reaction parallels were performed at room temperature with 2 equivalents lithium chloride and 5 mL acetonitrile as solvent. The amount (%) of starting material **1**, epoxide **2**, and chlorohydrin **3** are calculated from $^1\text{H-NMR}$ with deuterated chloroform as solvent.

Reaction parallel	c_2 [M]	AcOH [equiv.]	Reaction time [h]	% of 1	% of 2	% of 3
1	$4.6 \cdot 10^{-7}$	5	24	~ 0	~ 0	~ 100
2	$1.8 \cdot 10^{-7}$	5	27	1	1	98
3	$2.7 \cdot 10^{-7}$	3	27	1	1	98
4	$3.3 \cdot 10^{-7}$	2	27	~ 0	1	99

From Table 2.6 it was only reaction parallel 1 that achieved full conversion of epoxide **3**. This is also the reaction parallel with the highest concentration of the epoxide, thereby the reaction parallel with the highest concentration of acetic acid. It is believed that since the ring-opening of epoxide **2** is acid-catalyzed, a high concentration of acetic acid is needed. It seems that alkoxide $\mathbf{3}_{\text{Anion}}$ (Scheme 2.7) is resistant to protonation, and when the concentration of acetic acid is low, alkoxide $\mathbf{3}_{\text{Anion}}$, instead of being protonated and forming chlorohydrin **3**, restores epoxide **2** (reaction mechanism d, Scheme 2.2).

2.4 Formation of dimers as by-products

As previously mentioned in Section 2.2, two by-products were observed in the reaction between deprotonated phenol **1**, epichlorohydrin, and potassium carbonate as base forming epoxide **2** (Scheme 2.5). The first by-product was determined to be 3,3'-(((2-hydroxypropane-1,3-diyl)bis(oxy))bis(4,1-phenylene))dipropanoate (**A**) with molecular mass 416.45 g/mol. LC-MS analysis gave a peak with $m/z = 439.2$, molecular formula $\text{C}_{23}\text{H}_{28}\text{O}_7\text{Na}$, and IHD = 10 (Appendix G.5). This was also believed to be dimer **A** shown in Figure 1.8, which previously in the Biocatalysis research group has been observed for similar β -blocker precursor, and in the synthesis of epoxide **2**, as discussed in Section 1.5.^{1,39,40}

By purification of epoxide **2** by flash chromatography with dichloromethane and acetonitrile (11:1), dimer **A** was isolated in 6% yield (33.2 mg, 0.08 mmol) with a purity of 99%. Achiral HPLC-analysis confirmed that dimer **A** was isolated as seen in Figure 2.9 which gave $t_R(\mathbf{A}) = 9.1$ min.

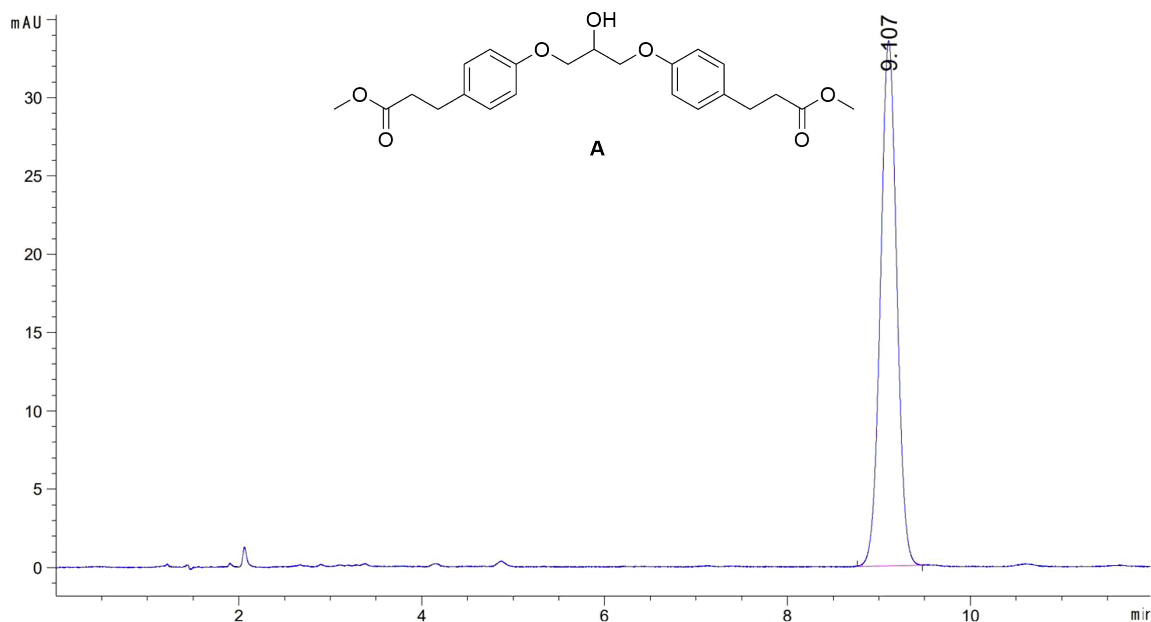
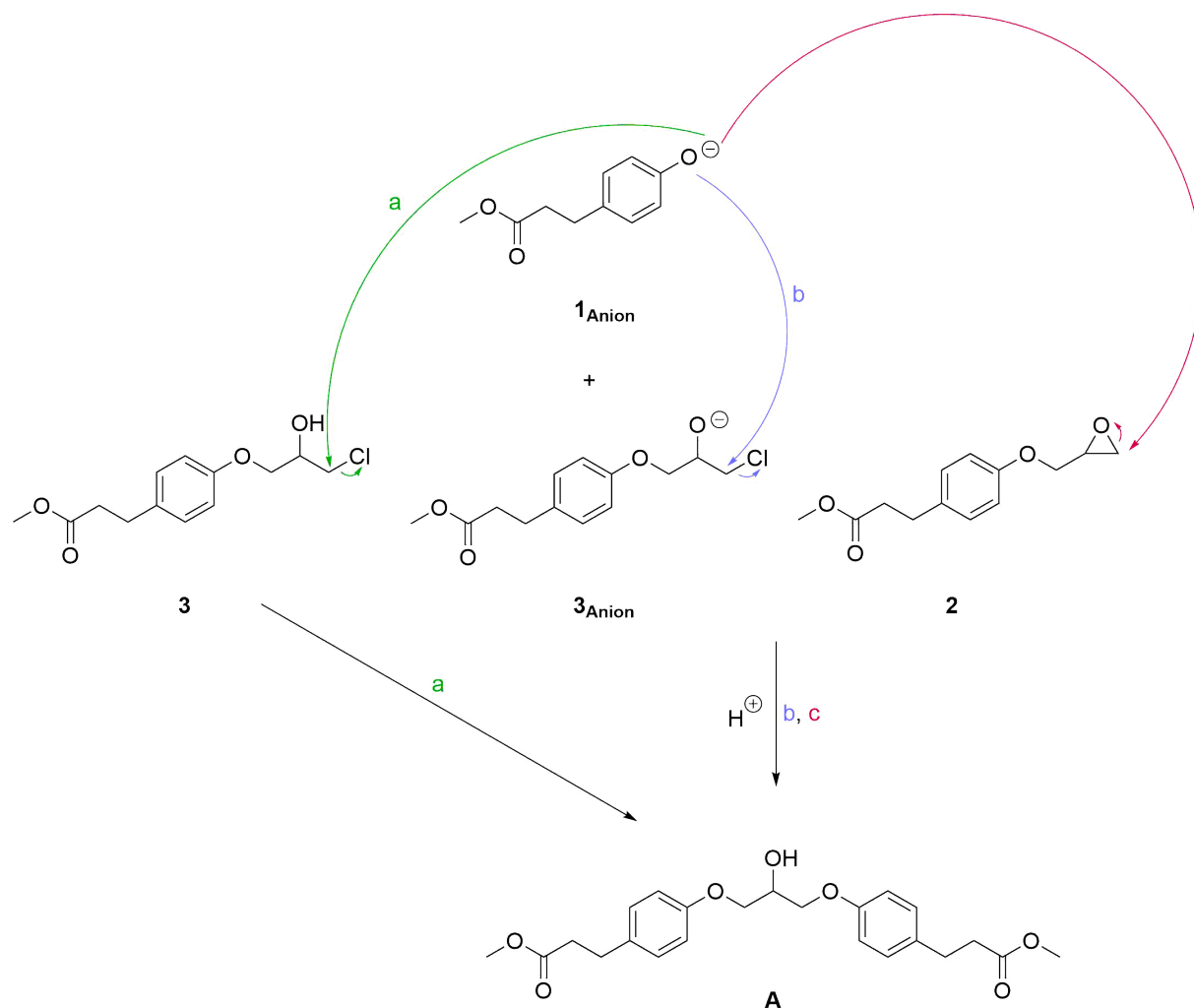


Figure 2.9: Achiral HPLC of isolated dimer **A** ($t_R = 9.1$ min) performed on a ACE Excel 5 C18 column with an isocratic mobile phase composition of water and acetonitrile (50:50) over 12 min, flow 1 mL/min.

2.4.1 Mechanistic studies of dimer **A** formation

It is suggested that dimer **A** can be formed in three ways by nucleophilic attacks of deprotonated phenol **1_{Anion}**, see Scheme 2.8. Reaction mechanism a shows a nucleophilic attack by alkoxide **1_{Anion}** on chlorohydrin **3**, b on alkoxide **3_{Anion}**, and c on epoxide **2**. Mechanism b and c requires a proton donor.



Scheme 2.8: Three suggested mechanistic pathways for formation of dimer **A**. Reaction mechanism a shows a nucleophilic attack by alkoxide **1_{Anion}** on chlorohydrin **3**, b on alkoxide **3_{Anion}**, and c on epoxide **2**. Mechanism b and c requires a proton donor.

2.4.2 Characterization of dimer **A**

Further confirmation that by-product **A** was formed in the reaction shown in Scheme 2.5 was achieved by NMR analysis. Characterization of dimer **A** was performed by NMR spectroscopy with deuterated chloroform as solvent. Dimer **A** with numbered carbons is given in Figure 2.10, and the corresponding shifts determined by 1H -, ^{13}C -, H,H-COSY-, HSQC- and HMBC-NMR spectroscopy are given in Table 2.7, including the OH-proton. All spectra for dimer **A** are given in Appendix E. The 1H -NMR spectrum (Appendix E.1) showed a water peak at $\delta = 1.56$ ppm which

indicated that the by-product wasn't completely dry. Because this was only a by-product, dimer **A** wasn't dried further. The $^1\text{H-NMR}$ spectrum also showed a doublet with $\delta = 2.56\text{-}2.55$ ppm which resonates for one proton, as for chlorohydrin **3**. This was again believed to be the proton in the OH-group, and a deuterated water test confirmed that this again was the OH-proton.

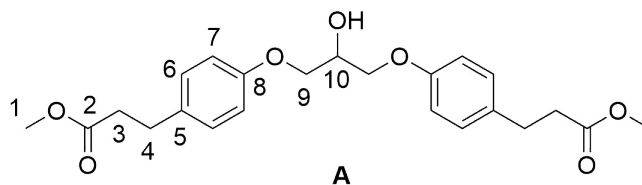


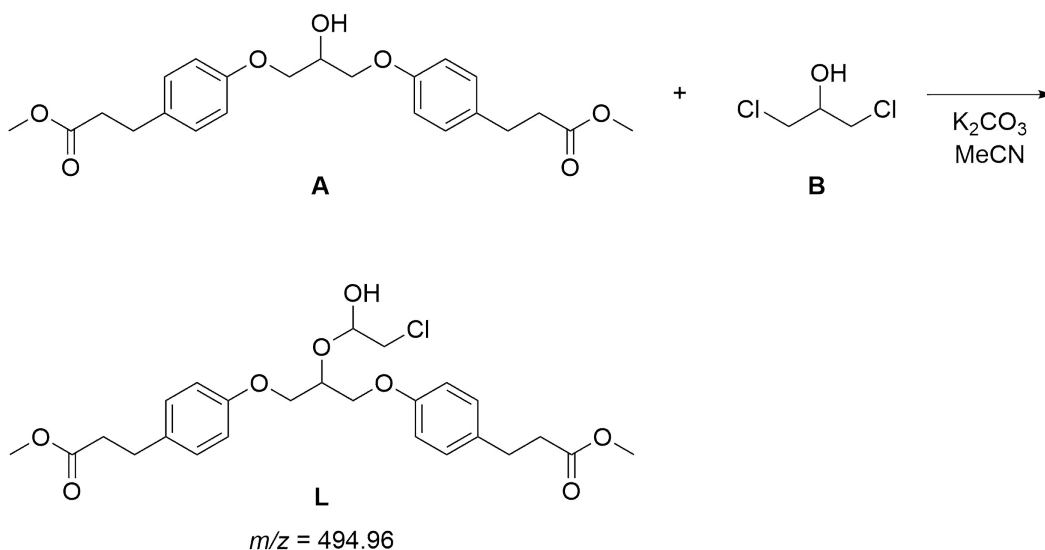
Figure 2.10: Synthesized by-product **A** with labeled carbon atoms. Assignment of chemical shifts are given in Table 2.7, and all spectra are given in Appendix E.

Table 2.7: Characterization of dimer **A** given $^1\text{H-}$, $^{13}\text{C-}$, H,H-COSY, HSQC- and HMBC-NMR (600 MHz, CDCl_3), see Appendix E.

Position	$^1\text{H-NMR}$ [ppm] (mult., int., ^3J)	$^{13}\text{C-NMR}$ [ppm]	COSY	HMBC
1	3.66 (s, 6H)	51.6	-	2
2	-	173.4	-	1, 3, 4
3	2.61-2.58 (t, 4H, 7.85 Hz)	36.0	4	2, 4, 5, 6
4	2.91-2.88 (t, 4H, 7.85 Hz)	30.1	3	2, 3, 5, 6
5	-	133.23	-	3, 4, 7
6	7.13-7.10 (m, 4H)	129.4	7	3, 4, 6, 7, 8
7	6.89-6.84 (m, 4H)	114.6	6	5, 6, 7, 8
8	-	156.0	-	6, 7, 9
9	4.15-4.09 (m, 4H)	68.9	10	8, 10
10	4.37-4.34 (quint., 1H, 5.40 Hz)	68.8	9	9
OH	2.56-2.55 (d, 1H, 5.10 Hz)	-	-	9, 10

2.4.3 Formation of a dimer derivative

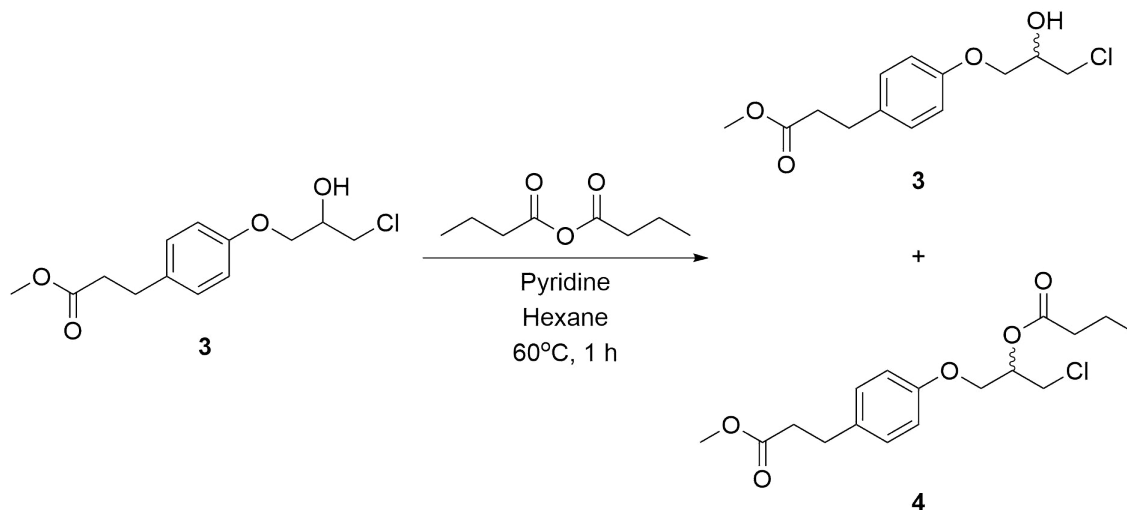
The second by-product was suggested to be dimethyl 3,3'-(((2-(2-chloro-1-hydroxyethoxy)propane-1,3-diyl)bis(oxy))bis(4,1-phenylene))dipropionate (**L**) with molecular mass 494.96 g/mol. LC-MS analysis gave a peak with $m/z = 517.2$, molecular formula $C_{25}H_{31}O_8NaCl$, and IHD = 10 (Appendix G.6). It was believed that dimer **L** can be formed in a reaction between dimer **A** and 1,3-dichloropropan-2-ol (**B**) (discussed in Section 1.5) as shown in Scheme 2.9. This is a base-catalyzed transesterification. Dimer **L** was not isolated, and could therefore not be confirmed by NMR analysis. In addition, as before, by-product **B** has not been observed on NMR.



Scheme 2.9: Side-reaction between dimer **A** and by-product **B** forming by-product **L** with molecular $m/z = 494.96$.

2.5 Derivatization reaction of methyl 3-(4-(3-chloro-2-hydroxypropoxy)phenyl)propanoate (**3**)

A derivatization reaction of racemic chlorohydrin **3** was performed in order to determine the retention times of the (*R*)- and (*S*)-enantiomers of chlorohydrin **3**. The derivatization reaction was performed by addition of pyridine and butyric anhydride, and run with air heating at 60°C for one hour, see Scheme 2.10. The reaction formed racemic 1-chloro-3-(4-(3-methoxy-3-oxopropyl)phenoxy)propan-2-yl butanoate (**4**).



Scheme 2.10: Chemical derivatization reaction of racemic chlorohydrin **3** with butyric anhydride and pyridine dissolved in hexane. The reaction was run with air heating at 60°C for one hour, forming racemic 1-chloro-3-(4-(3-methoxy-3-oxopropyl)phenoxy)propan-2-yl butanoate (**4**).

The derivatization reaction was analyzed by chiral HPLC using a Chiralcel OD-H column with an isocratic eluent of two different compositions of *n*-hexane and 2-propanol, and a flow of 1 mL/min. The different eluent compositions, analysis times, and resolution factors (R_S) of (*R*)/(*S*)-**4** and (*R*)/(*S*)-**3** are given in Table 2.8. The resolution factors, R_S , are calculated using Equation (1.7).

Table 2.8: Methods attempted to achieve baseline separation between (*R*)- and (*S*)-**3**, and (*R*)- and (*S*)-**4** by chiral HPLC analysis with a mobile phase composed of *n*-hexane and 2-propanol with different compositions, all isocratic. All methods were run with a mobile phase flow of 1 mL/min, and 10 μ L injection.

Entry	<i>n</i> -Hexane	2-propanol	Analysis time [min]	R_S	R_S
	[%]	[%]		((<i>R</i>)/(<i>S</i>)- 4)	((<i>R</i>)/(<i>S</i>)- 3)
1	90	10	30	-	1.98
2	97	3	30	1.56	-

In order to achieve baseline separation between two peaks, the resolution of two peaks should be above 1.5.⁴⁵ A resolution of the (*R*)/(*S*)-**4** and (*R*)/(*S*)-**3** above 1.5 were obtained for both pairs of enantiomers, but with different eluent compositions. Chiral HPLC analysis of the derivatization reaction with *n*-hexane and 2-propanol in a ratio of 90:10 gave t_R (*S*R)-**4**) = 9.87 min, t_R ((*S*)-**3**) = 22.32 min and t_R ((*R*)-**3**) = 24.62 min with $R_S = 1.98$. The chromatogram is shown in Figure 2.11.

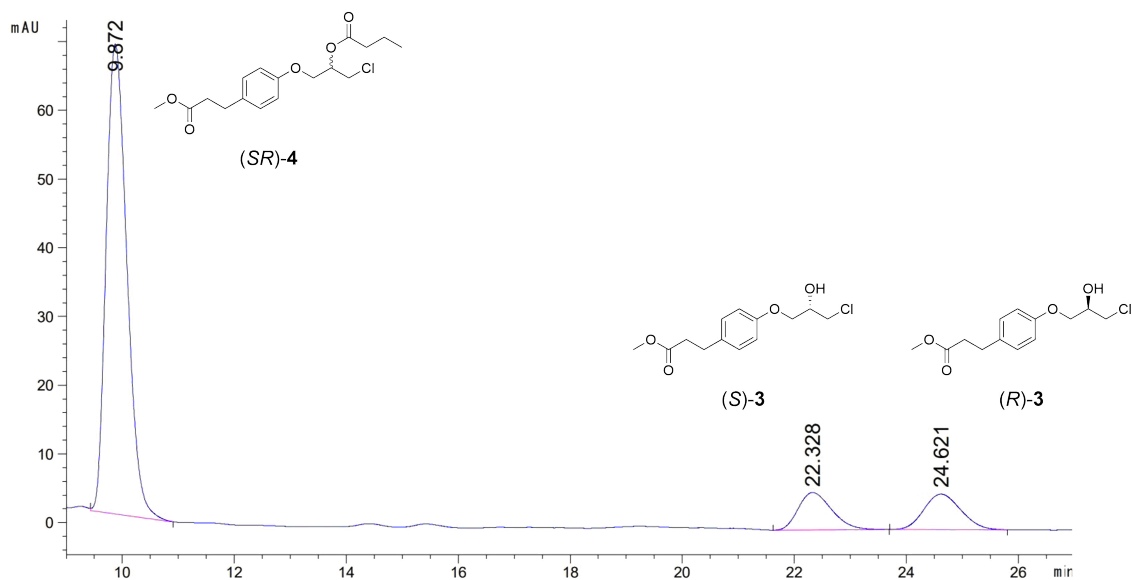


Figure 2.11: Chiral HPLC analysis of chlorohydrin **3**, derivatized with butyric anhydride. The analysis was performed on a Chiralcel OD-H column with hexane and 2-propanol (90:10) as eluent and 1 mL/min flow. The retention times of *(SR)*-**4** = 9.87 min, and *(S)*/*(R)*-**3** = 22.32 and 24.62 min respectively. R_S (*(R)*/*(S)*-**3**) = 1.98.

Chiral HPLC analysis of the derivatization reaction with *n*-hexane and 2-propanol in a ratio of 97:3 gave t_R (*(S)*-**4**) = 19.45 min and t_R (*(R)*-**4**) = 20.95 min with R_S = 1.56. The chromatogram is shown in Figure 2.12.

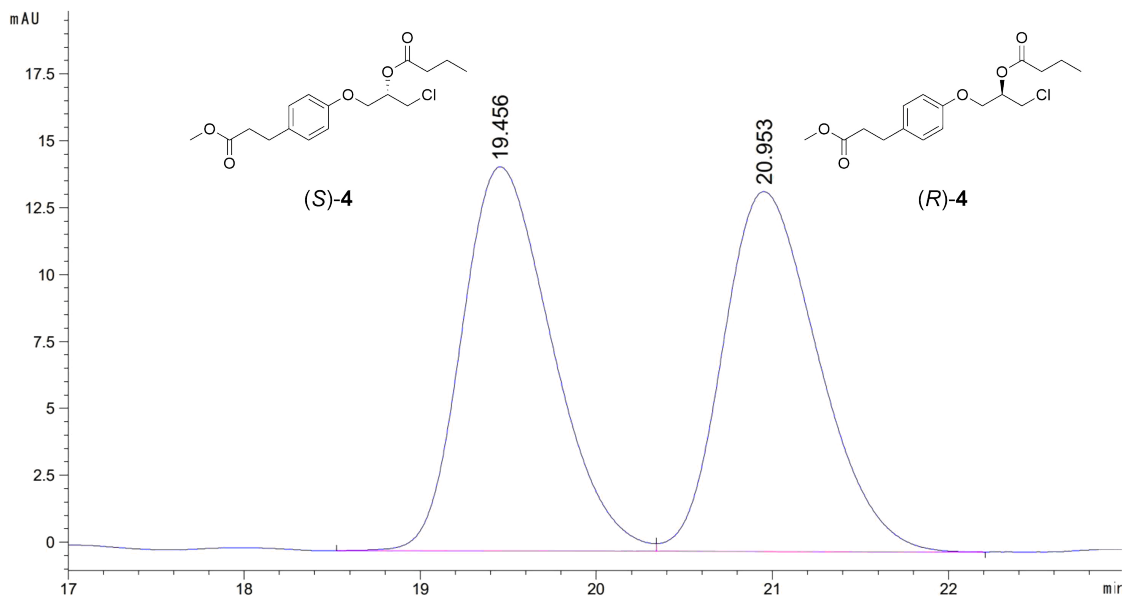
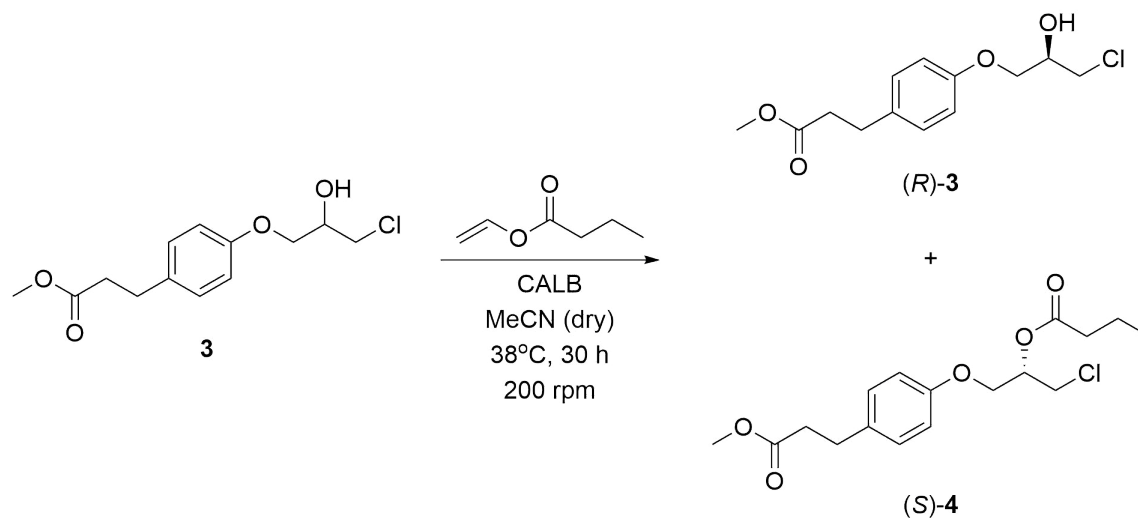


Figure 2.12: Chiral HPLC analysis of chlorohydrin **3**, derivatized with butyric anhydride. The analysis was performed on a Chiralcel OD-H column with hexane and 2-propanol (97:3) as eluent and 1 mL/min flow. The retention times of (*S*)/(*R*)-**4** = 19.45 and 20.95 min respectively. R_S ((*R*)/(*S*)-**4**) = 1.56.

2.6 Small-scale kinetic resolution of methyl 3-(4-(3-chloro-2-hydroxypropoxy)phenyl)propanoate (**3**) with CALB

In order to synthesize enantiopure (*S*)-esmolol ((*S*)-**5**) a kinetic resolution with racemic chlorohydrin **3** was performed with CALB as catalyst and vinyl butanoate as acyl donor forming enantiopure chlorohydrin (*R*)-**3** and ester (*S*)-**4** as shown in Scheme 2.11.



Scheme 2.11: Kinetic resolution of chlorohydrin **3** with CALB as catalyst, and vinyl butanoate as acyl donor forming enantiopure chlorohydrin *(R)*-**3** and enantiopure ester *(S)*-**4**.

Samples at different time intervals were analyzed by chiral HPLC using a Chiralcel OD-H column with an isocratic mobile phase composition of *n*-hexane and 2-propanol (90:10) and (97:3) for the enantiomers of chlorohydrin **3** and ester **4** respectively. This gave $t_R((S)\text{-}\mathbf{3}) = 21.6$ min and $t_R((R)\text{-}\mathbf{3}) = 23.8$ min, and $t_R((S)\text{-}\mathbf{4}) = 20.2$ min and $t_R((R)\text{-}\mathbf{4}) = 22.5$ min, see Figure 2.13 and 2.14 respectively.

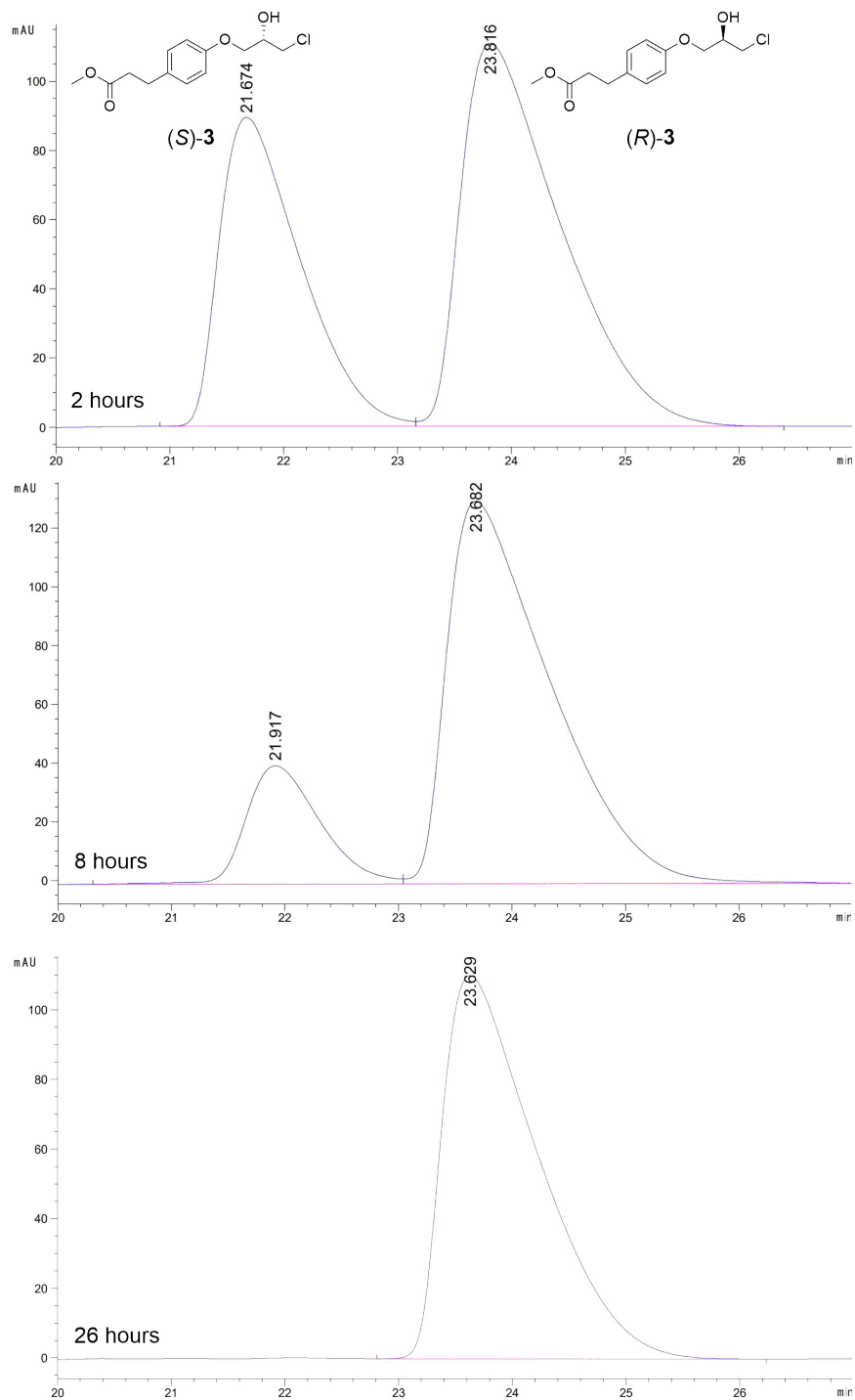


Figure 2.13: HPLC chromatograms of the CALB catalyzed kinetic resolution of chlorohydrin **3** after 2, 8 and 22 hours. The analyzes were performed on a Chiralcel OD-H column with an isocratic mobile phase composition of *n*-hexane and 2-propanol (90:10) and 1 mL/min flow. This gave $t_R((S)\text{-}\mathbf{3}) = 21.6$ min and $t_R((R)\text{-}\mathbf{3}) = 23.8$ min.

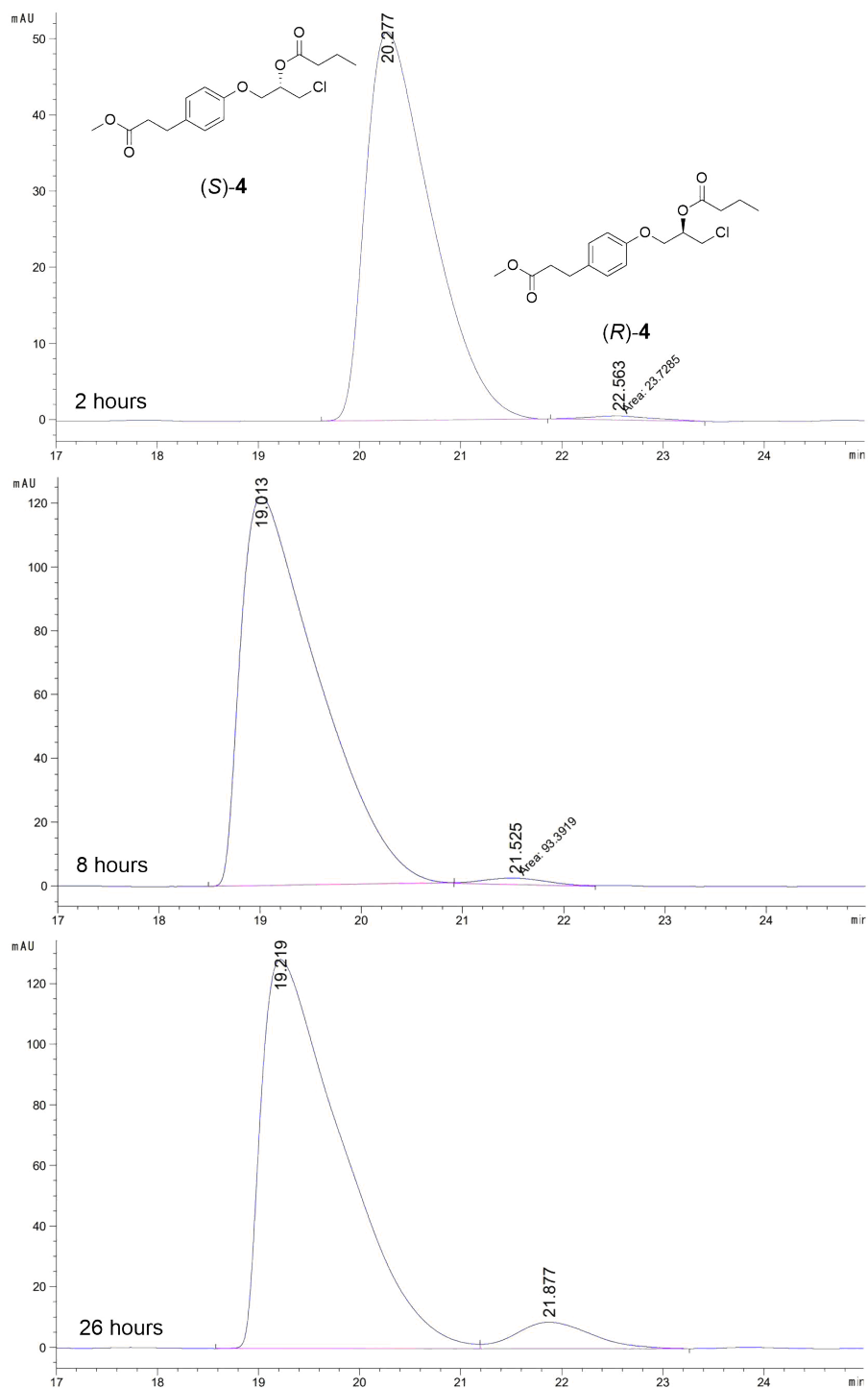


Figure 2.14: HPLC-chromatograms of the CALB catalyzed kinetic resolution of chlorohydrin **3** after 2, 8 and 22 hours. The analyzes were performed on a Chiralcel OD-H column with an isocratic mobile phase composition of *n*-hexane and 2-propanol (97:3) and 1 mL/min flow. This gave $t_R((S)\text{-}4) = 20.2$ min and $t_R((R)\text{-}4) = 22.5$ min.

The enantiomeric ratio, E , from the kinetic resolution of chlorohydrin **3** with CALB was calculated on the basis of the ping-pong bi-bi mechanism with the software *E & K Calculator*²², where ee_S and ee_P in percent is plotted against percentage conversion. ee_S -, ee_P -, and c -values are calculated using experimental data and Equation (1.1) and (1.2). The curve for the E -value is shown in Figure 2.15, and the E -value was calculated to be 157. The red and blue curve are generated from the experimental value of ee_S and ee_P respectively.

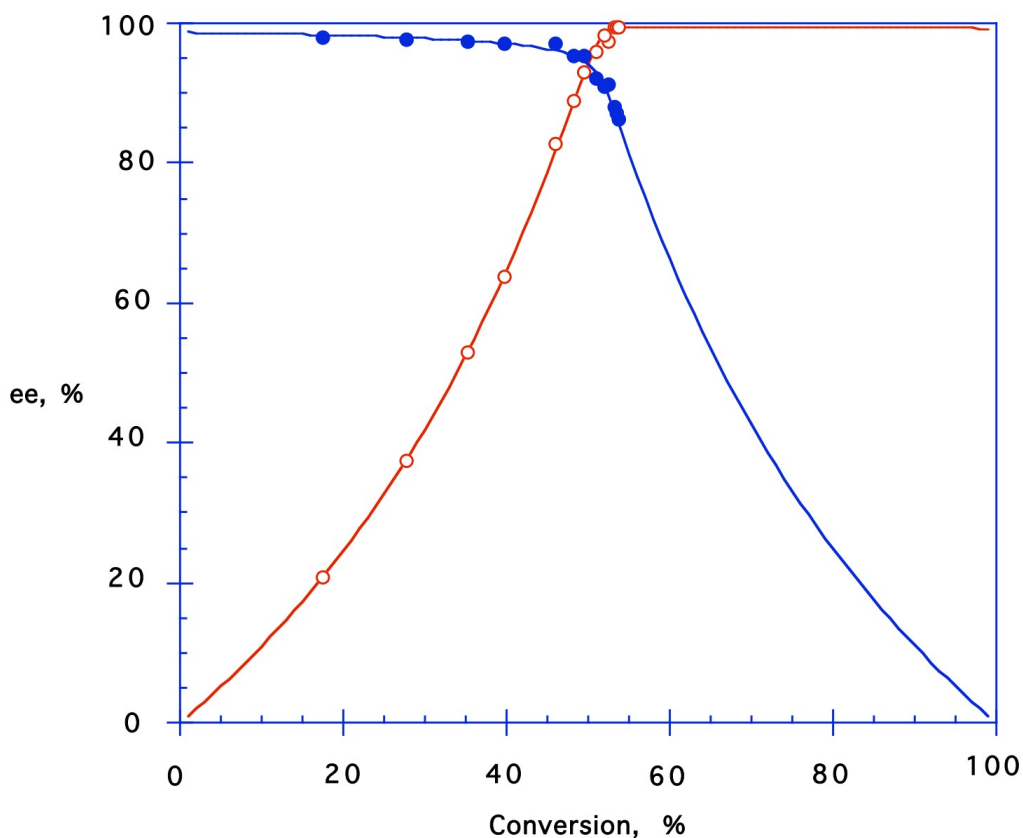


Figure 2.15: Graphical representation of the course of the kinetic resolution of chlorohydrin **3** with CALB in dry acetonitrile with vinyl butanoate as acyl donor. ee_S (red circles) and ee_P (blue circles) in percent against conversion in percent. The red and the blue curve are generated from the experimental values of ee_S and ee_P respectively. The E -value was calculated to be 157.

Kinetic resolution of chlorohydrin **3** with CALB gave an enantiomeric excess of (*R*)-**3** of 99% (determined by HPLC).

2.7 Large-scale kinetic resolution of methyl 3-(4-(3-chloro-2-hydroxypropoxy)phenyl)propanoate (**3**) with CALB

A large-scale kinetic resolution of chlorohydrin **3** catalyzed with CALB was performed to study the enantioselectivity of the enzyme in larger scaled reactions.

The large-scale kinetic resolution of chlorohydrin **3** was run for 30 hours in an incubator at 200 rpm and 38° C. Samples of 150 μ L were taken only after 24 hours and 28 hours and analyzed by chiral HPLC as the small-scale kinetic resolution of chlorohydrin **3** indicated that the reaction was finished after 26 hours. Therefore, the large-scale kinetic resolution would be finished approximately after the equal amount of hours. Table 2.9 show the time in hours, and the corresponding ee_S-values.

Table 2.9: Reaction progression of large-scale kinetic resolution of chlorohydrin **3** catalyzed by CALB with vinyl butanoate as acyl donor. The ee_S-values are calculated from chiral HPLC analyzes on a Chiralcel OD-H column.

Time [h]	ee _S [%]
24	96
28	98

The reaction was stopped after 30 hours as the HPLC analyzes indicated an ee_S = 98% after 28 hours. The product mixture, consisting of enantiopure chlorohydrin (*R*)-**3** and ester (*S*)-**4**, was separated by flash chromatography and resulted in (*R*)-**3** in 43% yield with 97% purity and an ee of 98 %, and (*S*)-**4** in 50% yield with 71% purity and an ee of 89%. The chromatograms from chiral HPLC analyzes are given in Figure 2.16 and 2.17. The HPLC chromatogram of the CALB catalyzed kinetic resolution of chlorohydrin **3** show that (*R*)-**3** was not completely separated from (*S*)-**4** (t_R = 9.7 min) by flash chromatography. It also show a small amount of epoxide **2** (t_R = 14.9 min), and an unknown impurity with t_R = 13.1 min, both which are from the previous synthetic step. It was first believed that the peak of the impurity was epoxide **2**, which was separated into its respective enantiomers, but it was later discovered that only the peak with t_R = 14.9 min was from the epoxide. The reason why will be discussed later in Section 2.8.

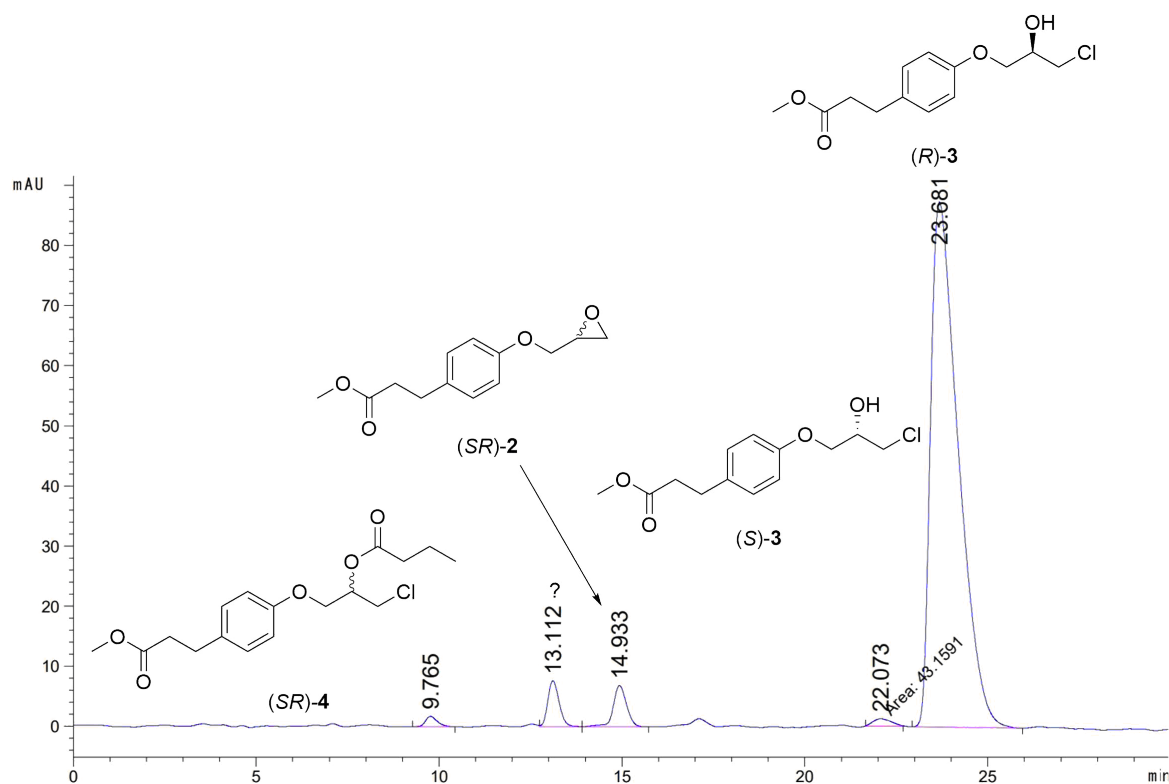


Figure 2.16: HPLC chromatogram of the CALB catalyzed kinetic resolution of chlorohydrin **3** after 30 hours. The analysis was performed on a Chiralcel OD-H column with an isocratic mobile phase composition of *n*-hexane and 2-propanol (90:10) and 1 mL/min flow. This gave $t_R((S)\text{-3}) = 22.0$ min and $t_R((R)\text{-3}) = 23.6$ min.

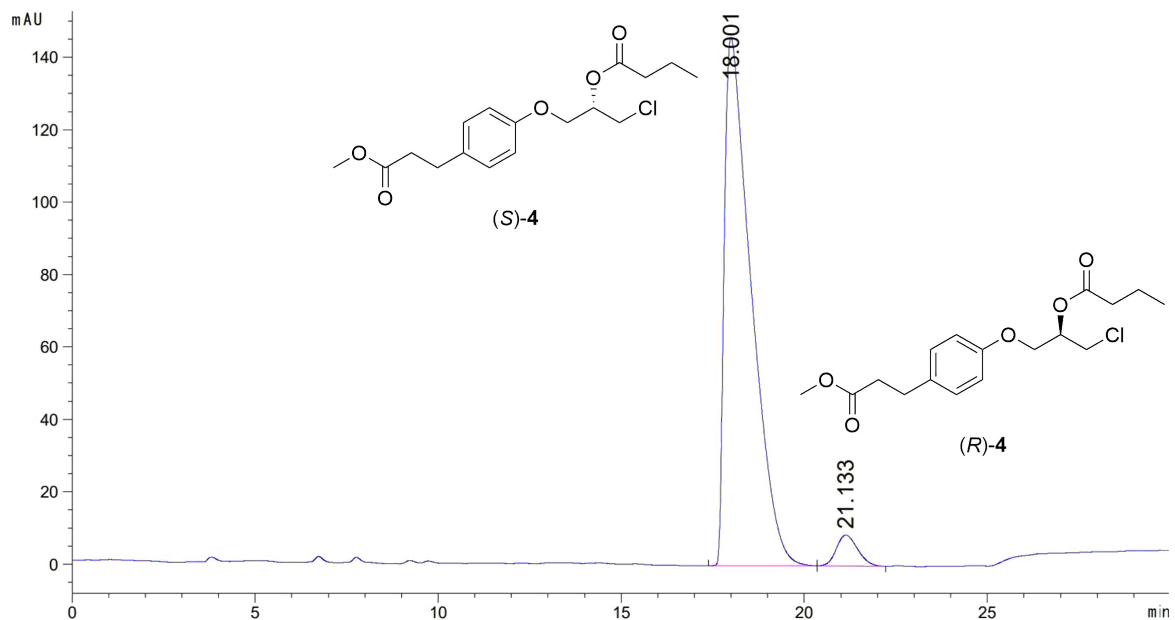


Figure 2.17: HPLC chromatogram of the CALB catalyzed kinetic resolution of ester **6** after 30 hours. The analysis was performed on a Chiralcel OD-H column with an isocratic mobile phase composition of *n*-hexane and 2-propanol (97:3) and 1 mL/min flow. This gave $t_R((S)\text{-4}) = 18.0$ min and $t_R((R)\text{-4}) = 21.1$ min.

Large-scale kinetic resolution of chlorohydrin **3** gave lower reaction rate, compared to small-scale kinetic resolution of chlorohydrin **3**, given the same reaction conditions. One possible reason is that the amount of CALB compared to the amount of chlorohydrin **3** and acyl donor wasn't the same. Therefore, the amount of active enzymes in the reaction is lower and thereby the reaction rate is lowered. Another reason for the lower reaction rate could be the equipment used. For the large-scale kinetic resolution of chlorohydrin **3** it was used a bigger flask which was longer, and giving more airspace at the top of the flask. This means that there may have been more humidity in the air, which can lead to more water in the reaction system and slow down the reaction rate. A solution is to flush the reaction flask with nitrogen each time it is opened.

The low purity of (*S*)-**4** is due to formation of butanoic acid as a by-product. This is formed due to water in the reaction. Butanoic acid and (*S*)-**4** eluted in the same fractions, and were not separated. Due to limited time, it was not attempted to remove butanoic acid from the ester.

2.7.1 Characterization of ester **4**

Characterization of ester **4** was performed by NMR spectroscopy with deuterated chloroform as solvent. Ester **4** with numbered carbon atoms is given in Figure 2.18,

and the corresponding shifts determined by ^1H -, ^{13}C -, H,H-COSY-, HSQC- and HMBC-NMR spectroscopy are given in Table 2.10. All spectra for ester **4** are given in Appendix C. From ^1H -NMR it was discovered that butanoic acid with chemical shifts at 0.99-0.95, 1.71-1.64, and 2.34-2.32 ppm overlapped with the chemical shifts of carbon 13, 14, and 15 in ester **4** (Appendix C.1). These three chemical shifts all resonate for one extra proton, which are the protons from butanoic acid. The experimental ^1H -NMR spectrum for butanoic acid in deuterated chloroform was obtained from the Integrated Spectral Database System of Organic Compounds (data obtained from the National Institute of Advanced Science and Technology (Japan)).⁵³ In addition, from ^{13}C -NMR the carbons for butanoic acid at 18.2, 35.8, and 179.0 ppm was observed (Appendix C.2). For carbon 13, 14, and 15 the number of hydrogens from the spectrum is given, and what the integrals should resonate for when subtracting butanoic acid protons are given in parentheses.

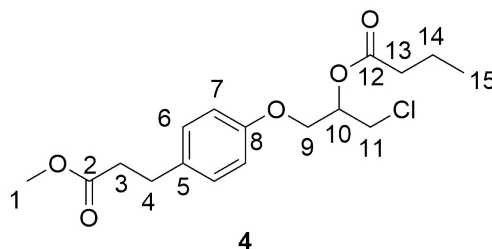


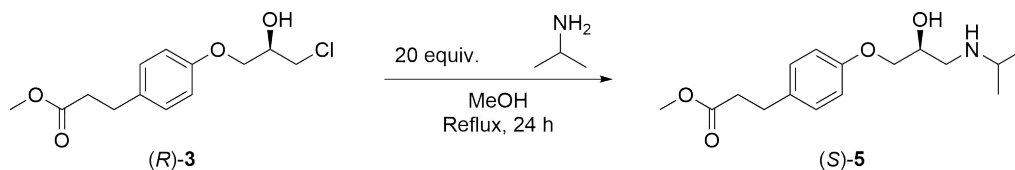
Figure 2.18: Synthesized ester **4** with labeled carbon atoms. Assignment of chemical shifts are given in Table 2.10, and all spectra are given in Appendix C.

Table 2.10: Characterization of ester **4** given ^1H -, ^{13}C -, H,H-COSY, HSQC- and HMBC-NMR (600 MHz, CDCl_3), see Appendix C.

Position	^1H -NMR [ppm] (mult., int., ^3J)	^{13}C -NMR [ppm]	COSY	HMBC
1	3.66 (s, 3H)	51.6	-	2
2	-	173.4	-	1, 3, 4
3	2.61-2.58 (t, 2H, 7.77 Hz)	36.0	4	2, 4, 5
4	2.90-2.88 (t, 2H, 7.77 Hz)	30.1	3	2, 3, 5, 6
5	-	133.5	-	3, 4, 7
6	7.13-7.11 (m, 2H)	129.4	7	4, 6, 8
7	6.85-6.82 (m, 2H)	114.7	6	5, 6, 8
8	-	156.8	-	6, 7, 9
9	4.16-4.11 (m, 2H)	66.2	10	8, 10, 11
10	5.35-5.31 (quint., 1H, 5.16 Hz)	70.9	9, 11	9, 12
11	3.86-3.76 (m, 2H)	42.6	10	9, 10
12	-	172.9	-	10, 13, 14
13	2.34-2.32 (m, 3H (2H))	36.1	14	12, 14, 15
14	1.71-1.64 (m, 3H (2H))	18.4	13, 15	12, 13, 15
15	0.99-0.95 (m, 4H (3H))	13.6	14	13, 14

2.8 Synthesis of enantiopure (*S*)-esmolol ((*S*)-**5**)

The synthesis of enantiopure (*S*)-esmolol ((*S*)-**5**) was carried out with basis in Banoth and Banerjee's¹³ description, but without triethylamine as this had been successfully performed for similar β -blockers.¹ The reaction is an amine alkylation of isopropylamine with (*R*)-**3** as alkylating agent. The reaction was performed as shown in Scheme 2.12.



Scheme 2.12: Amine alkylation of isopropylamine with (*R*)-**3** as alkylating agent forming (*S*)-**5**.

Banoth and Banerjee¹³ reported that (*RS*)-**5** was separated on a Chiralcel OD-H column with an isocratic eluent of *n*-hexane and 2-propanol in a ratio 90:10. This system was tried for separation of racemic **5**, but the enantiomers did not elute when the analysis was run for 80 minutes. In order to elute the enantiomers of esmolol (**5**) an additive had to be used. An eluent of *n*-hexane and 2-propanol with 0.4% diethylamine (DEA) was used in different ratios. In addition, it was tried to use a Chiralcel OD-RH column with an isocratic eluent of water and acetonitrile (50:50), but it didn't give any separation of the enantiomers of **5**. Table 2.11 show the different compositions of the eluents with DEA and the R_S -values obtained for the enantiomers of **5** with the Chiralcel OD-H column. All analyzes were performed with a flow of 0.4 mL/min.

Table 2.11: Test of eluent systems for separation of the enantiomers of esmolol (**5**) with a Chiralcel OD-H column.

Entry	<i>n</i> -Hexane [%]	2-Propanol [%]	DEA [%]	R_S ((<i>R</i>)/(<i>S</i>)- 5)
1	50	49.6	0.4	1.40
2	70	39.6	0.4	2.58
3	80	29.6	0.4	5.90
4	85	14.6	0.4	7.31
5	90	9.6	0.4	5.89

As seen from Table 2.11 several different eluent systems were tested for separation of the esmolol (**5**) enantiomers. The R_S values for the eluent compositions tested gave baseline separation of the esmolol (**5**) enantiomers for all entries except for entry 1. The problem with separation of the esmolol (**5**) enantiomers was that the peak of (*S*)-**3** overlapped with the peak of (*S*)-**5** for all entries. The HPLC method for separation of esmolol (**5**) enantiomers should be optimized further, but due to time constraints it was not performed in this thesis.

The chromatogram of (*S*)-esmolol ((*S*)-**5**) analyzed by chiral HPLC using a Chiralcel OD-H column with an isocratic eluent of *n*-hexane and 2-propanol (90:10) gave t_R

((*S*)-**5**) = 49.2 min and t_R ((*R*)-**5**) = 27.6 min with $R_S = 5.89$ (Figure 2.19). The chromatogram also show traces of (*R*)-**5** ($t_R = 27.6$ min), (*R*)-**3** ($t_R = 60.1$, and an unidentified impurity with $t_R = 31.2$ min (*S*)-**5** was obtained in 86% yield with 96% purity and an ee of 89%.

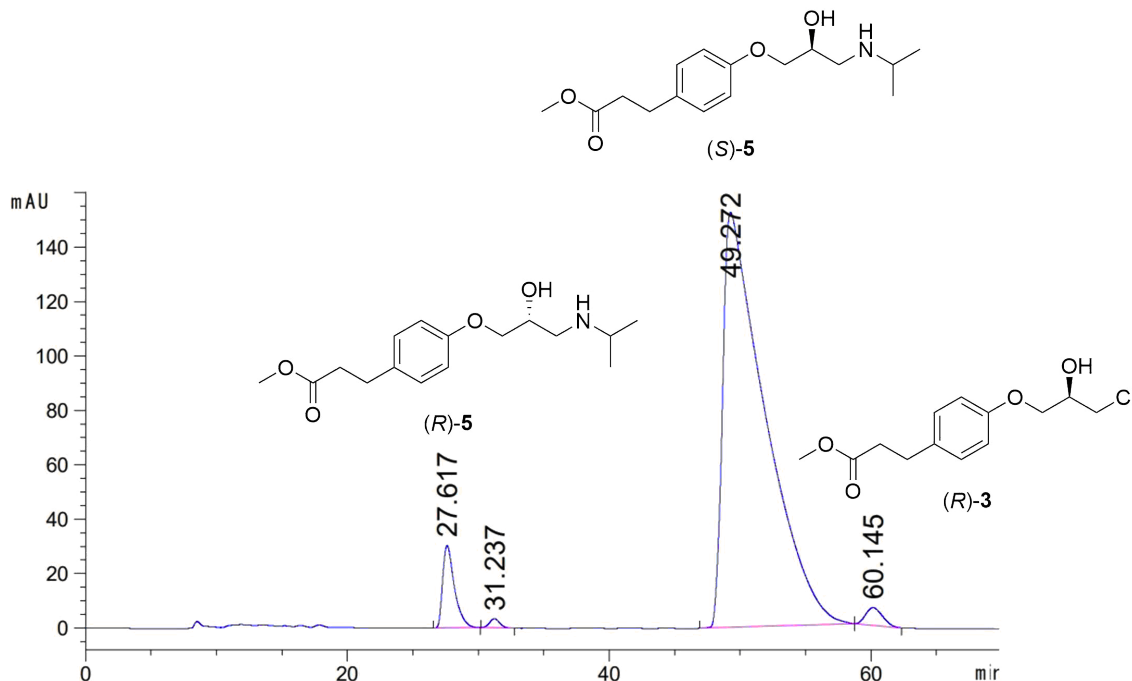
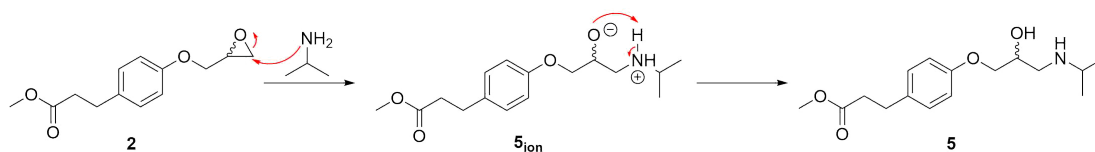


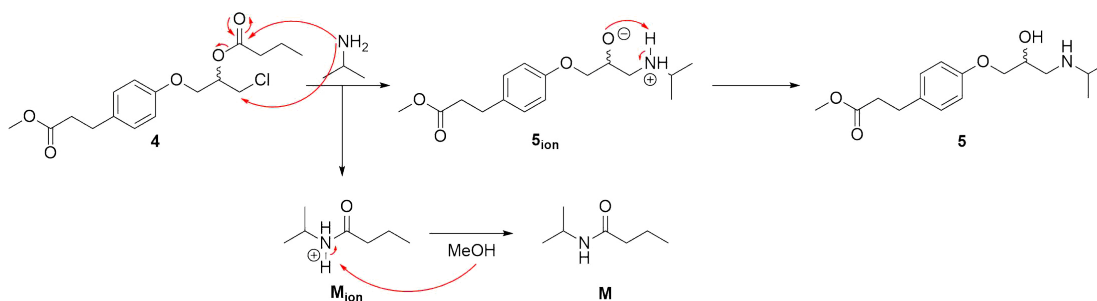
Figure 2.19: HPLC chromatogram of (*S*)-esmolol ((*S*)-**5**) ($t_R = 49.2$ min). The chromatogram also show traces of (*R*)-**5** ($t_R = 27.6$ min), (*R*)-**3** ($t_R = 60.1$, and an unidentified impurity with $t_R = 31.2$ min. $R_S = 5.89$.

The sample of (*R*)-**3** analyzed from the large-scale kinetic resolution (Figure 2.16) was analyzed with the same method as for separation of (*S*)-**5** (Entry 5 in Table 2.11) to identify which peaks corresponded to epoxide **2**, (*S*)/(*R*)-**3**, and ester **4**. As mentioned earlier it was discovered that epoxide **3** was not separated into its respective enantiomers. The reason why this could be seen from comparing the chromatograms (Figure 2.16 and 2.19) is because studies have shown that epoxide **2** in presence with isopropylamine reacts in a ring-opening to form esmolol, and one of the peaks from the large-scale chromatographic analysis with the esmolol-method disappeared. A suggested mechanism for formation of racemic esmolol (**5**) from epoxide **2** is given in Scheme 2.13.



Scheme 2.13: Reaction mechanism of formation of racemic esmolol (**5**) from epoxide **2** and isopropylamine.

Another observation that was made when comparing the chromatogram in Figure 2.19 and the large-scale analysis with this method was that the peak for ester **4** also disappeared. A theory is that the ester also can be amine alkylated to form esmolol **5**. This will in that case form a by-product, which is shown as by-product **M** in Scheme 2.14. Scheme 2.14 also show a suggested reaction mechanism to form racemic esmolol (**5**) from racemic ester (**4**). By-product **M** has not been analyzed by LC-MS due to time constraints.



Scheme 2.14: Reaction mechanism of formation of racemic esmolol (**5**) from ester (**4**) and isopropylamine with a possible by-product **M**.

If ester **4** can be amine alkylated as shown (Scheme 2.14) it would be mostly (*S*)-**4** which is formed into (*R*)-**5** because from the kinetic resolution the (*S*)-**4**/*(R)*-**4** ratio is high. As a consequence the enantiomeric excess is decreased, which could explain the decrease in enantiomeric excess of (*S*)-**5** (89% ee, $\Delta ee = 9\%$).

2.8.1 Characterization of esmolol (**5**)

Characterization of esmolol (**5**) was performed by NMR spectroscopy with deuterated chloroform as solvent. Esmolol (**5**) with numbered carbon atoms is given in Figure 2.20, and the corresponding shifts determined by ^1H -, ^{13}C -, H,H-COSY-, HSQC-, and HMBC-NMR spectroscopy are given in Table 2.12, including OH- and NH-protons. All spectra for esmolol (**5**) are given in Appendix D. The ^1H -NMR spectrum shows some impurities around the doublet at 1.08-1.07 ppm, and it is believed that some of these resonate for the protons in by-product **M** when comparing the shifts with the predicted spectrum in ChemDraw Professional.

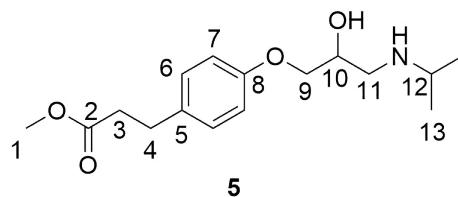


Figure 2.20: Synthesized esmolol (**5**) with labeled carbon atoms. Assignment of chemical shifts are given in Table 2.12, and all spectra are given in Appendix D.

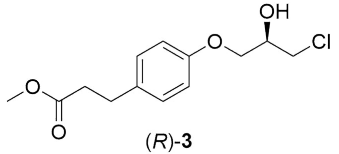
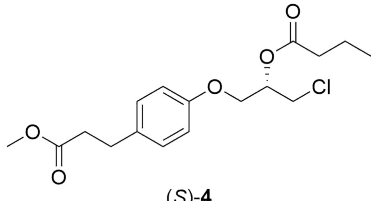
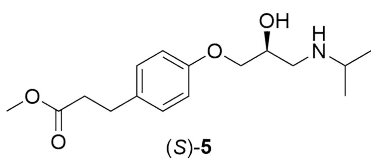
Table 2.12: Characterization of esmolol (**5**) given ^1H -, ^{13}C -, H,H-COSY, HSQC- and HMBC-NMR (600 MHz, CDCl_3), see Appendix D.

Position	^1H -NMR [ppm] (mult., int., ^3J)	^{13}C -NMR [ppm]	COSY	HMBC
1	3.66 (s, 3H)	51.6	-	2
2	-	173.4	-	1, 3, 4
3	2.60-2.58 (t, 2H, 7.83 Hz)	36.0	4	2, 4, 5
4	2.90-2.87 (t, 2H, 7.83 Hz)	30.1	3	2, 3, 6
5	-	133.0	-	3, 7
6	7.11-7.09 (m, 2H)	129.3	7	4, 6, 8
7	6.84-6.83 (m, 2H)	114.6	6	5, 7, 8
8	-	157.3	-	6, 7
9	3.95-3.94 (m, 2H)	70.6	-	10
10	4.01-3.96 (m, 1H)	68.6	-	10, 11
11	2.72-2.69 (dd, 1H, 7.40 Hz) 2.86-2.85 (d, 1H, 3.76 Hz)	49.3	11	10, 12, 13
12	2.83-2.79 (quint., 1H, 6.22 Hz)	48.9	13	11, 13
13	1.08-1.07 (d, 6H, 6.22 Hz)	23.1/23.2	12	11, 13
OH	Not observed	-	-	-
NH	Not observed	-	-	-

2.9 Optical rotation of enantiopure compounds

The optical rotation was determined for (*R*)-**3**, (*S*)-**4**, and (*S*)-**5**, and the results are given in Table 2.13. The optical rotation, α , was measured at 589 nm (D) and 20°C, and calculated using Equation (1.8) to give the correct value for the exact concentration.

Table 2.13: Optical rotation of (*R*)-**3**, (*S*)-**4**, and (*S*)-**5**, measured at 20°C and 589 nm (D). The optical rotation, α , was calculated using Equation (1.8) for the exact concentration.

Compound	ee [%]	$[\alpha]_D^{20}$
 (<i>R</i>)- 3	98	-5.19° (<i>c</i> 1.5, <i>i</i> -PrOH)
 (<i>S</i>)- 4	89	$+53.80^\circ$ (<i>c</i> 1.7, <i>i</i> -PrOH)
 (<i>S</i>)- 5	89	-5.48° (<i>c</i> 1.5, <i>i</i> -PrOH) -5.59° (<i>c</i> 1.4, CHCl ₃)

The absolute configuration of compound (*R*)-**3**, (*S*)-**4**, and (*S*)-**5** was determined by the enantioselectivity of CALB, which previously has been reported.^{54,55} There are no previous reported values for the optical rotation of (*R*)-**3** or (*S*)-**4**. Narsaiah and Kumar⁵⁶ reported in 2011 an optical rotation of (*S*)-**5** of $[\alpha]_D^{21} = +4.5$ (*c* 1, CHCl₃), while in this thesis an optical rotation of (*S*)-**5** was determined to be $[\alpha]_D^{20} = -5.59$ (*c* 1.4, CHCl₃) (Table 2.13). The reported optical rotation and the one determined in this thesis are quite similar, but have opposite sign. Narsaiah and Kumar⁵⁶ haven't report a value for the enantiomeric excess of (*S*)-esmolol ((*S*)-**5**) nor how the absolute configuration was determined. Therefore, their value of the optical rotation of (*S*)-**5** is unreliable and doesn't give any information about (*S*)-**5**.

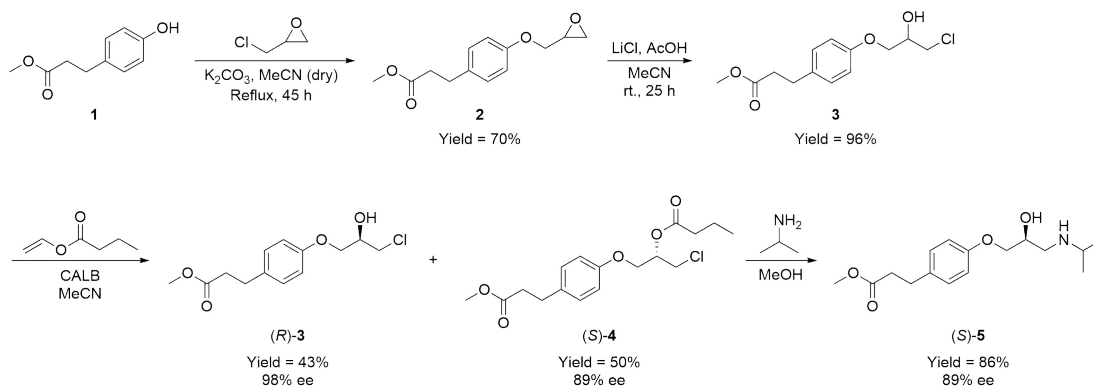
The optical rotation of (*S*)-**5** was also measured in 2-propanol, and when comparing the values of optical rotation for (*R*)-**3** and (*S*)-**5**, they are quite similar. Because both samples had some impurities, purity of 97% and 96% respectively, it is believed that the values of optical rotation of these compounds should be higher, and closer

to each other as there is a small difference in purities of the compounds. Further, the enantiomeric excess of (*S*)-**5** (89% ee) is lower than for (*R*)-**3** (98% ee), which means that the optical purity of (*S*)-**5** should be more increased than for (*R*)-**3**.

For (*S*)-**4**, the optical rotation should be lower or higher depending on the impurities. From NMR analysis (*S*)-**4** was only 71% pure, and from HPLC an enantiomeric excess of only 89% was determined.

3 Conclusion

The main aim of this thesis was to synthesize enantiomerically pure (*S*)-esmolol ((*S*)-**5**) by the use of biocatalysis. The synthetic pathway with yields and enantiomeric excess (ee) obtained for each compound is shown in Scheme 3.1.



Scheme 3.1: Synthetic pathway with yields of each compound leading to the target compound (*S*)-**5**.

The initial synthesis step was to synthesize epoxide **2** from deprotonated phenol **1** and epichlorohydrin. Both sodium hydroxide and potassium carbonate was used as base, but the reaction was not successful using sodium hydroxide. The synthesis of epoxide **2** was performed with 2 equivalents of potassium carbonate and epichlorohydrin, and epoxide **2** was isolated in 70% yield and a purity of 99% (determined by 1H -NMR) after purification by flash chromatography. The low yield of epoxide **2** can be explained by formation of dimer **A** and dimer derivative **L** as by-products.

In the second synthesis step, epoxide **2** was ring-opened using 2 equivalents of lithium chloride and 5 equivalents of acetic acid. The reaction did not proceed to full conversion of epoxide **2**, and unknown by-products were formed. Chlorohydrin **3** was obtained in 96% yield with 98% purity.

Kinetic resolution of racemic chlorohydrin **3** was performed using CALB as a catalyst and vinyl butanoate as an acyl donor. The enantiomeric ratio was determined to be 157, and enantiomerically pure (*R*)-**3** was obtained in 43% yield with 97% purity and 98% ee (determined by HPLC). Ester (*S*)-**4** was obtained in 50% yield with 71% purity and 89% ee. The low purity of (*S*)-**4** is due to formation of butanoic acid because of water in the reaction system. This was determined by comparing 1H -NMR spectra of butanoic acid and (*S*)-**4**. Optical rotation of (*R*)-**3** and (*S*)-**4** was determined to be $[\alpha]_D^{20} = -5.19^\circ$ (*c* 1.5, *i*-PrOH) and $+53.80^\circ$ (*c* 1.7, *i*-PrOH) respectively.

Enantiopure (*S*)-esmolol ((*S*)-**5**) was synthesized by alkylation of isopropylamine

with (*R*)-**3**. Isopropylamine was used in large excess, but the reaction did not proceed to full conversion of (*R*)-**3**. (*S*)-**5** was obtained in 86% yield with 96% purity and 89% ee. The HPLC showed formation of racemic **5** from racemic epoxide **2** and enantiopure (*S*)-**4**, which is the reason for the low enantiomeric excess. The optical rotation of (*S*)-**5** was determined to be $[\alpha]_{\text{D}}^{20} = -5.48^{\circ}$ (*c* 1.5, *i*-PrOH).

4 Future Work

It would be of interest to improve each synthetic step leading to (*S*)-esmolol ((*S*)-**5**).

The first synthesis step forming epoxide **2** could be improved to produce chlorohydrin **3** and epoxide **2** in a high ratio as seen when using sodium hydroxide as base. It would therefore be of interest to do a study of different bases for this reaction step to achieve full conversion of phenol **1**, and ideally avoid heating, excess use of base, and by-product formation. The amount of epichlorohydrin can also be of interest to increase to achieve full conversion of phenol **1** at a higher rate. It would be of interest to perform a time-analysis in order to get better understanding of the reaction pathway.

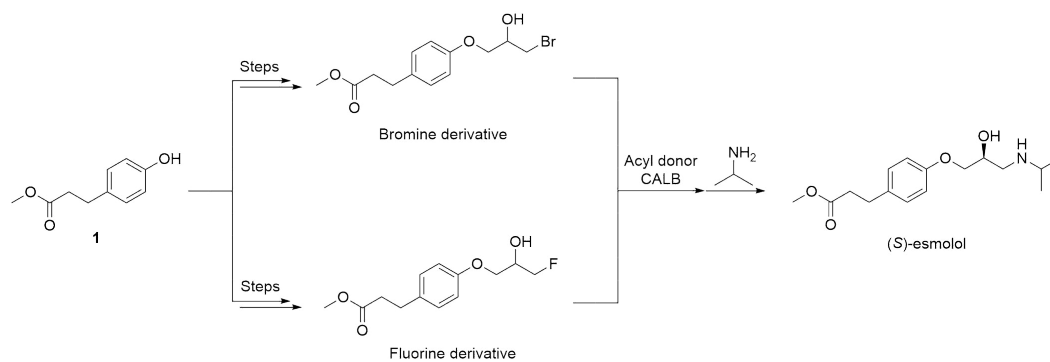
The second synthesis step forming chlorohydrin **3** could be improved in order to achieve full conversion of epoxide **2**. This would include optimization of the number of equivalents used of lithium chloride and acetic acid, and varying the concentration of the substrate and reagents. In addition, it would be optimal to find an efficient purification method if by-products are formed.

Kinetic resolution of chlorohydrin **3** was very time-consuming due to the use of two different HPLC analysis methods for the enantiomers of chlorohydrin **3** and ester **4**. It would be of interest to try to separate the enantiomers of **3** and **4** by the same HPLC method by the use of an additive (DEA or TFA) or a different chiral column like a Chiralcel OD-RH column. Since the kinetic resolution of racemic chlorohydrin **3** maximally can form (*R*)-**3** in 50% yield, it would be of interest to perform dynamic kinetic resolution of the racemic mixture of chlorohydrin **3** in order to be able to achieve (*R*)-**3** in yields above 50%.

Finally, the fourth synthesis step should be optimized by using a larger excess of isopropylamine to achieve full conversion of (*R*)-**3**. Increasing the amount of isopropylamine could also reduce the reaction time, which is optimal due to less heating-time and the possibility of less by-product formation. It would also be of interest to find a suitable purification method, and HPLC method for separation of the enantiomers from other compounds in the product.

To take it one step further, it would be of interest to synthesize (*S*)-esmolol via the bromine and fluorine derivatives of chlorohydrin **3** in order to study the effects of changing halogen substituent, where fluorine is the least effective leaving group and bromine the most effective leaving group, see Scheme 4.1. Although epifluorohydrin is more expensive than epichlorohydrin, it would be interesting to study the effect of changing to a less effective leaving group, as this preferably will form fluorohydrin over epoxide. In this way, the synthetic pathway to enantiopure (*S*)-esmolol may be reduced by one reaction step. However, the last step may not proceed due to fluorine being a less effective leaving group. On the other hand, the bromine derivative may

be a better choice of precursor for (*S*)-esmolol regarding the last reaction step.



Scheme 4.1: Suggested route to (*S*)-esmolol via bromine and fluorine derivatives as building blocks.

5 Experimental

5.1 General methods

All experiments and analyzes were performed at the Department of Chemistry, Faculty of Natural Sciences, University of Science and Technology (NTNU), Trondheim, Norway.

5.1.1 Chemicals, solvents and enzymes

All chemicals used in the syntheses and analyzes are commercially available, and of analytical quality. The chemicals were bought from Sigma Aldrich (Oslo, Norway) and VWR, (Oslo, Norway). The water used was of distilled grade and heating of chemical reactions were performed by use of an oil bath. The laboratory work was carried out under the university's HSE guidelines.

All solvents used for HPLC analyzes were of HPLC grade.

Dry solvents

Dry solvents (MeCN) were acquired from a solvent purifier from MBraun (München, Germany). The dry solvents were dried by storage with molecular sieve (4Å), and flushed with nitrogen before use.

Activation of molecular sieve

Molecular sieve (1/8 pellets, pore diameter 4Å) were dried at 1000°C for 24 hours and stored in a desiccator.

Enzymes

Candida antarctica Lipase B (activity > 10 000 PLU/g, lot# 20170315) immobilized on styrene/methacrylate polymer. Gifted from SyncoZymes Co, Ltd. (Shanghai, China).

5.1.2 Chromatographic analyzes

Chromatography methods used were thin layer chromatography (TLC), flash chromatography, high-performance liquid chromatography (HPLC), and liquid chromatography-mass spectroscopy (LC-MS).

Thin layer chromatography

TLC was performed using precoated Merck silica gel 60 F₂₅₄ (0.2 mm) plates from Sigma Aldrich, (Oslo, Norway), and separated compounds were identified under

ultraviolet (UV) light (254 nm).

Flash Chromatography

Flash chromatography was performed with silica gel (pore size 60 Å, 230-240 mesh particle size, 40-63 µm particle size) from Sigma Aldrich, (Oslo, Norway). All separations were performed with an eluent of MeCN:CH₂Cl₂ (1:11).

Achiral HPLC

Achiral HPLC was performed on an Agilent 1290 system from Matriks AS, (Oslo, Norway), equipped with an auto injector (4 µL), and detection was performed by a diode array detector (DAD, λ = 254 nm). All separations of **1**, **2**, **3** and by-products were performed on a ACE Excel 5 C18 column from Matriks AS, (Oslo, Norway) (150 mm × 4.6 mm ID; 5 µm), with an isocratic eluent of water and acetonitrile (50:50) over 12 minutes, flow = 1 mL/min.

Chiral HPLC

Chiral HPLC was performed on an Agilent 1100 system (Santa Clara, CA, USA) equipped with a manual injector (Rheodyne 77254i/Agilent, 20 µL loop), and a variable wavelength detector (VWD, 254 nm). All separations of (*S*)/(*R*)-**3**, (*S*)/(*R*)-**4**, and (*S*)/(*R*)-**5** were performed on a Chiralcel® OD-H column from Daicel (Chiral Technologies Europe, Gonthier d'Andernach, Illkirch, France) (250 mm × 4.6 mm ID; 5 µm).

Method for separation of chlorohydrin **3** enantiomers: *n*-hexane:2-propanol (90:10), 1 mL/min, 10 µL injection.

Method for separation of ester **4** enantiomers: *n*-hexane:2-propanol (97:3), 1 mL/min, 10 µL injection.

Method for separation of esmolol (**5**) enantiomers: *n*-hexane:2-propanol:diethylamine (90:9.6:0.4), 0.4 mL/min, 10 µL injection.

Liquid Chromatography-Mass Spectroscopy (LC-MS)

LC-MS analyzes of by-products were performed on a AQUITY UPLC I-Class system (Waters, Milford, USA) coupled to a quadrupole time of flight mass analyzer (QTOF; SYNAPT-G2S) with a ZSpray EIS ion source (Waters, Milford, USA). A AQUITY UPLC BEH C18 column (130Å, 1.7 µm ID, 2.1 mm × 100 mm) was used for chromatographic separation with a mobile phase composition of water (A) and acetonitrile (B), both with 0.1% formic acid. Method: Isocratic (80% A:20% B) over 12 min, then gradient (0% B:%B) from 12-13.5 min, and then back to (80% A:20% B) until 15 min, flow = 0.25 mL/min.

5.1.3 Spectroscopic analyzes

Nuclear magnetic resonance (NMR)

NMR characterizations were performed on a 600 MHz Bruker Avance III UltraShield from Bruker Corporation (Fällanden, Switzerland), equipped with a CryoProbe 5 mm TCI probehead. All other NMR analyzes were performed on a 400 MHz Bruker Avance III HD NMR Spectrometer from Bruker Corporation (Fällanden, Switzerland), equipped with a SmartProbe 5 mm probehead. The spectroscopic data were analyzed with Bruker TopSpin 3.6.2.

5.1.4 Other methods

Shaker

The enzyme reactions were performed in a New Brunswick G24 Environmental Incubator Shaker from New Brunswick Co. (Edison, New Jersey, USA).

Optical rotation

Optical rotation was performed with a Anton Paar MCP 5100 polarimeter with a 2.5 mm long cell from Dipl. Ing. Houm AS (Oslo, Norway). The samples were dissolved in *i*-PrOH at room temperature (20°C). The light had a wavelength of 589 nm (D).

5.2 Synthesis of racemic building blocks and achiral compounds

5.2.1 Synthesis of a mixture of methyl 3-(4-(oxiran-2-ylmethoxy)phenyl)propanoate (**2**) and methyl 3-(4-(3-chloro-2-hydroxypropoxy)phenyl)propanoate (**3**) with NaOH

To a mixture of methyl 3-(4-hydroxyphenyl)propanoate (**1**) (0.58 g, 3.22 mmol) and epichlorohydrin (0.50 mL, 6.44 mmol), NaOH (0.2 M, 4.81 mL, 0.97 mmol) was added and set to stir at rt. for 24 h. NaOH (1 M, 3.21 mL, 3.22 mmol) was added and the reaction was stirred for another 144 hours. The reaction was monitored by TLC (CH₂Cl₂:MeOH) (20:1); R_f (**1**) = 0.52, R_f (**2**) = 0.77, and R_f (**3**) = 0.61. EtOAc (50 mL) was added and the phases were separated. The organic phase was washed with distilled H₂O (20 mL), and the combined water phase was extracted with EtOAc (2 × 30 mL). The combined organic layer was washed with saturated NaCl-solution (30 mL) and dried over MgSO₄. Organic solvent was removed under reduced pressure, and epoxide **2** and chlorohydrin **3** were separated by flash chromatography (CH₂Cl₂:MeCN) (11:1). Epoxide **2** was obtained in 2% yield (14.3 mg, 0.06 mmol)

with 96% purity ($^1\text{H-NMR}$) as a light yellow liquid, and chlorohydrin **3** in 49% yield (0.43 g, 1.57 mmol) with 86% purity ($^1\text{H-NMR}$) as a light yellow liquid. The total conversion of phenol **1** was determined by HPLC analysis using a ACE Excel 5 C18 column with an isocratic mobile phase ($\text{H}_2\text{O}:\text{MeCN}$) (50:50) over 12 min, flow = 1.0 mL/min, which gave t_{R} (**1**) = 2.8 min, t_{R} (**2**) = 4.8 min, and t_{R} (**3**) = 4.4 min.

5.2.2 Synthesis of methyl 3-(4-(oxiran-2-ylmethoxy)phenyl)propanoate (**2**) with K_2CO_3

To a mixture of methyl 3-(4-hydroxyphenyl)propanoate (**1**) (0.26 g, 1.42 mmol) and K_2CO_3 (0.51 g, 3.70 mmol) in anhydrous MeCN (15 mL) epichlorohydrin (0.22 mL, 2.84 mmol) was added and the reaction mixture was set to stir and heated under reflux for 45 h. The reaction was monitored by TLC ($\text{MeCN}:\text{CH}_2\text{Cl}_2$) (1:11); R_{f} (**1**) = 0.28, R_{f} (**2**) = 0.50. The reaction mixture was cooled, filtered under vacuum and washed with MeCN. The filtrate was concentrated under reduced pressure, EtOAc (25 mL) was added, and the solution washed with distilled H_2O (10 mL). The water phase was extracted with EtOAc (3×15 mL), and the combined organic layer was washed with saturated NaCl-solution (15 mL) and dried over MgSO_4 . Organic solvent was removed under reduced pressure, and phenol **1** and epoxide **2** was separated by flash chromatography ($\text{CH}_2\text{Cl}_2:\text{MeCN}$) (11:1). Epoxide **2** was obtained in 70% yield (0.24 g, 1.00 mmol) with 99% purity ($^1\text{H-NMR}$) as a light yellow liquid. The total conversion of phenol **1** was determined by HPLC analysis using a ACE Excel 5 C18 column with an isocratic mobile phase composition of $\text{H}_2\text{O}:\text{MeCN}$ (50:50) over 12 min, flow = 1 mL/min, which gave t_{R} (**1**) = 2.8 min and t_{R} (**2**) = 4.8 min; $^1\text{H-NMR}$ (600 MHz, CDCl_3) δ : 7.10-7.09 (m, 2H, Ar-H), 6.85-6.82 (m, 2H, Ar-H), 4.19-4.17 (dd, 1H, $^3\text{J} = 14.27$, -CH-O-), 3.94-3.91 (m, 1H, -CH-O-), 3.65 (s, 3H, -CH₃), 3.34-3.31 (m, 1H, -CH-O-), 2.89-2.87 (m, 3H, -CH₂-Ar/-CH-O-), 2.74-2.73 (m, 1H, -CH-O-), 2.60-2.57 (m, 2H, -CH₂-CO₂-); $^{13}\text{C-NMR}$ (600 MHz, CDCl_3) δ : 173.4, 157.0, 133.2, 129.3 (2C), 114.7 (2C), 68.8, 51.6, 50.2, 44.7, 35.9, 30.1. The analysis is consistent with previous reported data.¹³

5.2.3 Synthesis of methyl 3-(4-(3-chloro-2-hydroxypropoxy)phenyl)propanoate (**3**) by ring-opening of methyl 3-(4-(oxiran-2-ylmethoxy)phenyl)propanoate (**2**)

To a mixture of methyl 3-(4-(oxiran-2-ylmethoxy)phenyl)propanoate (**2**) (0.21 g, 0.88 mmol), LiCl (0.08, 1.94 mmol), and MeCN (5 mL), AcOH (0.25 mL, 3.98 mmol) was added and the reaction mixture was set to stir at rt. for 25 h. The reaction was monitored by TLC ($\text{MeCN}:\text{CH}_2\text{Cl}_2$) (1:11): R_{f} (**3**) = 0.31 The reaction mixture was quenched with Na_2CO_3 (pH 12) to a neutral pH followed by extraction with CH_2Cl_2 (3×20 mL). The combined organic layer was washed with saturated

NaCl-solution (15 mL) and dried over MgSO_4 . Organic solvent was removed under reduced pressure, giving chlorohydrin **3** in 96% yield (0.23 g, 0.84 mmol) with 98% purity ($^1\text{H-NMR}$) as a light yellow liquid. The total conversion of epoxide **2** was determined by HPLC analysis using a ACE Excel 5 C18 column with an isocratic mobile phase composition of $\text{H}_2\text{O}:\text{MeCN}$ (50:50) over 12 min, flow = 1 mL/min, which gave t_{R} (**2**) = 24.8 min and t_{R} (**3**) = 4.4 min; $^1\text{H-NMR}$ (600 MHz, CDCl_3) δ : 7.13-7.10 (m, 2H, Ar-**H**), 6.85-6.83 (m, 2H, Ar-**H**), 4.22-4.18 (m, 1H, -**CH**-), 4.09-4.04 (m, 2H, -**CH**₂-O-), 3.79-3.71 (m, 2H, -**CH**₂-Cl), 3.66 (s, 3H, -**CH**₃), 2.91-2.88 (m, 2H, -**CH**₂-Ar), 2.61-2.58 (m, 2H, -**CH**₂-CO₂-), 2.56-2.55 (d, 1H, $^3J = 5.93$ Hz, **OH**); $^{13}\text{C-NMR}$ (600 MHz, CDCl_3) δ : 173.4, 156.8, 133.5, 129.4 (2C), 114.7 (2C), 68.9, 68.6, 51.6, 46.0, 36.0, 30.1. The analysis is consistent with previous reported data.¹³

5.3 Enzyme catalyzed kinetic resolutions of racemates

5.3.1 Derivatization reaction of methyl 3-(4-(3-chloro-2-hydroxypropoxy)phenyl)propanoate (**3**)

To a GC-glass methyl 3-(4-(3-chloro-2-hydroxypropoxy)phenyl)propanoate (**3**) (23 mg, 0.09 mmol), butyric anhydride (2 droplets) and pyridine (2 droplets) were dissolved in hexane (0.5 mL). The reaction was run with air heating to 60°C for 1 h, and analyzed by chiral HPLC. A Chiralcel OD-H column with isocratic mobile phase composition of *n*-hexane and *i*-PrOH (90:10), flow 1 mL/min gave t_{R} (*(S)*/*(R)*-**4**) = 9.87 min, and t_{R} (*(S)*/*(R)*-**3**) = 22.32 min and 24.62 min, R_{S} (*(S)*/*(R)*-**3**) = 1.98. A Chiralcel OD-H column with isocratic mobile phase composition of *n*-hexane and *i*-PrOH (97:3), flow 1 mL/min gave t_{R} (*(S)*/*(R)*-**4**) = 19.45 min and 20.95 min, R_{S} (*(S)*/*(R)*-**4**) = 1.56. Analytes were dissolved in *i*-PrOH before analysis. The retention times corresponds to what is previously reported.^{13,40}

5.3.2 Small-scale kinetic resolution of methyl 3-(4-(3-chloro-2-hydroxypropoxy)phenyl)propanoate (**3**) with CALB

Methyl 3-(4-(3-chloro-2-hydroxypropoxy)phenyl)propanoate (**3**) (58.7 mg, 0.22 mmol) was dissolved in dry MeCN (3 mL), and vinyl butanoate (98.2 mg, 0.86 mmol), CALB (53 mg), and molecular sieves (4Å) were added. The reaction was run for 30 h in an incubator at 200 rpm and 38°C. Samples of 150 μL were taken regularly until 30 hours of reaction, and analyzed by chiral HPLC using a Chiralcel OD-H column, and ee_{S} , ee_{P} , and c were calculated from the chromatograms.

5.3.3 Large-scale kinetic resolution of methyl 3-(4-(3-chloro-2-hydroxypropoxy)phenyl)propanoate (**3**) with CALB

Methyl 3-(4-(3-chloro-2-hydroxypropoxy)phenyl)propanoate (**3**) (0.52 g, 1.91 mmol) was dissolved in dry MeCN (3 mL), and vinyl butanoate (0.88 g, 7.73 mmol), CALB (0.51 g), and molecular sieves (4Å) were added. The reaction was run for 30 h in an incubator at 200 rpm and 38°C. The reaction was analyzed by chiral HPLC after 24 and 28 h. After 30 h, the reaction was stopped, CALB and molecular sieves were filtered off and the solvent was removed under reduced pressure. (*S*)-**4** and (*R*)-**3** were separated by flash chromatography (*n*-hexane:*i*-PrOH) (90:10). (*R*)-**3** was obtained in 43% yield (0.22 g, 0.81 mmol) with 97% purity (¹H-NMR) and an ee of 98% as a light yellow liquid, $[\alpha]_{\text{D}}^{20} = -5.19^\circ$, and (*S*)-**4** in 50% yield (0.32 g, 0.95 mmol) with 71% purity (¹H-NMR) and an ee of 89% as a yellow liquid, $[\alpha]_{\text{D}}^{20} = +53.80^\circ$. The ee-values were calculated from chiral HPLC analysis. **4**: ¹H-NMR (600 MHz, CDCl₃) δ : 7.13-7.11 (m, 2H, Ar-**H**), 6.85-6.82 (m, 2H, Ar-**H**), 5.35-5.31 (quint., 1H, ³J = 5.16 Hz, -**CH**-), 4.16-4.11 (m, 2H, -**CH**₂-O-), 3.86-3.76 (m, 2H, -**CH**₂-Cl), 3.66 (s, 3H, -**CH**₃), 2.90-2.88 (t, 2H, ³J = 7.77 Hz, -**CH**₂-Ar), 2.61-2.58 (t, 2H, ³J = 7.77 Hz, -**CH**₂-CO₂-), 2.34-2.32 (m, 2H, -**CH**₂-CO₂), 1.71-1.64 (m, 2H, -**CH**₂-CH₃), 0.99-0.95 (m, 3H, -**CH**₃); ¹³C-NMR (600 MHz, CDCl₃) δ : 173.4, 172.9, 156.8, 133.5, 129.4 (2C), 114.7 (2C), 70.9, 66.2, 51.6, 42.6, 36.1, 36.0, 30.1, 13.6, 18.4.

5.4 Synthesis of (*S*)-esmolol ((*S*)-**5**)

A mixture of (*R*)-**3** (0.15 g, 0.54 mmol), isopropylamine (0.89 mL, 10.83 mmol), and MeOH (5 mL) was heated under reflux for 24 h. The reaction was monitored by TLC (MeCN:CH₂Cl₂) (1:11); R_f ((*S*)-**5**) = 0.16. The reaction mixture was diluted with EtOAc (50 mL) and washed with distilled H₂O (20 mL). The organic layer was dried over MgSO₄, and solvent was removed under reduced pressure giving (*S*)-**5** in 86% yield (0.14 g, 0.47 mmol) with 96% purity (¹H-NMR) and an ee of 89% (HPLC) as a light yellow liquid; $[\alpha]_{\text{D}}^{20} = -5.48^\circ$; ¹H-NMR (600 MHz, CDCl₃) δ : 7.11-7.09 (m, 2H, Ar-**H**), 6.84-6.83 (m, 2H, Ar-**H**), 4.01-3.96 (m, 1H, -**CH**-), 3.95-3.94 (m, 2H, -**CH**₂-O-), 3.66 (s, 3H, -**CH**₃), 2.90-2.87 (t, 2H, ³J = 7.83 Hz, -**CH**₂-Ar), 2.86-2.85 (d, 1H, ³J = 3.76 Hz, -**CH**-NH-), 2.83-2.79 (quint., 1H, ³J = 6.22 Hz, -NH-**CH**-C₂H₆), 2.72-2.69 (dd, 1H, ³J = 7.40 Hz, -**CH**-NH-), 2.60-2.58 (t, 2H, ³J = 7.83 Hz, -**CH**₂-CO₂-), 1.08-1.07 (d, 6H, ³J = 6.22, -**CH**₃); ¹³C-NMR (600 MHz, CDCl₃) δ : 173.4, 157.3, 133.0, 129.3 (2C), 114.6 (2C), 70.6, 68.6, 51.6, 49.3, 48.9, 36.0, 30.1, 23.2, 23.1. The analysis is consistent with previous reported data.¹³

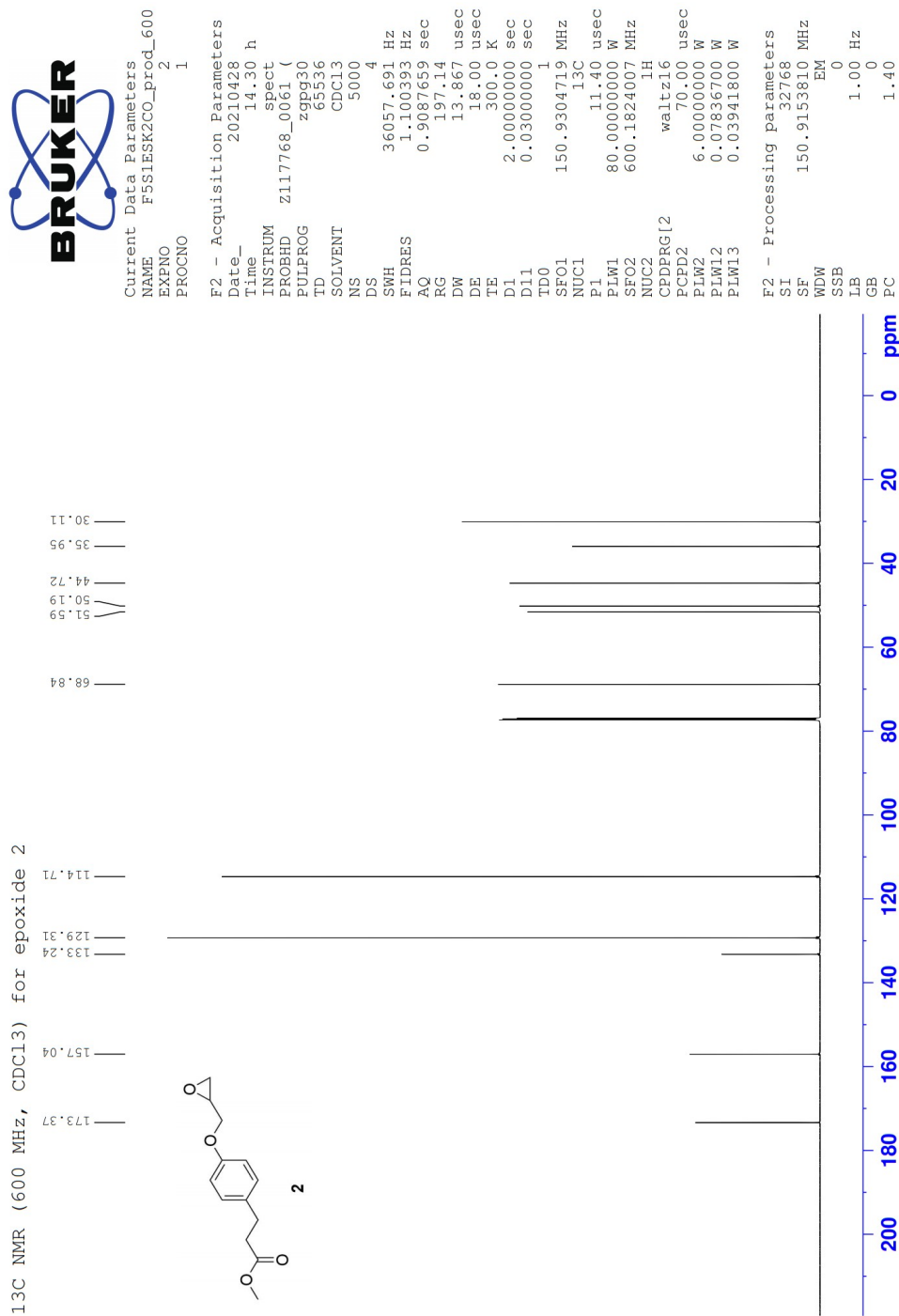
References

- (1) Gundersen, M.; Austli, G.; Løvland, S.; Hansen, M.; Rødseth, M.; Jacobsen, E. Lipase Catalyzed Synthesis of Enantiopure Precursors and Derivatives for β -Blockers Practolol, Pindolol and Cateolol. *Catalysts*. **2021**, *11*, 503.
- (2) Solomons, T.; Fryhle, C.; Snyder, S., *Organic Chemistry*, 11th ed., pp 199-200, 241, 246-247, 265-268, 271, 518-519, 525-527; John Wiley & Sons Inc.: 2014.
- (3) Tucker, G. Chiral Switches. *The Lancet (British edition)*. **2000**, *355*, 1085–1087.
- (4) Calcaterra, A.; D'Acquarica, I. The Market of Chiral Drugs: Chiral Switches Versus *de novo* Enantiomerically Pure Compounds. *J. Pharm. Biomed. Anal.* **2018**, *147*, 323–340.
- (5) Agranat, I.; Caner, H.; Caldwell, J. Putting Chirality to Work: The Strategy of Chiral Switches. *Nat. Rev. Drug Discov.* **2002**, *1*, 753–768.
- (6) Gellad, W.; Choi, P.; Mizah, M.; Good, C.; Kesselheim, A. Assessing the Chiral Switch: Approval and Use of Single-Enantiomer Drugs, 2001 to 2011. *Am. J. Manag. Care.* **2014**, *20*, 90–97.
- (7) Agustian, J.; Kamaruddin, A.; Bhatia, S. Single Enantiomeric β -Blockers - The Existing Technologies. *Process Biochem.* **2010**, *45*, 1597–1604.
- (8) Helseinformatikk, N. Betablokkere, <https://nhi.no/sykdommer/hjertekar/lakemedel/betablokkere/>, Accessed: 21.01.20, 2018.
- (9) Khan, M., *Cardiac Drug Therapy*, 8th ed., p 7; Humana Press: 2015.
- (10) Patric, G., *An Introduction to Medicinal Chemistry*, 2nd ed, p 789; Oxford University Press: 2001.
- (11) Friedman, P. Esmolol and Other Intravenous Beta-Blockers. *Card. Electrophysiol. Rev.* **2000**, *4*, 240.
- (12) Esmolol, <https://www.legemiddelhandboka.no/L8.2.2.5/Esmolol>, Accessed: 04.03.21, 2019.
- (13) Banoth, L.; Banerjee, U. New Chemical and Chemo-Enzymatic Synthesis of (*RS*)-, (*R*)-, and (*S*)-Esmolol. *Arab. J. Chem.* **2017**, *10*, 3603–3613.
- (14) Wiest, D.; Haney, J. Clinical Pharmacokinetics and Therapeutic Efficacy of Esmolol. *Clin. Pharmacokinet.* **2012**, *51*, 347–356.
- (15) Anastas, P. Introduction: Green Chemistry. *Chem. Rev.* **2007**, *107*, 2167–2168.
- (16) N.S., K.; Kumar, R. Chiral Synthesis: An Overview. *IJPRD.* **2014**, *6*, 70–78.
- (17) Rouf, A.; Taneja, S. Synthesis of Single-enantiomer Bioactive Molecules: A Brief Overview. *Chirality.* **2014**, *26*, 63–78.
- (18) Kagan, H.; Fiaud, J., *Topics in Stereochemistry*, p 251; John Wiley & Sons, Inc.: 1988; Vol. Vol. 18.
- (19) Faber, K., *Biotransformations in Organic Chemistry*, 6. ed., pp 22-23, 31, 40-41; Springer: 2011.

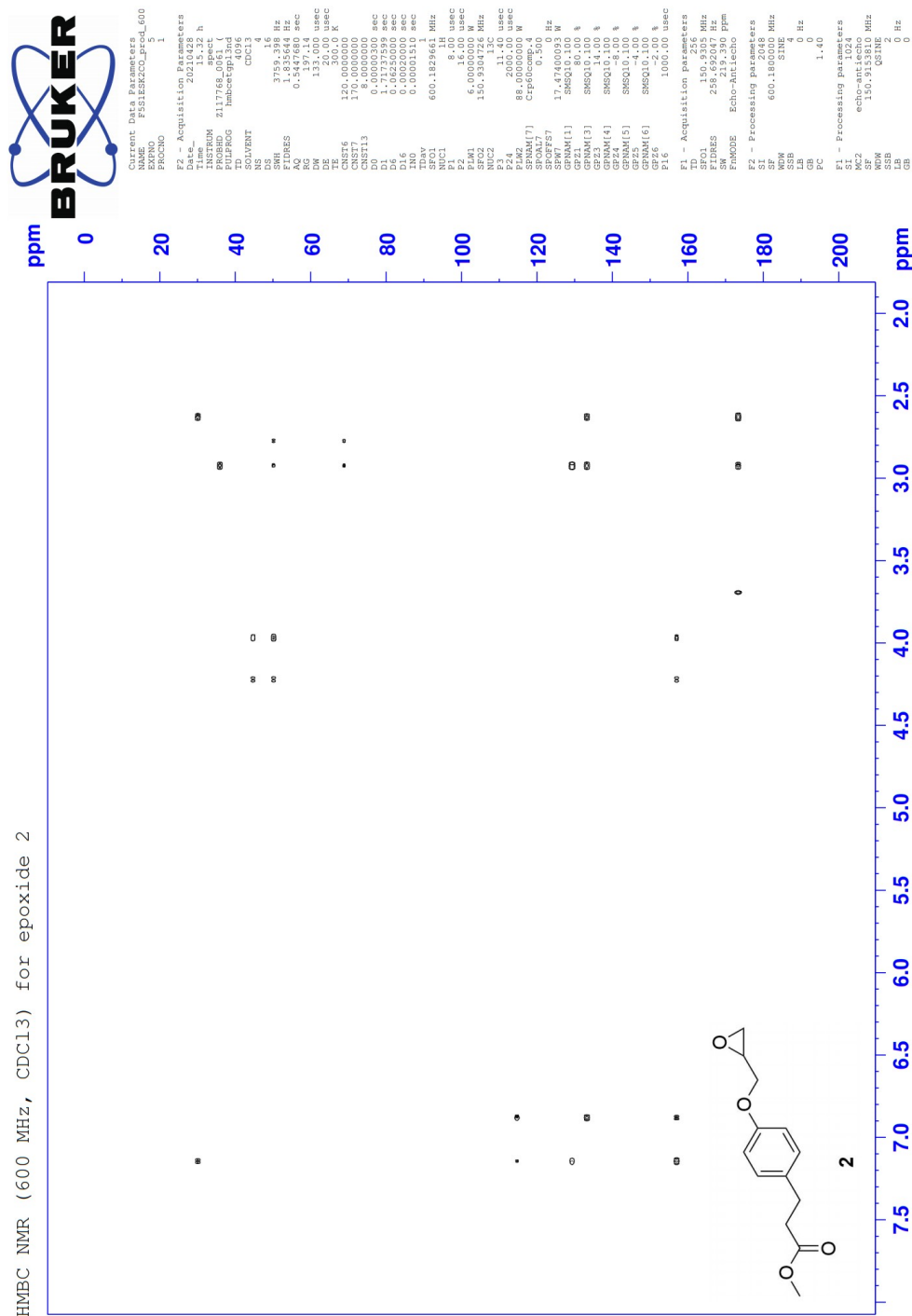
-
- (20) Galende, P.; Cuadrado, N.; Kostetsky, E.; Roig, M.; Villar, E.; Shnyrov, V.; Kennedy, J. Kinetics of Spanish Broom Peroxidase Obeys a Ping-Pong Bi-Bi Mechanism with Competitive Inhibition by Substrates. *Int. J. Biol. Macromol.* **2015**, *81*, 1005–1011.
- (21) Clealand, W. The Kinetics of Enzyme-Catalyzed Reactions with Two or More Substrates or Products. *Biochimica Et Biophysica Acta (BBA) - Specialized Section on Enzymological Subjects.* **1963**, *67*, 104–137.
- (22) Anthonsen, H.; Hoff, B.; Anthonsen, T. Calculation of Enantiomer Ratio and Equilibrium Constants in Biocatalytic Ping-Pong Bi-Bi Resolutions. *Tetrahedron: Asymmetry.* **1996**, *7*, 2633–2638.
- (23) Straathof, A.; A., J. J. The Enantiomeric Ratio: Origin, Determination and Prediction. *Enzyme Microb. Technol.* **1997**, *21*, 559–571.
- (24) Adlercreutz, P. Immobilisation and Application of Lipases in Organic Media. *Chem. Soc. Rev.* **2013**, *42*, 6406.
- (25) Bezborodov, A.; Zagustina, N. Lipases in Catalytic Reactions of Organic Chemistry. *Appl. Biochem. and Microbiol.* **2014**, *50*, 313–337.
- (26) Wu, X.; Sun, W.; Xin, J.; Xia, C. Lipase-Catalysed Kinetic Resolution of Secondary Alcohols with Improved Enantioselectivity in Propylene Carbonate. *World J. Microbiol. Biochem.* **2008**, *24*, 2421–2424.
- (27) Jing, Q.; Kazlauskas, R. Determination of Absolute Configuration of Secondary Alcohols Using Lipase-Catalyzed Kinetic Resolutions. *Chirality.* **2008**, *20*, 724–735.
- (28) Duleba, J.; Czirson, K.; Siódmiak, T.; M.P., M. Lipase B from *Candida antarctica* - The Wide Applicable Biocatalyst in Obtaining Pharmaceutical Compounds. *Med. Res. J.* **2019**, *4*, 174–177.
- (29) Stauch, B.; Fisher, S.; Cianci, M. Open and Closed States of *Candida antarctica* Lipase B: Protonation and the Mechanism of Interfacial Activation. *J. Lipid Res.* **2015**, *56*, 2348–2358.
- (30) Trodler, P.; Pleiss, J. Modeling Structure and Flexibility of *Candida antarctica* Lipase B in Organic Solvents. *BMC Struct. Biol.* **2008**, *8*, 9.
- (31) Raza, S. Enantioselectivity in *Candida antarctica* Lipase B: A Molecular Dynamics Study. *Protein Sci.* **2001**, *10*, 329–338.
- (32) Bøckmann, P. Synthesis of Enantiopure β -Blocker (*S*)-Metoprolol and Derivatives by Lipase Catalysis, MA thesis, Norwegian University of Science and Technology, 2016.
- (33) Kazlauskas, R.; Weissfloch, N.; Rappaport, A.; Cuccia, L. A Rule to Predict which Enantiomer of a Secondary Alcohol Reacts Faster in Reactions Catalyzed by Cholesterol Esterase, Lipase from *Pseudomonas cepacia*, and Lipase from *Candida rugosa*. *J. Org. Chem.* **1991**, *56*, 2656–2665.
- (34) Kumar, A.; Dhar, K.; Kanwar, S.; Arora, P. Lipase Catalysis in Organic Solvents: Advantages and Applications. *Biol. Proced. Online.* **2016**, *18*.

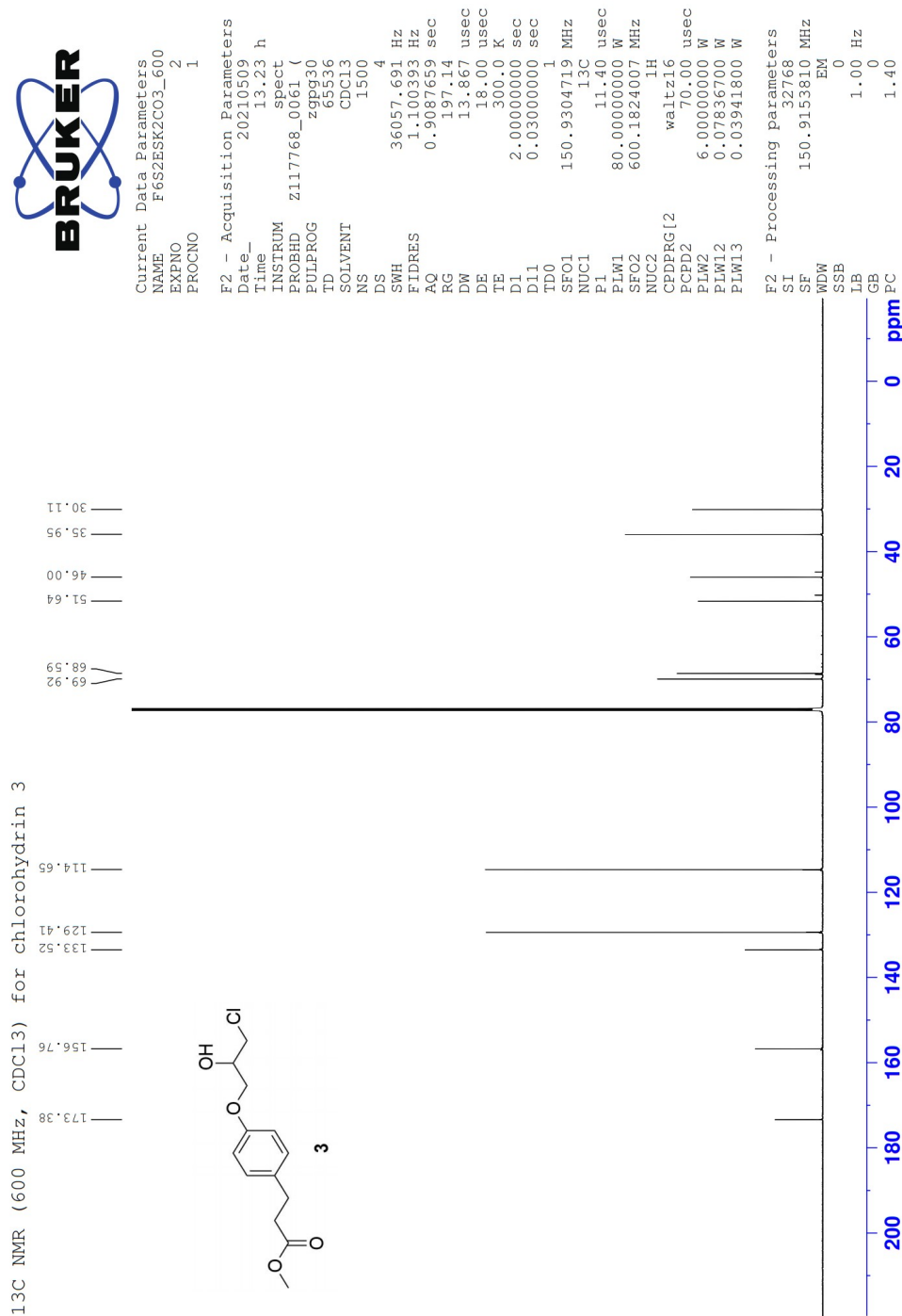
- (35) Ducret, A.; Trani, M.; Lortie, R. Lipase-Catalyzed Enantioselective Esterification of Ibuprofen in Organic Solvents Under Controlled Water Activity. *Enzyme Microb. Technol.* **1998**, *22*, 212–216.
- (36) Jacobsen, E.; Anthonsen, T. Water Content Influences the Selectivity of CALB-Catalyzed Kinetic Resolution of Phenoxyethyl-Substituted Secondary Alcohols. *Can. J. Chem.* **2002**, *80*, 557–581.
- (37) Lund, I.; Bøckmann, P.; Jacobsen, E. Highly Enantioselective CALB-Catalyzed Kinetic Resolution of Building Blocks for β -Blocker Atenolol. *Tetrahedron.* **2016**, *72*, 7288–7292.
- (38) Lund, I. Mekanistiske studier i kjemo-enzymatisk syntese av enantiomert rene byggestener for betablokkeren Atenolol, MA thesis, Norwegian University of Science and Technology, 2015.
- (39) Hansen, M. Improved Understanding of Reagents Used in the Synthesis of Enantiopure Precursors for (*S*)-Atenolol and (*S*)-Metoprolol, MA thesis, Norwegian University of Science and Technology, 2018.
- (40) Buvarp, F. Kjemo-enzymatisk syntese av enantiomert ren (*S*)-esmolol, MA thesis, Norwegian University of Science and Technology, 2018.
- (41) Austli, G. Synthesis of Enantiopure β -Blocker (*S*)-Practolol by Lipase Catalysis, MA thesis, Norwegian University of Science and Technology, 2018.
- (42) Feitsma, K.; B.F.H., D. Chromatographic Separation of Enantiomers. *Pharm. Weekbl. Sci.* **1988**, *10*, 1–11.
- (43) Okamoto, Y.; Ikai, T. Chiral HPLC for Efficient Resolution of Enantiomers. *Chem. Soc. Rev.* **2008**, *37*, 2593.
- (44) Mayer, S.; Schurig, V. Enantiomer Separation by Electrochromatography on Capillaries Coated With Chirasil-Dex. *J. High Resolut. Chromatogr.* **1992**, *15*, 129–131.
- (45) Lundanes, E.; Reubsæet, L.; Greibrokk, T., *Chromatography: Basic Principles, Sample Preparations and Related Methods*, p 12; Wiley-VCH: 2014.
- (46) Cranwell, P.; Hardwood, L.; Moody, C., *Experimental Organic Chemistry*, 3rd ed., pp 197-199; John Wiley & Sons Ltd.: 2017.
- (47) March, J., *Advanced Organic Chemistry: Reactions, Mechanisms, and Structures*, 4th ed., pp 411-413; John Wiley & Sons, Inc: 1992.
- (48) Transesterification, <https://chem.libretexts.org/@go/page/5914>, Accessed: 11.05.21, 2020.
- (49) Anslyn, E.; Dougherty, D., *Modern Physical Organic Chemistry*, pp 380-381; University Science Books: 2006.
- (50) Carey, F.; Sundberg, R., *Advanced Organic Chemistry: Part B: Reaction and Synthesis*, 5th ed, pp 5-6; Springer US: 2007.
- (51) Fulmer, G.; Miller, A.; Sherden, N.; Gottlieb, H.; Nudelman, A.; Stoltz, B.; Bercaw, J.; Goldberg, K. NMR Chemical Shifts of Trace Impurities: Common Laboratory Solvents, Organics, and Gases in Deuterated Solvents Relevant to the Organometallic Chemist. *Organometallics.* **2010**, *29*, 2176–2179.

-
- (52) Gottlieb, H.; Kotylar, V.; Nudelman, A. NMR Chemical Shifts of Common Laboratory Solvents as Trace Impurities. *J. Org. Chem.* **1997**, *62*, 7512–7515.
- (53) Yamaji, T.; Saito, T.; Hayamizu, K.; Yanagisawa, M.; Yamamoto, O.; Wasada, N.; Someno, K.; Kinugasa, S.; Tanabe, K.; Tamura, T.; Hirasishi, J. AIST: Integrated Spectral Database System of Organic Compounds. (Data were obtained from the National Institute of Advanced Science and Technology (Japan), SDBSWeb: <https://sdb.sdb.aist.go.jp/sdb/cgi-bin/landingpage?sdbno=1227>, Accessed: 25.05.2021, 1997.
- (54) Jacobsen, E.; Hoff, B.; Anthonsen, T. Enantiopure Derivatives of 1,2-Alkanediols: Substrate Requirements of Lipase B from *Candida antarctica*. *Chirality*. **2000**, *12*, 654–659.
- (55) Jacobsen, E.; Anthonsen, T.; El-Beairy, M.; Sundby, E.; Aboul-Enein, M.; M.I., A.; El-Azzouny, A.; Amin, K.; Abdel-Rehim, A. Lipase Catalyzed Kinetic Resolution of Stiripentolol. *Int. J. Chem.* **2012**, *4*, 7–13.
- (56) Narsaiah, A.; Kumar, J. Novel Asymmetric Synthesis of (S)-Esmolol Using Hydrolytic Kinetic Resolution. *Synth. Commun.* **2011**, *41*, 1603–1608.

A.2 ^{13}C -NMR spectrum of epoxide 2Figure A.2: ^{13}C -NMR spectrum (600 MHz, CDCl_3) of epoxide 2.

A.5 HMBC-NMR spectrum of epoxide 2

Figure A.5: HMBC-NMR spectrum (600 MHz, CDCl₃) of epoxide 2.

B.2 ^{13}C -NMR spectrum of chlorohydrin **3**Figure B.2: ^{13}C -NMR spectrum (600 MHz, CDCl_3) of chlorohydrin **3**.

C Characterization of 1-chloro-3-(4-(3-methoxy-3-oxopropyl)phenoxy)propan- 2-yl butyrate (4)

C.1 $^1\text{H-NMR}$ spectrum of ester 4

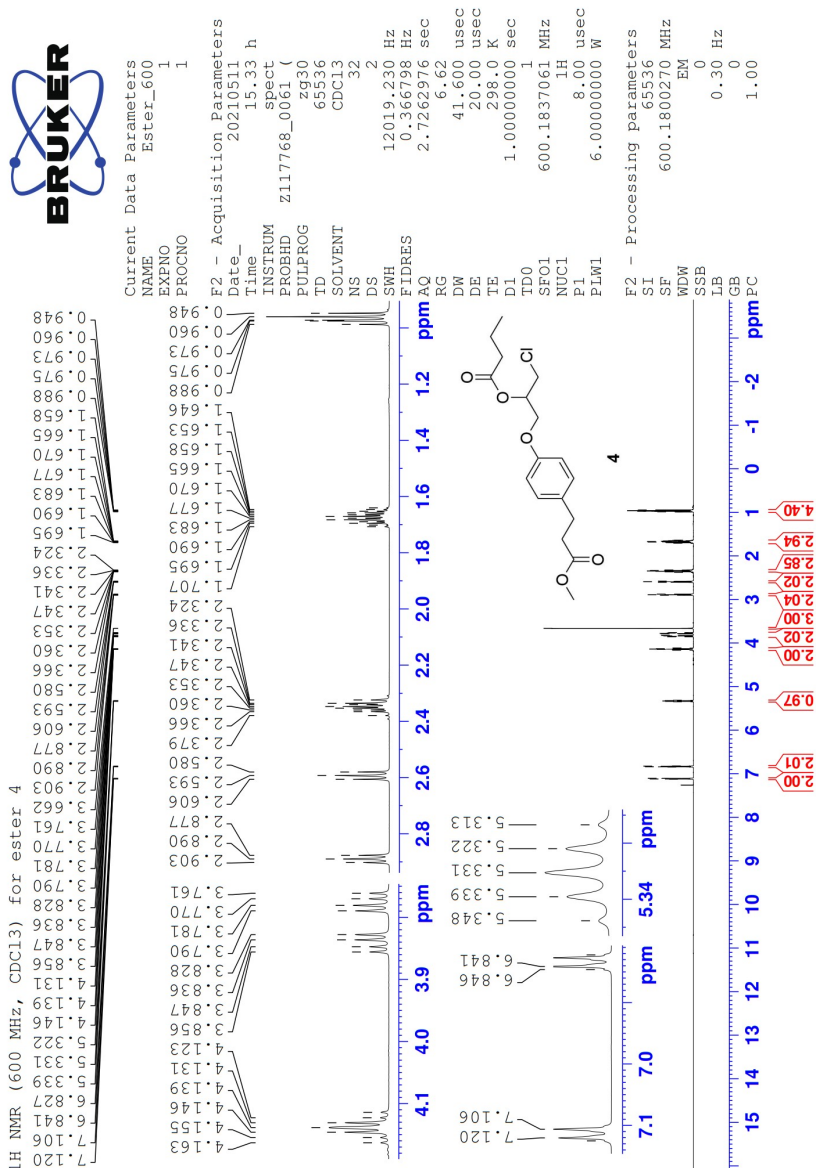


Figure C.1: $^1\text{H-NMR}$ spectrum (600 MHz, CDCl_3) of ester 4. $\delta = 2.34\text{-}2.32$, $1.71\text{-}1.64$, and $0.99\text{-}0.95$ ppm resonate for one proton extra which is from butanoic acid.

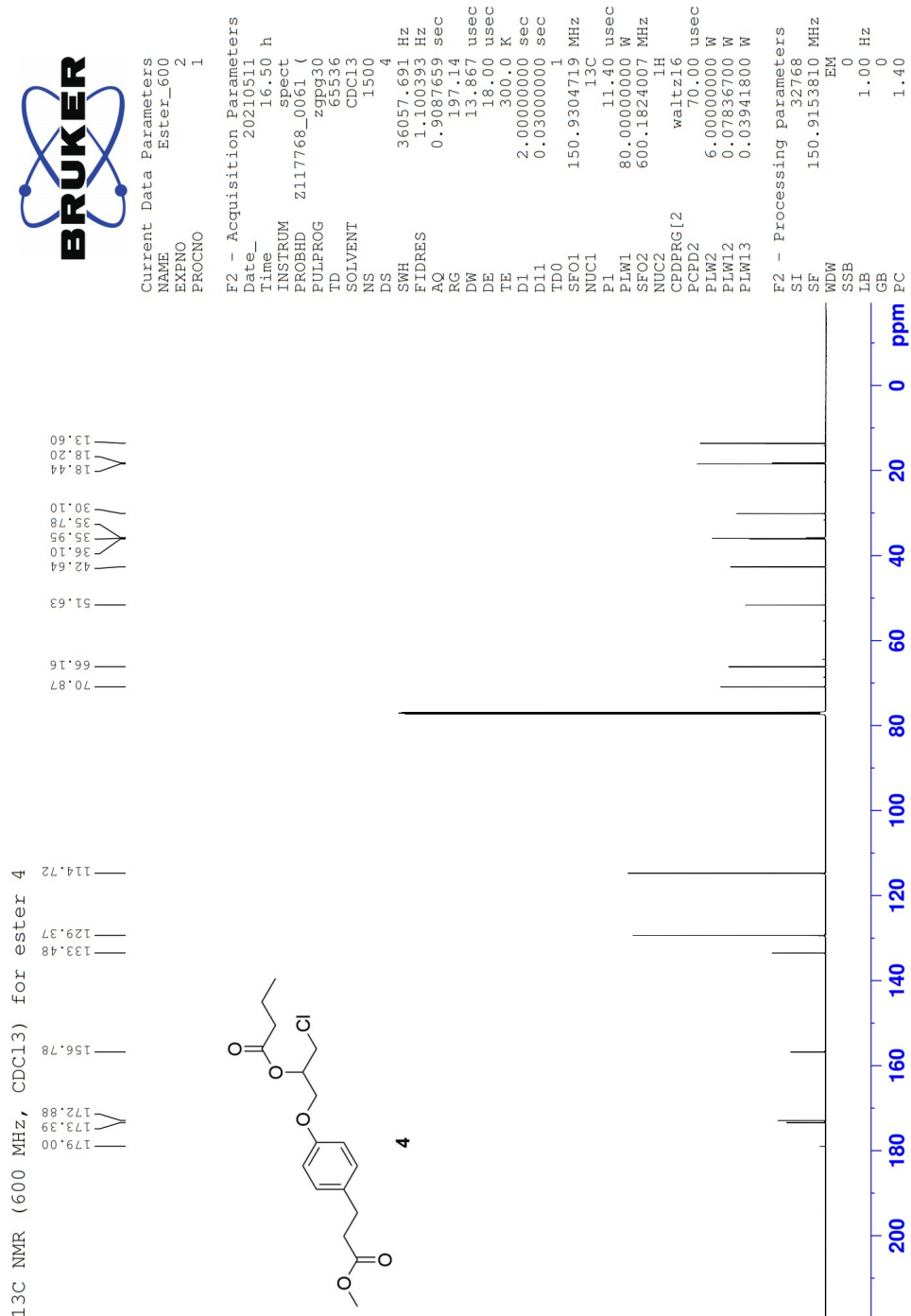
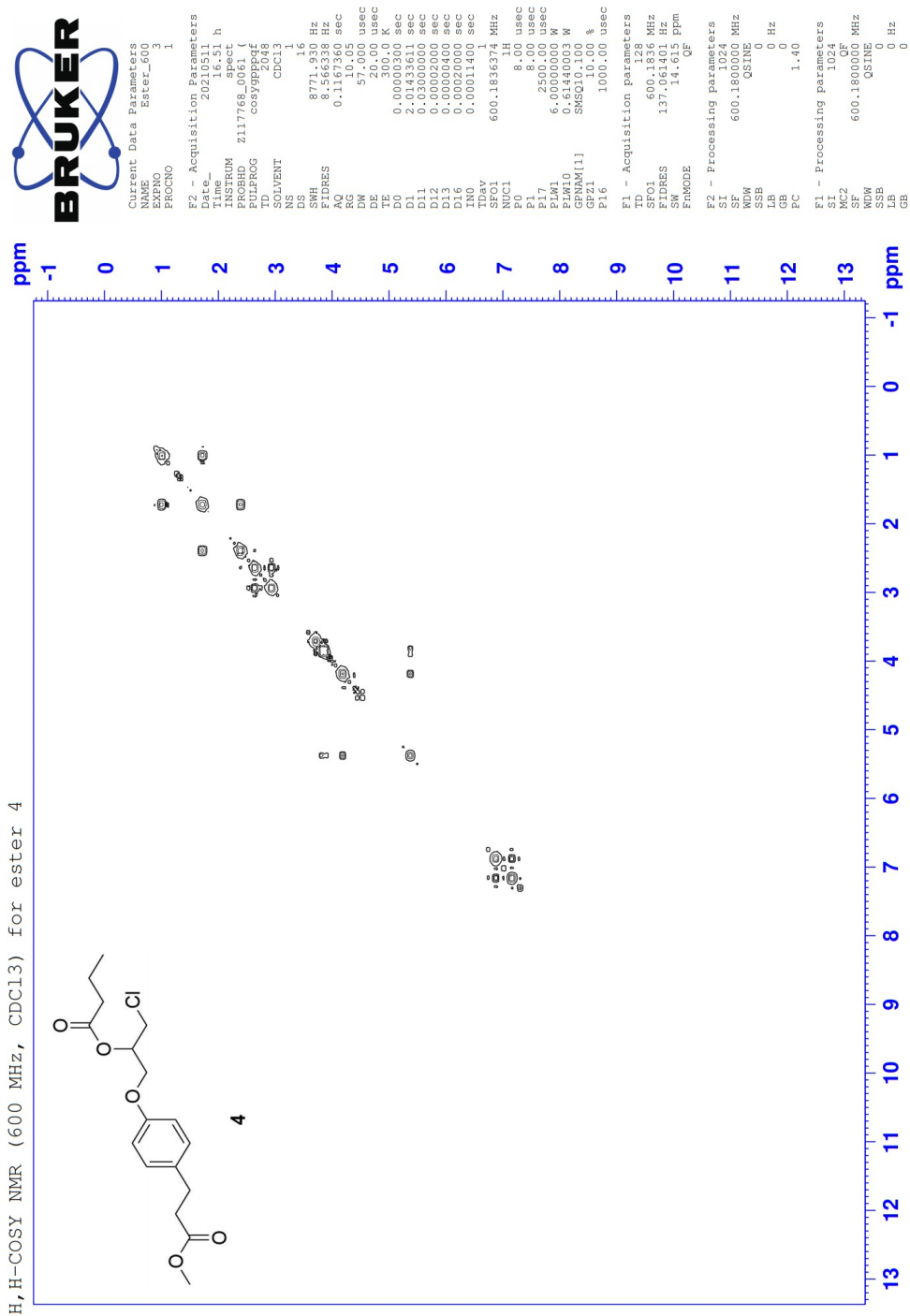
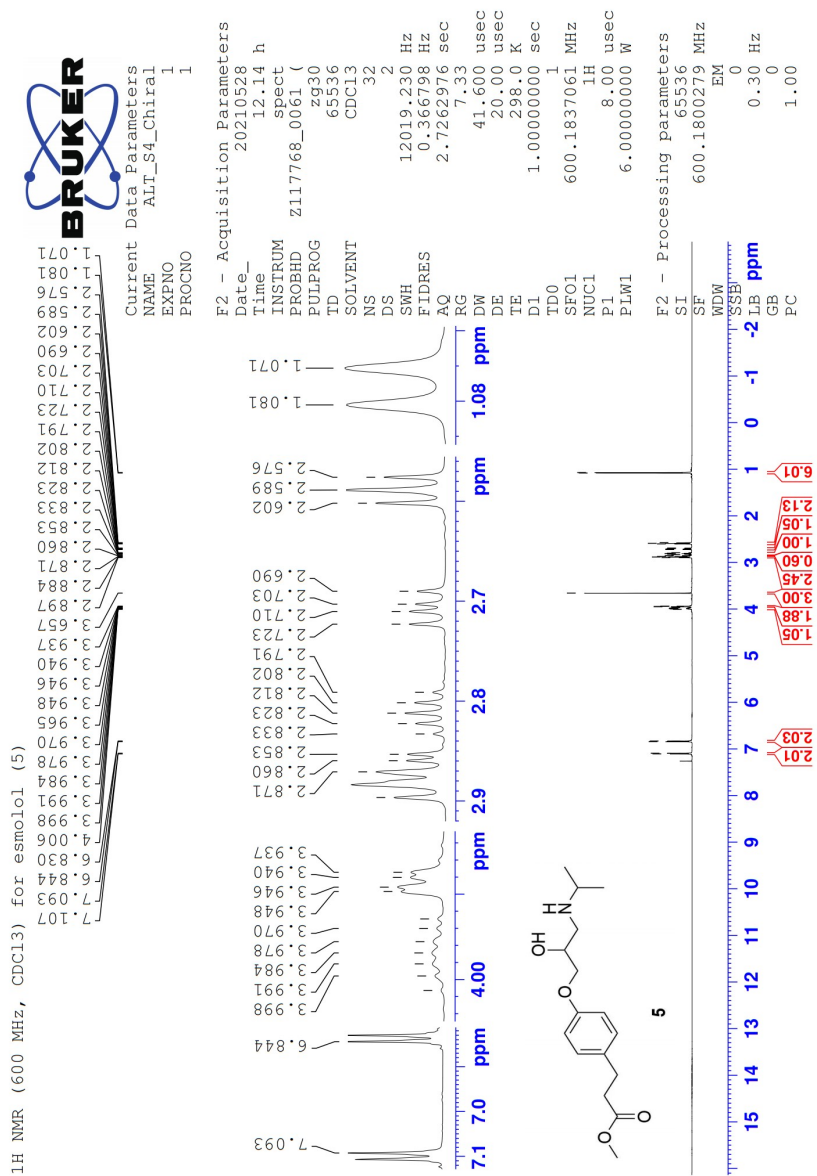
C.2 ^{13}C -NMR spectrum of ester 4

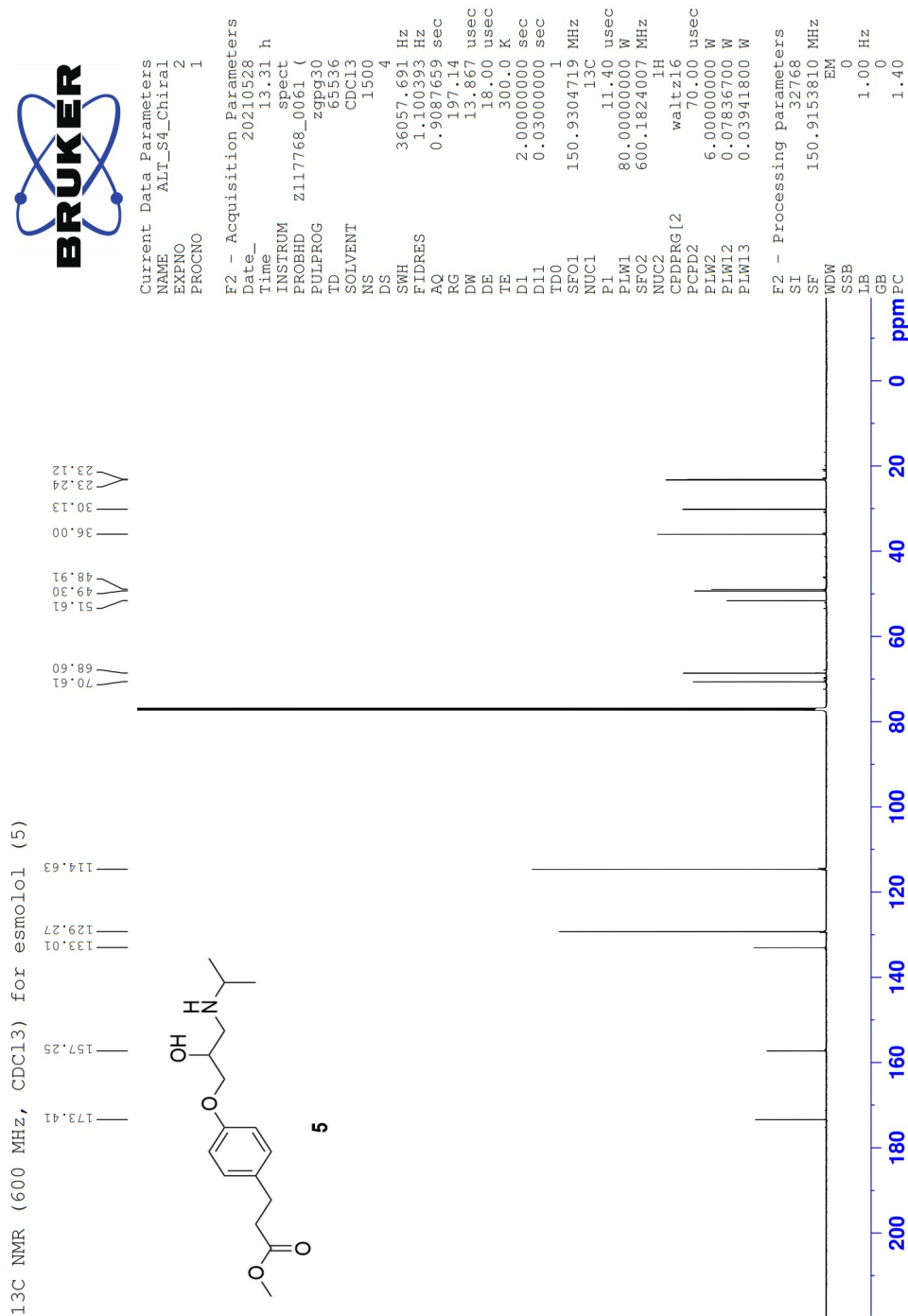
Figure C.2: ^{13}C -NMR spectrum (600 MHz, CDCl_3) of ester 4. $\delta = 179.0$, 35.8, and 18.2 ppm are from butanoic acid.

C.3 H,H-COSY-NMR spectrum of ester 4

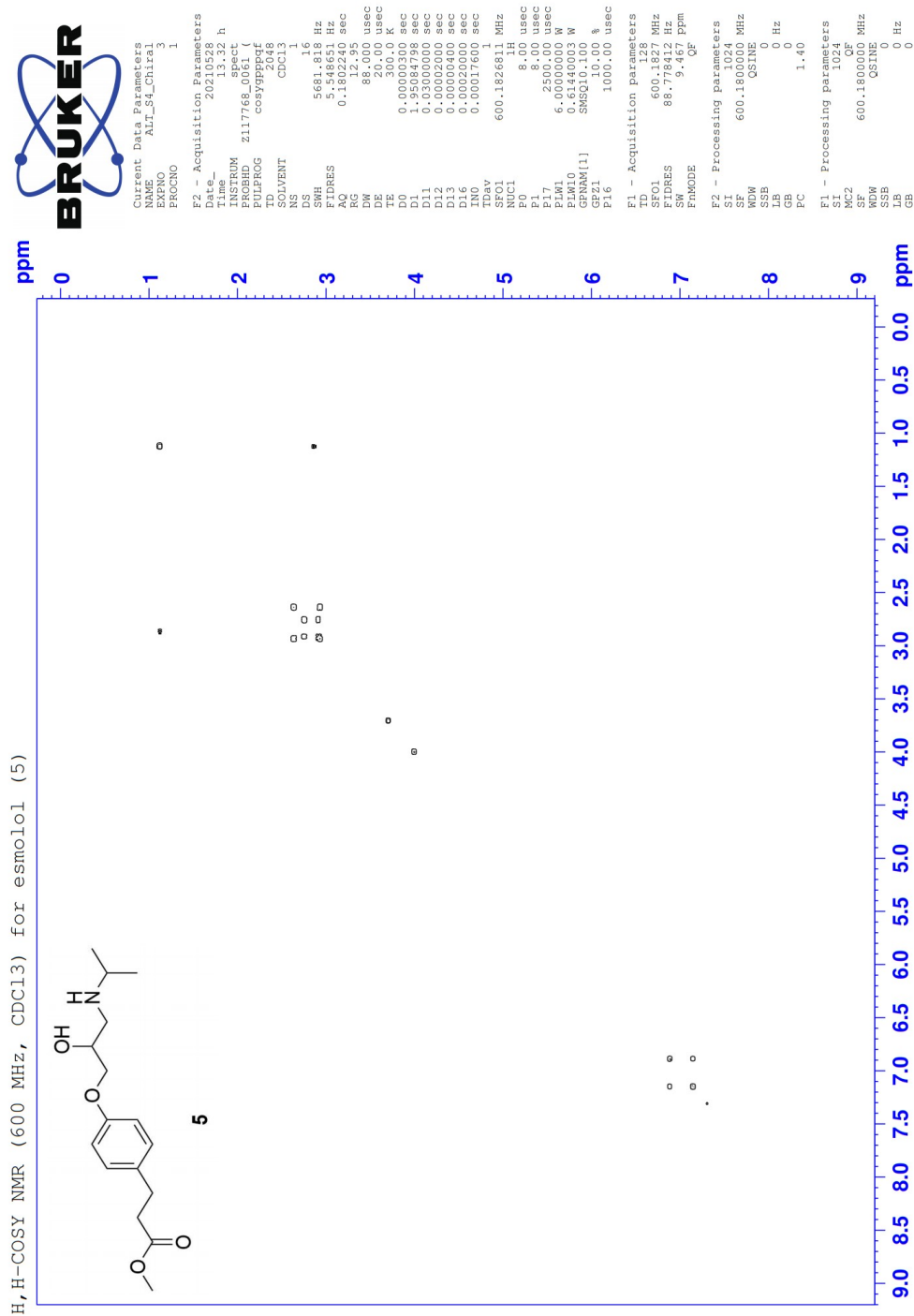
Figure C.3: H,H-COSY-NMR spectrum (600 MHz, CDCl₃) of ester 4.

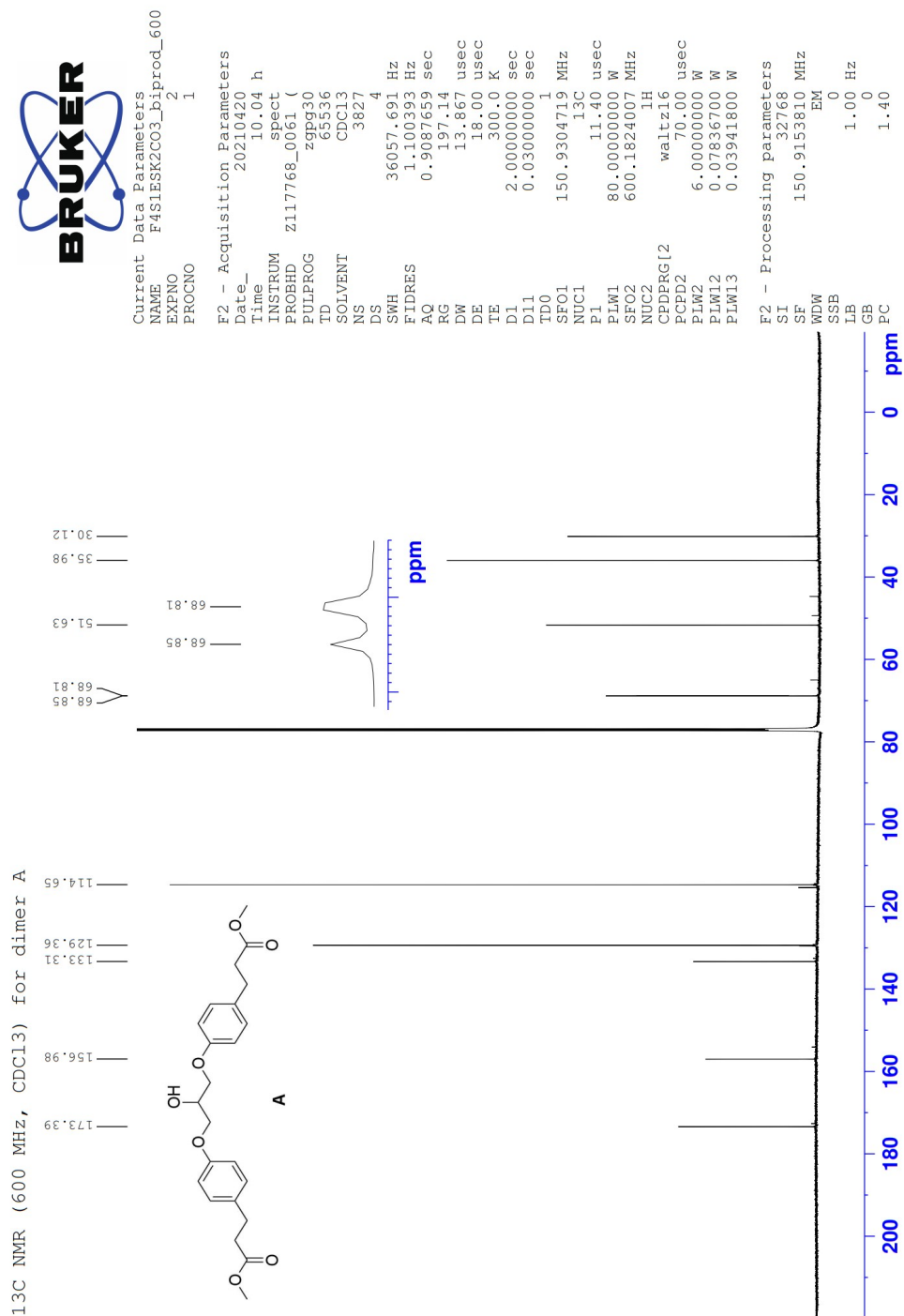
D Characterization of esmolol (5)

D.1 $^1\text{H-NMR}$ spectrum of esmolol (5)Figure D.1: $^1\text{H-NMR}$ spectrum (600 MHz, CDCl_3) of esmolol (5).

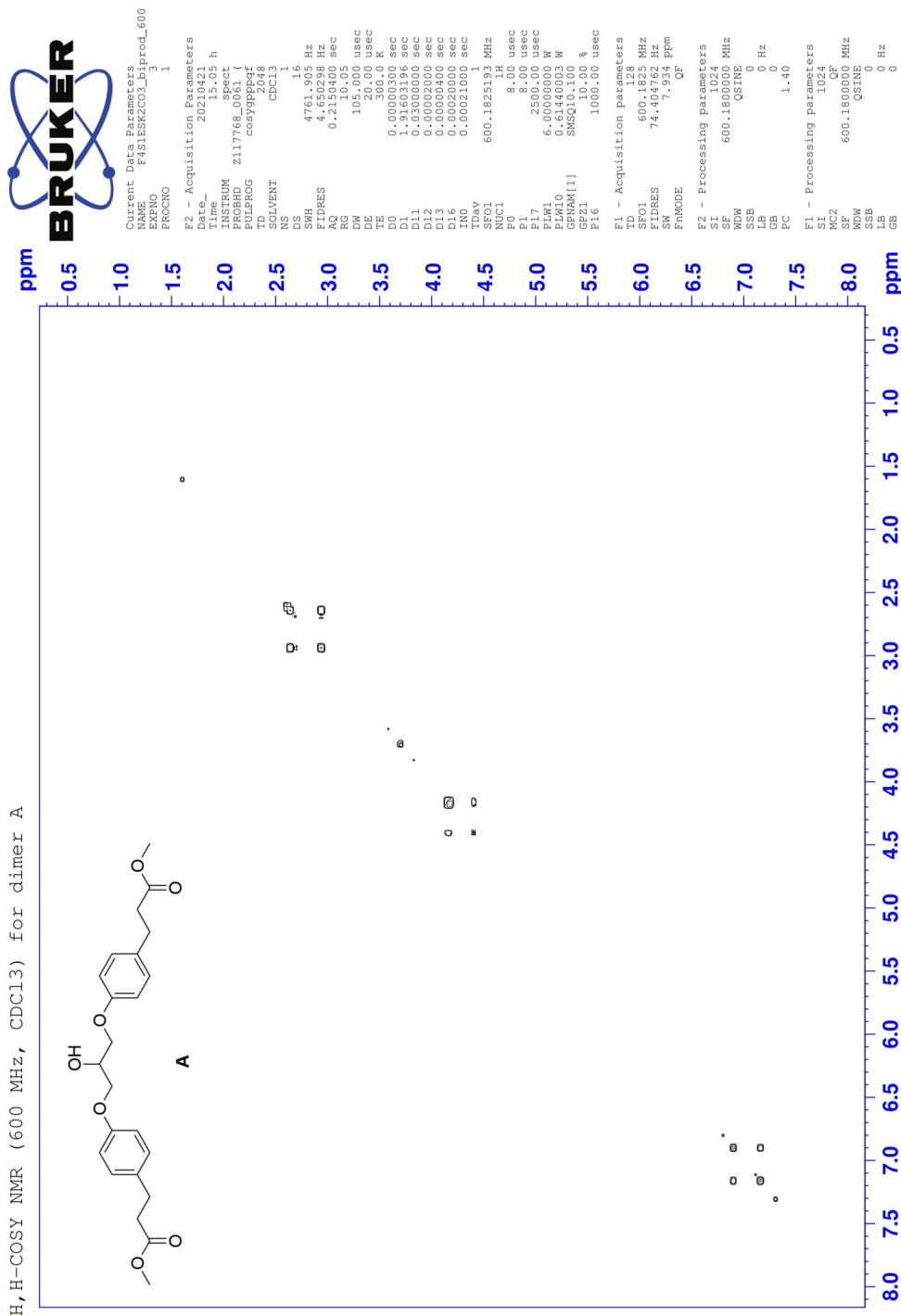
D.2 ^{13}C -NMR spectrum of esmolol (5)Figure D.2: ^{13}C -NMR spectrum (600 MHz, CDCl_3) of esmolol (5).

D.3 H,H-COSY-NMR spectrum of esmolol (5)

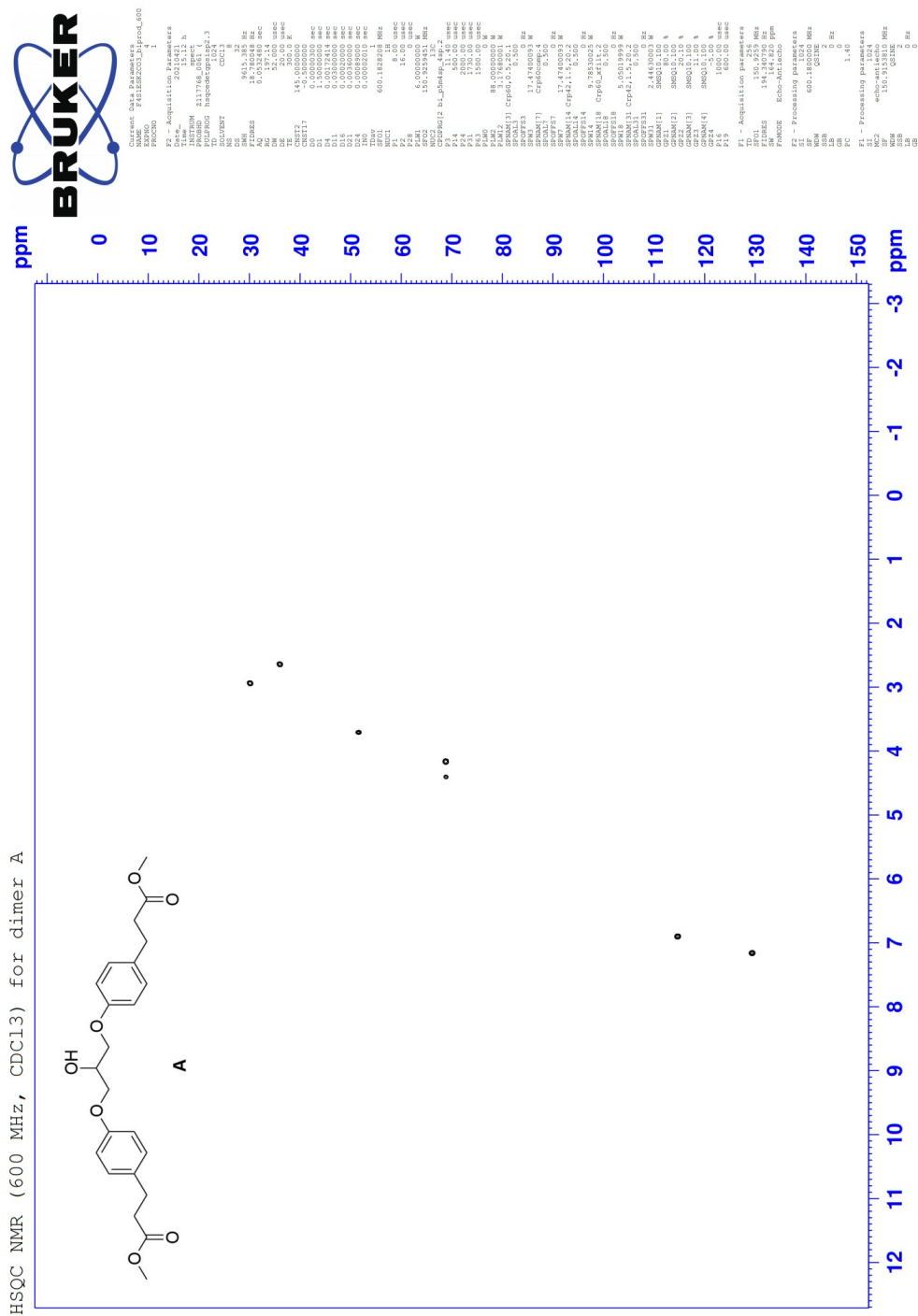
Figure D.3: H,H-COSY-NMR spectrum (600 MHz, CDCl₃) of esmolol (5).

E.2 ^{13}C -NMR spectrum of dimer AFigure E.2: ^{13}C -NMR spectrum (600 MHz, CDCl_3) of dimer A.

E.3 H,H-COSY-NMR spectrum of dimer A

Figure E.3: H,H-COSY-NMR spectrum (600 MHz, CDCl₃) of dimer A.

E.4 HSQC-NMR spectrum of dimer A

Figure E.4: HSQC-NMR spectrum (600 MHz, CDCl₃) of dimer A.

F Characterization of 3-chloro-2-hydroxypropyl 3-(4-(oxiran-2-ylmethoxy)phenyl)propanoate (J)

F.1 $^1\text{H-NMR}$ spectrum of by-product J

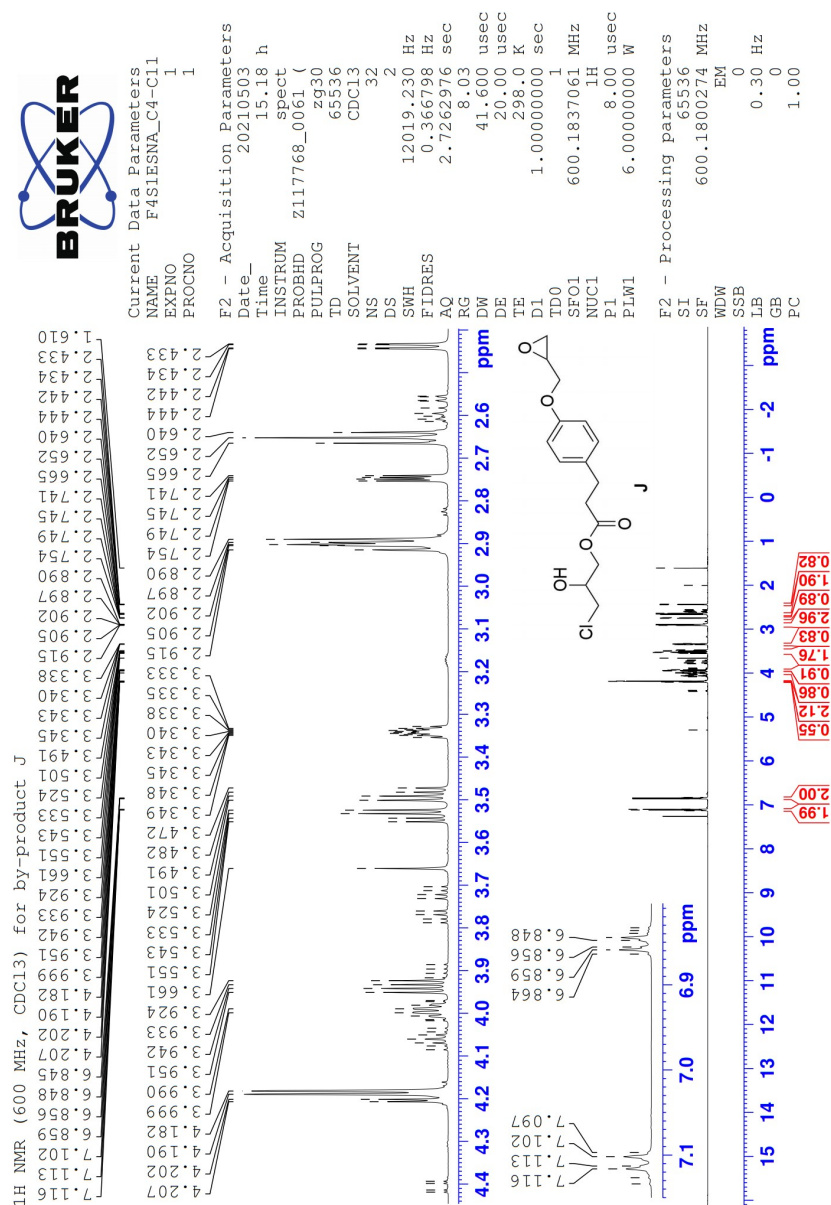
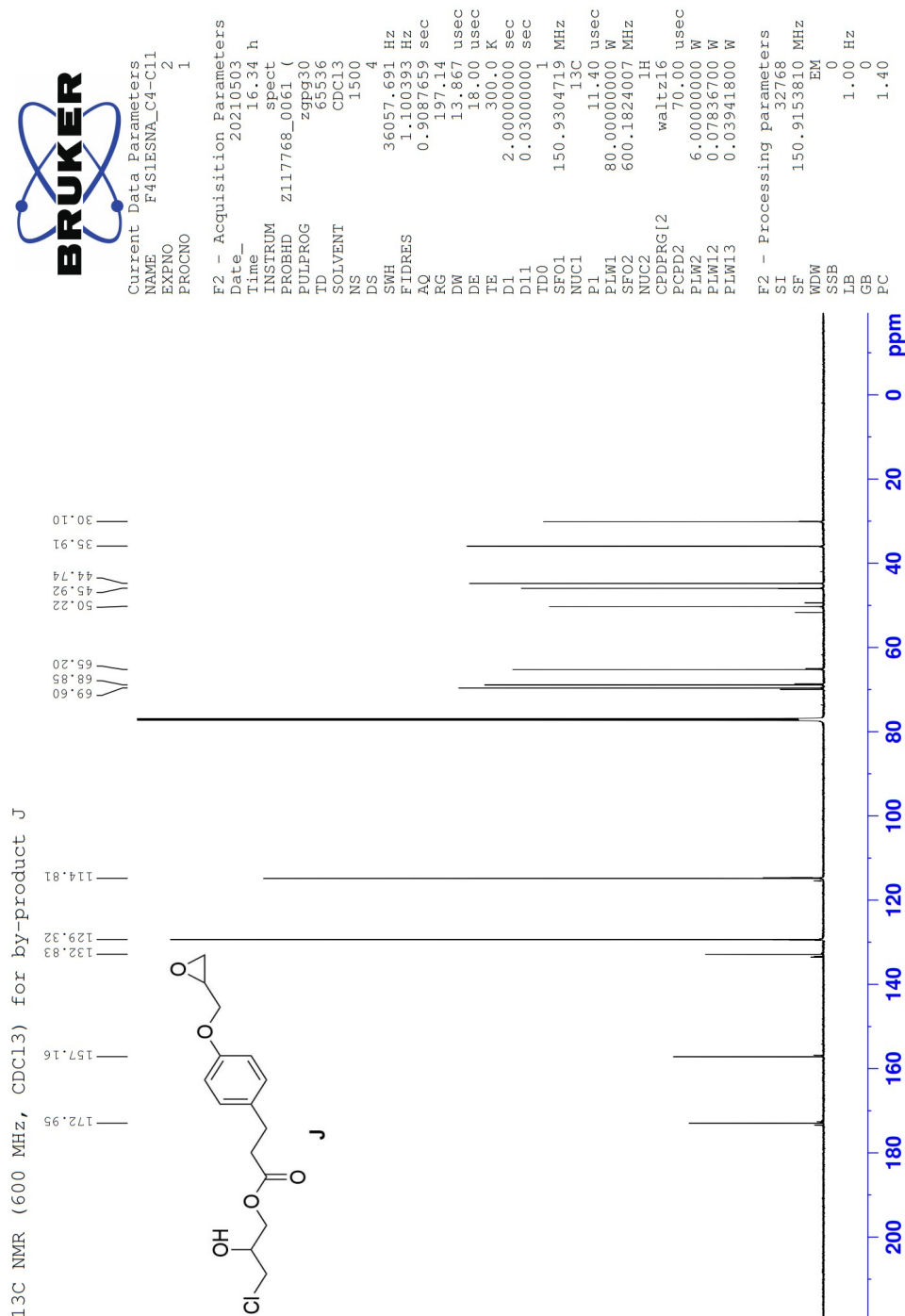
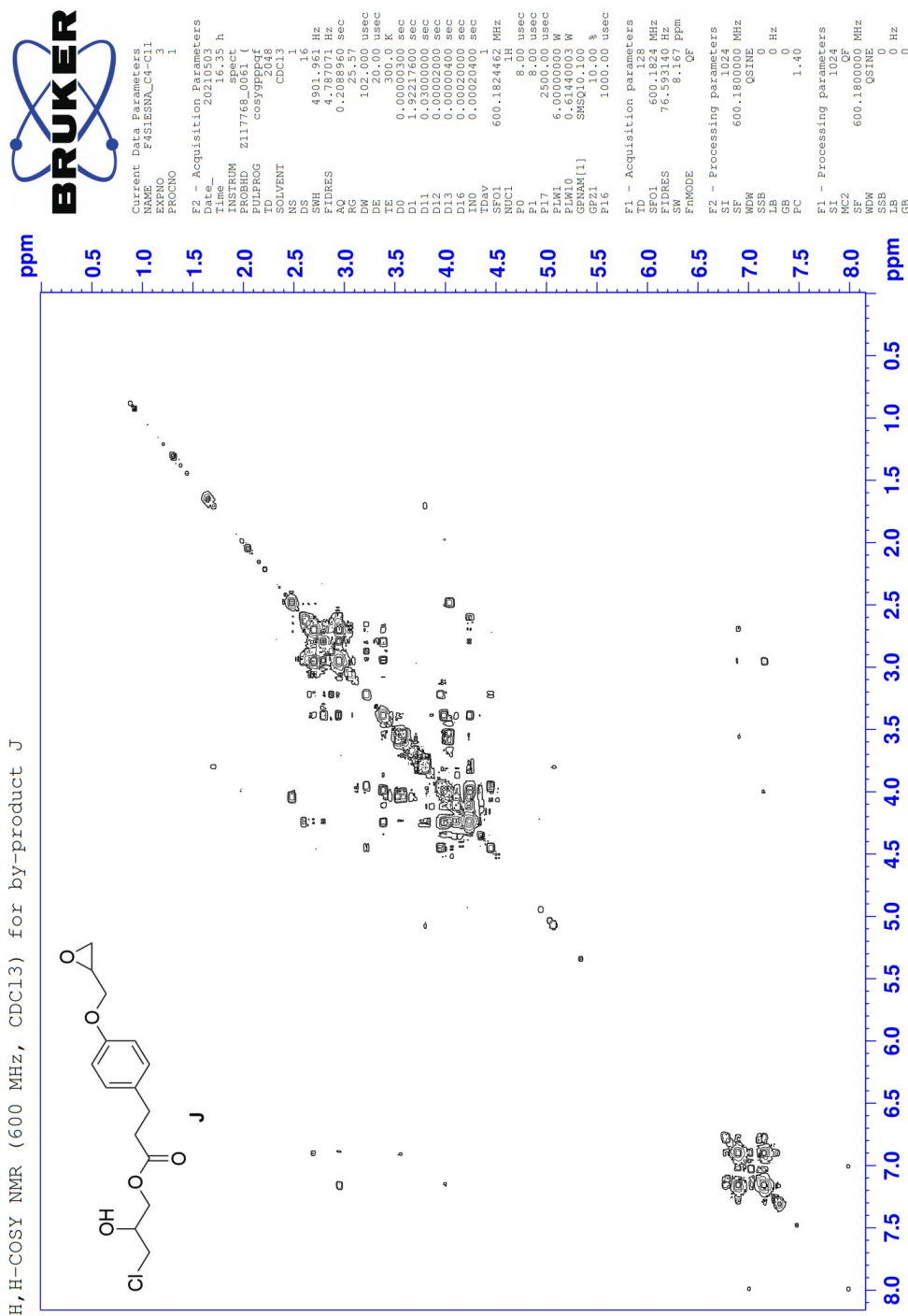


Figure F.1: $^1\text{H-NMR}$ spectrum (600 MHz, CDCl_3) of by-product **J**. $\delta = 1.61$ ppm corresponds to water from the solvent.

F.2 ^{13}C -NMR spectrum of by-product JFigure F.2: ^{13}C -NMR spectrum (600 MHz, CDCl_3) of by-product J.

F.3 ^1H , ^1H -COSY-NMR spectrum of by-product JFigure F.3: ^1H , ^1H -COSY-NMR spectrum (600 MHz, CDCl₃) of by-product J.

G LC-MS-analysis of by-products

G.1 LC-MS-chromatogram for reaction with NaOH

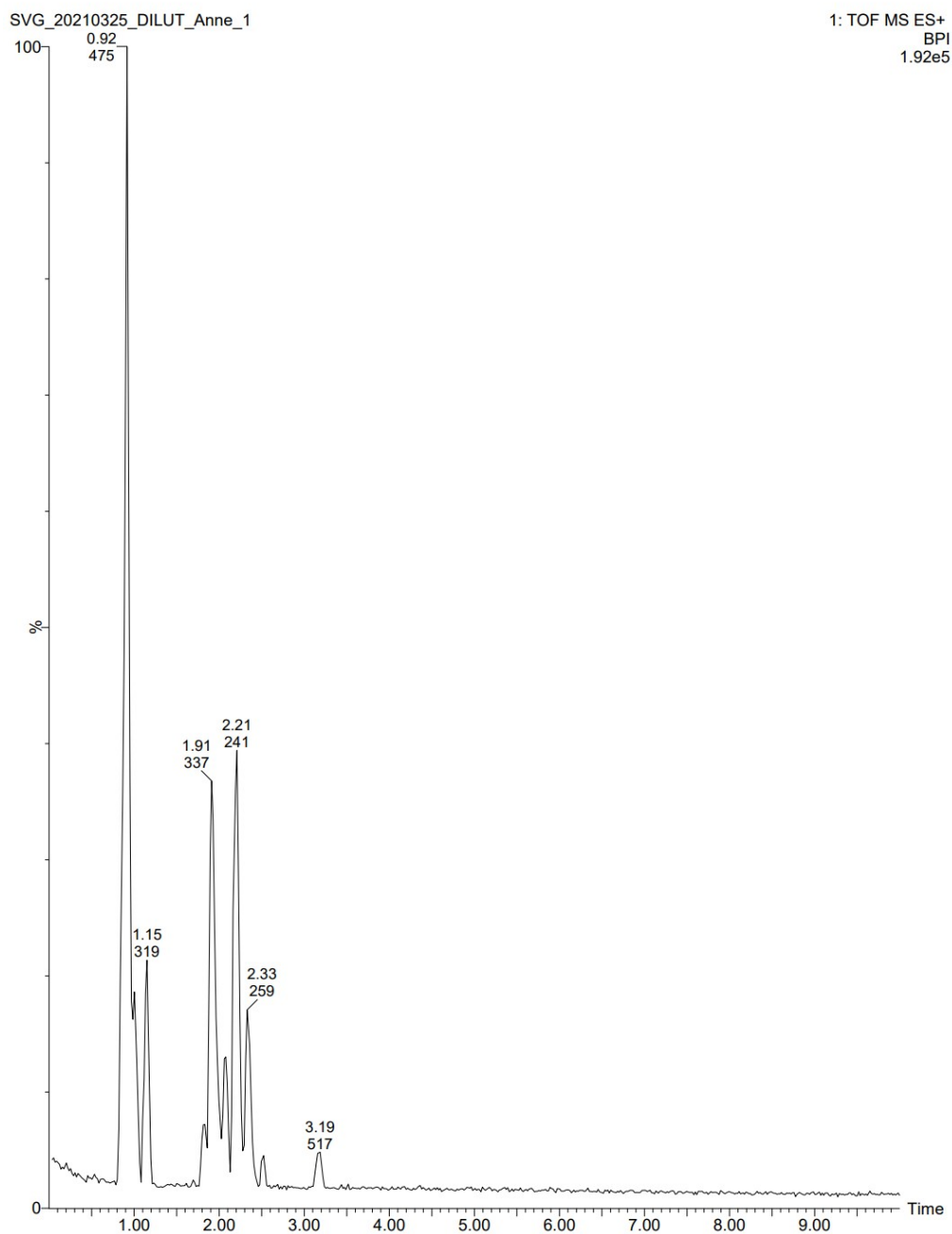


Figure G.1: LC-MS-chromatogram for reaction between phenol **1** and epichlorohydrin with sodium hydroxide as base.

G.2 MS-spectrum of by-product H or I

Elemental Composition Report

Page 1

Single Mass Analysis

Tolerance = 3.0 PPM / DBE: min = -1.5, max = 50.0

Element prediction: Off

Number of isotope peaks used for i-FIT = 3

Monoisotopic Mass, Even Electron Ions

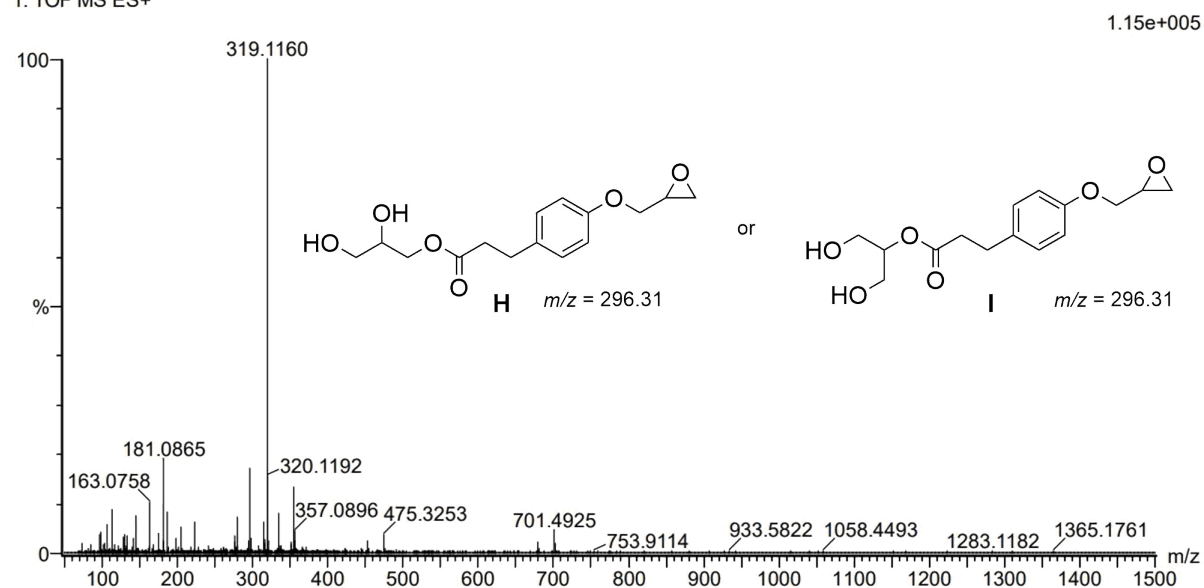
298 formula(e) evaluated with 2 results within limits (up to 50 closest results for each mass)

Elements Used:

C: 0-500 H: 0-1000 N: 0-1 O: 0-10 Na: 0-1 Cl: 0-1

SVG_20210325_DILUT_Anne_1 62 (1.151)AM2 (Ar,35000.0,0.00,0.00)

1: TOF MS ES+



Minimum: -1.5
 Maximum: 5.0 3.0 50.0

Mass	Calc. Mass	mDa	PPM	DBE	i-FIT	Norm	Conf (%)	Formula
319.1160	319.1160	0.0	0.0	-0.5	784.0	25.146	0.00	C11 H24 O8 Cl
	319.1158	0.2	0.6	5.5	758.9	0.000	100.00	C15 H20 O6 Na

Figure G.2: MS-spectrum of by-product H or I with $m/z = 296.31$.

G.3 MS-spectrum of by-product J or K

Elemental Composition Report

Page 1

Single Mass Analysis

Tolerance = 10.0 PPM / DBE: min = -1.5, max = 50.0

Element prediction: Off

Number of isotope peaks used for i-FIT = 3

Monoisotopic Mass, Even Electron Ions

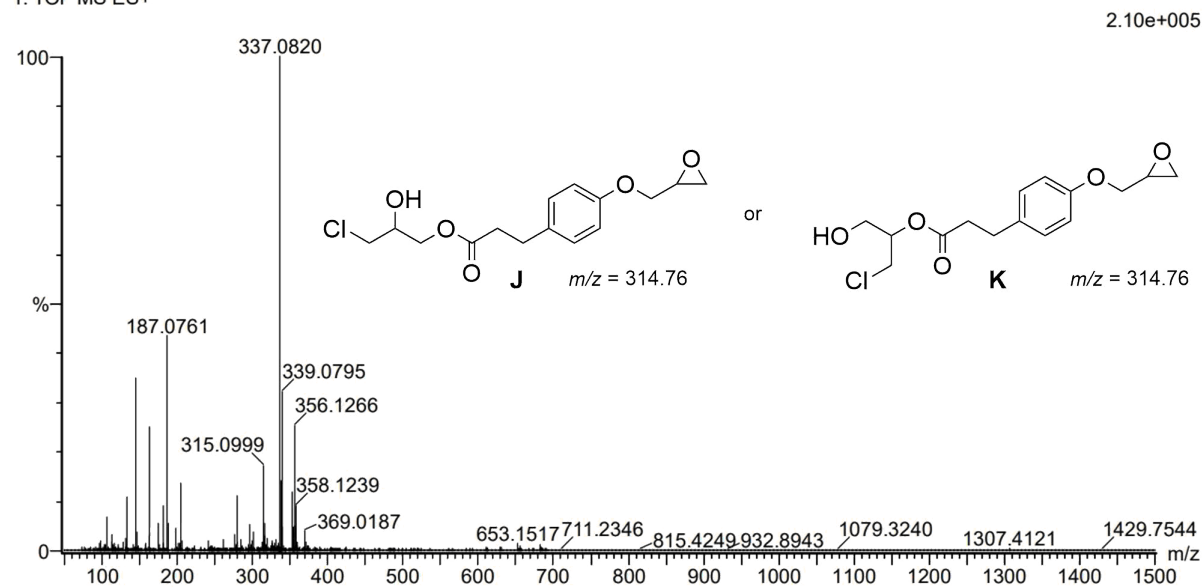
318 formula(e) evaluated with 3 results within limits (up to 50 closest results for each mass)

Elements Used:

C: 0-500 H: 0-1000 N: 0-1 O: 0-10 Na: 0-1 Cl: 0-1

SVG_20210325_DILUT_Anne_1 103 (1.912)AM2 (Ar,35000.0,0.00,0.00)

1: TOF MS ES+



Minimum: -1.5
Maximum: 5.0 10.0 50.0

Mass	Calc. Mass	mDa	PPM	DBE	i-FIT	Norm	Conf (%)	Formula
337.0820	337.0819	0.1	0.3	5.5	970.9	0.015	98.55	C15 H19 O5 Na Cl
	337.0841	-2.1	-6.2	14.5	991.2	20.325	0.00	C21 H14 O3 Na
	337.0843	-2.3	-6.8	8.5	975.2	4.234	1.45	C17 H18 O5 Cl

Figure G.3: MS-spectrum of by-product J or K with $m/z = 314.76$.

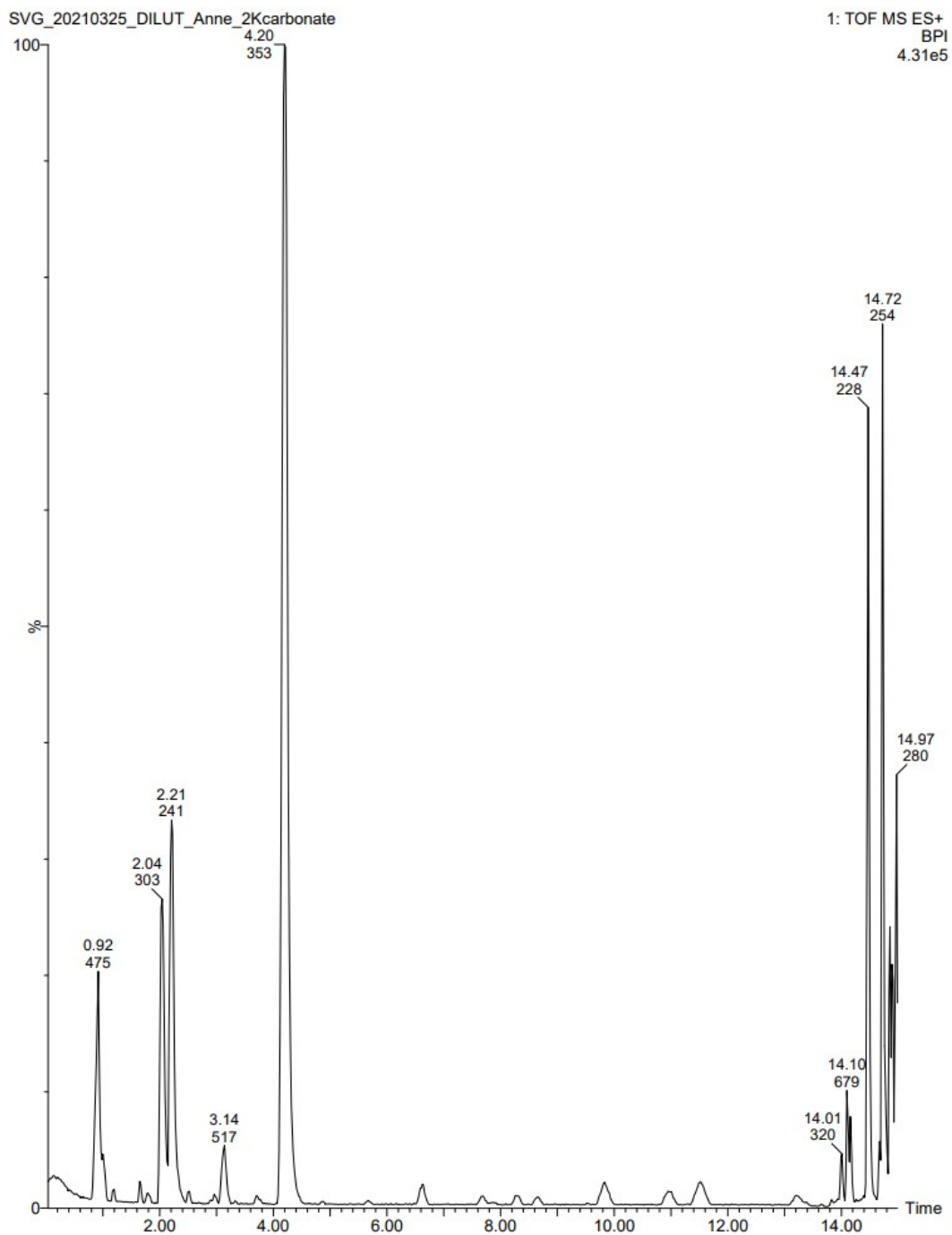
G.4 LC-MS-chromatogram for reaction with K_2CO_3 

Figure G.4: LC-MS chromatogram for reaction between phenol **1** and epichlorohydrin with potassium carbonate as base.

G.5 MS-spectrum of dimer A

Elemental Composition Report

Page 1

Single Mass Analysis

Tolerance = 10.0 PPM / DBE: min = -1.5, max = 50.0

Element prediction: Off

Number of isotope peaks used for i-FIT = 3

Monoisotopic Mass, Even Electron Ions

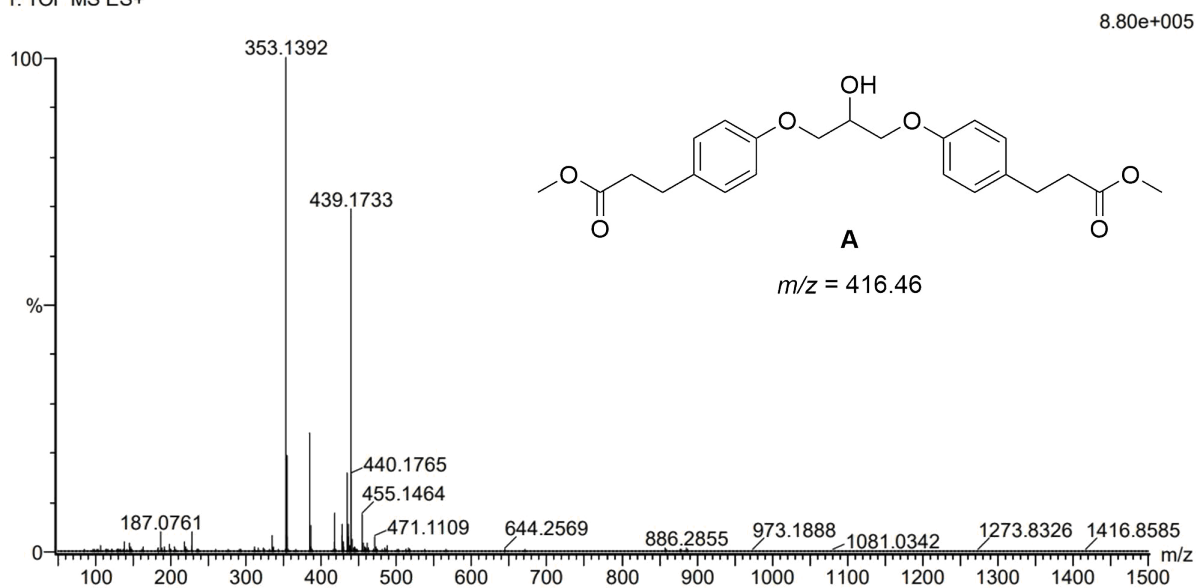
423 formula(e) evaluated with 5 results within limits (up to 50 closest results for each mass)

Elements Used:

C: 0-500 H: 0-1000 N: 0-1 O: 0-10 Na: 0-1 Cl: 0-1

SVG_20210325_DILUT_Anne_2Kcarbonate 226 (4.180)AM2 (Ar,35000.0,0.00,0.00)

1: TOF MS ES+



Minimum: -1.5
 Maximum: 5.0 10.0 50.0

Mass	Calc. Mass	mDa	PPM	DBE	i-FIT	Norm	Conf (%)	Formula
439.1733	439.1733	0.0	0.0	9.5	813.1	0.047	95.45	C23 H28 O7 Na
	439.1735	-0.2	-0.5	3.5	833.5	20.417	0.00	C19 H32 O9 Cl
	439.1711	2.2	5.0	0.5	833.6	20.521	0.00	C17 H33 O9 Na Cl
	439.1757	-2.4	-5.5	12.5	816.2	3.113	4.45	C25 H27 O7
	439.1698	3.5	8.0	21.5	820.0	6.925	0.10	C32 H23 O2

Figure G.5: MS-spectrum of dimer A with $m/z = 416.46$.

G.6 MS-spectrum of dimer L

Elemental Composition Report

Page 1

Single Mass Analysis

Tolerance = 10.0 PPM / DBE: min = -1.5, max = 50.0

Element prediction: Off

Number of isotope peaks used for i-FIT = 3

Monoisotopic Mass, Even Electron Ions

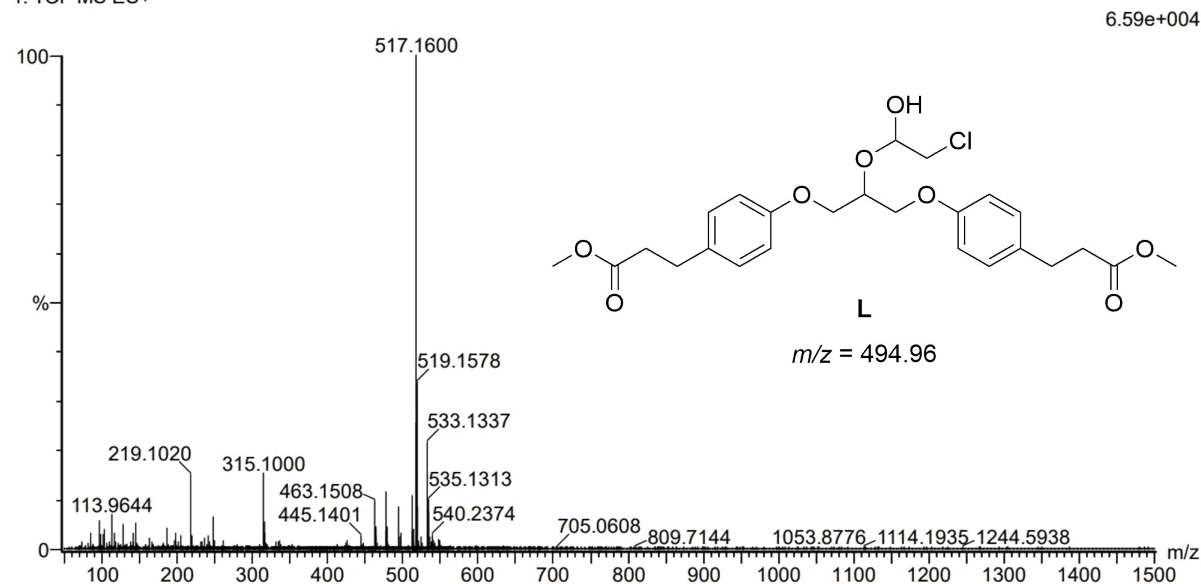
507 formula(e) evaluated with 7 results within limits (up to 50 closest results for each mass)

Elements Used:

C: 0-500 H: 0-1000 N: 0-1 O: 0-10 Na: 0-1 Cl: 0-1

SVG_20210325_DILUT_Anne_2Kcarbonate 168 (3.106)AM2 (Ar,35000.0,0.00,0.00)

1: TOF MS ES+



Minimum: -1.5
Maximum: 5.0 10.0 50.0

Mass	Calc. Mass	mDa	PPM	DBE	i-FIT	Norm	Conf (%)	Formula
517.1600	517.1605	-0.5	-1.0	9.5	508.9	0.042	95.92	C25 H31 O8 Na Cl
	517.1592	0.8	1.5	30.5	527.3	18.448	0.00	C40 H21 O
	517.1627	-2.7	-5.2	18.5	527.0	18.074	0.00	C31 H26 O6 Na
	517.1629	-2.9	-5.6	12.5	512.1	3.236	3.93	C27 H30 O8 Cl
	517.1570	3.0	5.8	21.5	515.4	6.539	0.14	C34 H26 O3 Cl
	517.1568	3.2	6.2	27.5	527.2	18.369	0.00	C38 H22 O Na
	517.1651	-5.1	-9.9	21.5	527.1	18.188	0.00	C33 H25 O6

Figure G.6: MS-spectrum of dimer L with $m/z = 494.96$.

